Synthesis and Biochemical Screening of Novel Non-Purine Based Xanthine Oxidase Inhibitors

A thesis submitted to the Central University of Punjab

For the award of
Master of Pharmacy

In
Medicinal Chemistry

By
Deependra Kumar

Supervisor
Dr. Raj Kumar

Centre for Chemical and Pharmaceutical Sciences
School of Basic and Applied Sciences
Central University of Punjab, Bathinda
October, 2013

DECLARATION

I declare that the thesis entitled "**Synthesis and Biochemical Screening of Novel Non-purine Based Xanthine Oxidase Inhibitors**" has been prepared by me under the guidance of Dr. Raj Kumar, Assistant Professor, Centre for Chemical and Pharmaceutical Sciences, School of Basic and Applied Sciences, Central University of Punjab. No part of this thesis has formed the basis for the award of any degree or fellowship previously.

Deependra Kumar
Centre for Chemical and Pharmaceutical Sciences
School of Basic and Applied Sciences,
Central University of Punjab,
Bathinda - 151001

Date:

CERTIFICATE

I certify that Deependra Kumar has prepared his thesis entitled "**Synthesis and Biochemical Screening of Novel Non-purine Based Xanthine Oxidase Inhibitors**", for the award of M.Pharm. degree of the Central University of Punjab, under my guidance. He has carried out this work at the Centre for Chemical and Pharmaceutical Sciences, School of Basic and Applied Sciences, Central University of Punjab.

Dr. Raj Kumar
Centre for Chemical and Pharmaceutical Sciences
School of Basic and Applied Sciences
Central University of Punjab
Bathinda - 151001

Date:

ABSTRACT

Synthesis and Biochemical Screening of Novel Non-purine Based Xanthine Oxidase Inhibitors

Name of student	**:**	Deependra Kumar
Registration Number	**:**	CUP/M.Phm.-PhD./SBAS/CPS/2011-12/06
Degree for which submitted	**:**	Master of Pharmacy (Medicinal Chemistry)
Supervisor	**:**	Dr. Raj Kumar
Centre	**:**	Chemical and Pharmaceutical Sciences
School of Studies	**:**	Basic and Applied Sciences

Key words	**:**	Non-purine based compounds, Synthesis, Xanthine oxidase inhibitory activity.

Xanthine oxidase (XO), or xanthine oxidoreductase (XOR), is a complex molybdoflavoenzyme which, in humans, is recognized as the terminal enzyme of purine catabolism, catalysing the hydroxylation of purines to uric acid, overproduction of which usually leads to a pathological condition called hyperuricemia and gout. XO inhibitors (XOI) are proved to be promising urate lowering agents. Purine based XOI (allopurinol) however, are associated with various lethal side effects like hypersensitivity syndrome (Stevens Johnson syndrome and Tissue Epidermal Necrolysis), bone marrow depression, rash etc. On the other hand non-purine based XOI (febuxostat) are found to be safer and effective antihyperuricemic and antigout agents.

Present investigation describes synthesis, characterization of some non-purine based compounds and their evaluation for xanthine oxidase inhibitory activity.

(Deependra Kumar) (Dr. Raj Kumar)

DEDICATED

TO

MY FATHER

L. RAJENDRA PRASAD SINHA

ACKNOWLEDGEMENTS

This thesis is product of a large measure of serendipity, fortuitous encounters with people who have changed the course of my academic career. It would not have been possible without the help, support, guidance and efforts of so many people in so many ways.

First of all, I am grateful to The Almighty God for the wisdom and perseverance that he has been bestowed upon me during this research work, and indeed, throughout my life.

I would like to express my grateful and sincere gratitude to my supervisor **Dr. Raj Kumar** for instilling in me the qualities to do this work. His infectious enthusiasm and unlimited zeal, guidance, understanding, patience, encouragement and support have been major driving forces through my post graduate career at the Central University of Punjab, Bathinda.

Let me place on record my gratitude to all my former teachers who made me what I am today especially to **"Dr. Rahul Shrivastava", "Dr. Virender Singh", "Dr. Ajit Vikram". Dr. Vikas Jaitak, Dr. Harish Holla** and **"Dr. Vinod Pathania**" for the useful comments, remarks and engagement through the learning process of this master's course

I also take this opportunity to express a deep sense of gratitude to Assistant Professor **Dr. Sanjeev K. Thakur** and **Dr. Sandeep Singh** for valuable information and guidance in their respective fields which helped me in completing this task through various stages.

Beside my supervisor, I would like to devote my thanks to Dean-Academic affairs and Coordinator **Prof. P. Rama Rao** for the blessings, help and guidance given by him time to time which carry me long way in the journey of life, on which I am about to embark.

I would like to avail this opportunity to express my gratitude to Examination Controller **"Prof. R.G Saini"** and appreciate the guidance that has improved our presentation skills by his comments and tips.

I express my deepest appreciation to my class mates, **Jimi, Arvind, Monica, Vinay, Ramit, Prakriti** and **Yashika** who supported and helped me throughout my work. Thanks to all of my juniors **Anil, Vijender, Ashish, Gaurav, Gagandeep, Akansha, Sheetal** and **Mayank** for being with me always.

Special thanks goes to **Gaurav** and **Gagandeep** for helping me during synthesis and **Monica** and **Sheetal Sharma** for helping me in biological screening.

Last but not least I couldn't imagine to be anywhere without the undying support, blessings and motivational encouragement of my mother **Fula Sinha** and brother **Kumar Brajendra**.

TABLE OF CONTENTS

LIST OF TABLES

LIST OF FIGURES

LIST OF SCHEMES

LIST OF ABBREVIATIONS

Sr. No.	Full form	Abbreviation
1.	Xanthine Oxidase	XO
2.	Reactive Oxygen Species	ROS
3.	Xanthine Oxidase Inhibitors	XOI
4.	Food and Drug Administration	FDA
5.	Xanthine Oxidoreductase	XOR
6.	Xanthine Dehydrogenase	XDH
7.	Flavin Adenine Dinucleotide	FAD
8.	Non-steroidal Anti-inflammatory Drugs	NSAIDs
9.	Chronic Kidney Disease	CKD
10.	Glucose Transporter	GLUT
11.	Adenosine Triphosphate	ATP
12.	Urate Transporter 1	URAT1
13.	Tumour Lysis Syndrome	TLS
14	Poly (ethylene) Glycol	PEG

15.	Randomized Controlled Trials	RCTs
16.	Lithospermic Acid	LSA
17.	1-methyl-1,2,3,4-tetrahydro-β-carboline-3-carboxylic acid	MTCA
18.	Uric Acid Lowering Therapy	ULT
19.	Liver Function Tests	LFTs
20.	Adverse Effects	AEs
21.	National Institute for Health and Clinical Excellence	NICE
22.	Drug Rash with Eosinophilia and Systemic Symptoms	DRESS
23.	European Medicines Evaluation Agency	EMEA
24.	Renin-Angiotensin System	RAS
25.	Cyclooxygenase-2	COX 2
26.	Dithiothreitol	DTT
27.	High-Performance Liquid Chromatography	HPLC
28.	Dimethyl Sulfoxide	DMSO
29.	Nuclear Magnetic Resonance	NMR
30.	Infrared Spectroscopy	IR

31.	Mass Spectrometry	MS
32.	Thin Layer Chromatography	TLC
33.	ATP-Binding Cassette Sub-Family G	ABCG
34.	Ultraviolet	UV
35.	Molecular Operating Environment	MOE

CHAPTER 1

INTRODUCTION

The majority of the xanthine metabolizing organisms acquire a molybdopterin cofactor-containing enzyme that oxidizes xanthine to uric acid and transfers electrons to NAD+ (xanthine dehydrogenase) or oxygen (xanthine oxidase) (Hille *et al.*, 1998). Even though mammalian xanthine oxidase (XO) exists originally as a dehydrogenase form, but it can be easily converted to oxidase form either irreversibly or reversibly. XO is capable of oxidizing varieties of purines, pterines and aromatic heterocycles as well as aliphatic and aromatic aldehydes and hence plays an important role in the detoxification or activation of endogenous compounds and xenobiotics. Human beings have higher levels of uric acid because of a deficiency of the hepatic enzyme, uricases and a lower fractional excretion of uric acid. Higher levels of uric acid (hyperuricemia) not only leads to gout but also results in the development of hypertension, cardiovascular diseases, diabetes, obesity, cancer and hyperlipidaemia (Hediger *et al*., 2005). During the catalytic oxidative hydroxylation of purine substrates, XO generates superoxide anions and H_2O_2, which in the presence of chelated iron are converted into highly reactive hydroxyl radicals. These reactive oxygen species (ROS) are associated with pathological events including inflammation, metabolic disorders, cellular aging, reperfusion damage, atherosclerosis and carcinogenesis. ROS induce apoptosis or necrosis, induce or suppress the expression of many genes and activate cell signalling cascades (Neogi *et al*., 2012).

Allopurinol, a purine based xanthine oxidase inhibitors (XOI) approved by the FDA in 1966 for treatment of gout and remains a mainstay in the therapy of gout and hyperuricemia. One of the major concern in purine based XOI is that they are associated with life threatening hypersensitivity reactions, including Stevens-Johnson syndrome, toxic epidermal necrolysis (*Saka et al*., 2013), vacuities, nephrotoxicity and hepatotoxicity (Menon and Nair, 2013). Such hypersensitivity syndromes have been fatal in some cases. Non-purine based XOI are the recent development in this field and they are devoid of severe life threatening adverse effect unlike purine based XOI (Becker *et al*., 2013). Therefore, the non-purine based inhibition of XO may result in a broad spectrum therapeutic for gout, cancer, inflammation and oxidative damage.

CHAPTER 2

LITERATURE REVIEW

2.1 Xanthine Oxidase

2.1.1 Biology

Xanthine oxidase (XO; EC 1.1.3.22) and xanthine dehydrogenase (XDH) (EC 1.17.1.4) are interconvertible forms of the same enzyme, known as xanthine oxidoreductase (XOR). The enzymes are molybdopterin-containing flavoproteins that consist of two identical subunits of around 145 kDa (Pacher *et al*., 2006). XO was first isolated from bovine milk by Schardinger as aldehyde reductase in 1902 (Nishino *et al.*, 2008), but Dixon showed in 1926 (Dixon, 1926) that the enzyme was identical to the xanthine oxidizing enzyme reported by Hopkins in 1920 (Becker, 1983). Historically, xanthine oxidase (XO) and xanthine dehydrogenase (XDH) were considered to be distinct enzymes; the enzyme was isolated in its XO form, using oxygen as the electron acceptor, from mammalian sources such as cow's milk (Waud *et al.*, 1975), whereas it was always purified in its XDH form, with NAD+ as the preferred electron acceptor, from other species, such as chicken (Rajagopalan and Handler, 1967) or insects (Barrett and Davidson, 1975). However, it has become clear that XDH and XO are products of the same gene.

2.1.2 Structure

XO is a highly versatile enzyme that is widely distributed among different species from bacteria to man and within the various tissues of mammals. It is a member of group of enzymes known as molybdenum iron/sulphur flavin hydroxylases. Stirpe & Della Corte reported that the enzyme originally exists in its XDH form, but is readily converted to XO either irreversibly by proteolysis or reversibly by oxidation of Cys residues to form disulphide bridges (Corte and Stirpe, 1972; Stirpe and Corte, 1969). Structurally, XDH is divided into three major domains and two connecting loops (figure 2.1). The two monomers have symmetry related domains in the same colours, in lighter shades for the monomer on the left and in darker shades for the monomer on the right.

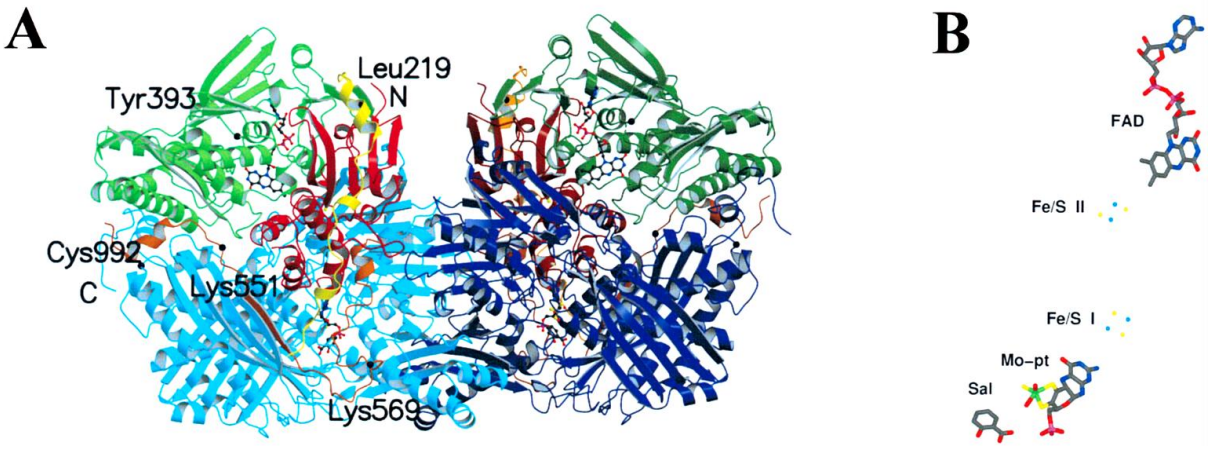

Figure 2.1: (A) Molecular structure of the XDH dimer, (B) Cofactors and salicylate in one subunit of XDH. (Enroth and Pai, 2000)

From N to C terminal, the present domains are: iron/sulphur centre domain (residues 3–165; red), FAD domain (residues 226–531; green), and Mo-Pt domain (residues 590–1,331; blue). The loop connecting the iron/sulphur domain with the FAD domain (residues 192–225) is shown in yellow, the one connecting the FAD domain with the Mo-Pt domain (residues 537–589) is in brown, and the N and C termini are labelled. The FAD cofactor, the two iron/sulphur canters, the molybdopterin cofactor, and the salicylate also are included. The positions of residues discussed in the text are indicated. (B) The arrangement of the cofactors and salicylate in one subunit of XDH are presented. The Mo ion is in green, the iron ions are in light blue, and the sulphur atoms in yellow.

2.1.3 Purine Metabolism

Physiologically, XO and XDH participate in a variety of biochemical reactions including the hydroxylation of various purines, pterins, and aromatic heterocycles, as well as aliphatic and aromatic aldehydes, thereby contributing to the detoxification or activation of endogenous compounds and xenobiotics. Inherited xanthine oxidase reductase (XOR) deficiency leads to xanthineuria and multiple organ failure syndrome caused by the accumulation of xanthine in different tissues. One of XOR's primary role is the conversion of hypoxanthine to xanthine and xanthine to uric acid (Pacher *et al.*, 2006) as depicted in figure 2.2.

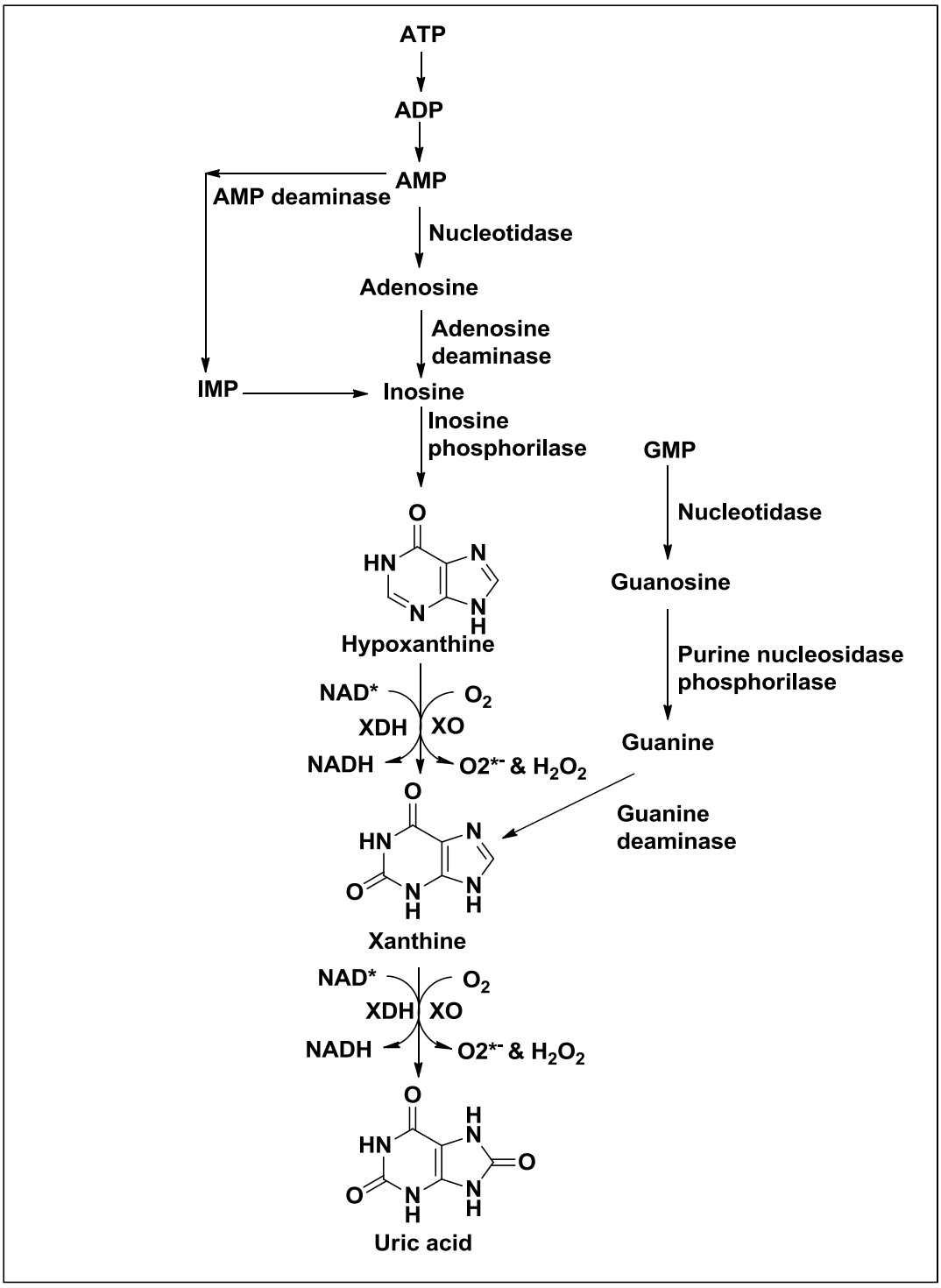

Figure 2.2: Pathway of purine metabolism (Pacher *et al.*, 2006).

2.1.4 Mechanism for XO

The process of XO catalysis is started by a base assisted nucleophilic attack by the equatorial Mo-OH on the C-8 carbon of xanthine with simultaneous hydride transfer from C-8 to Mo=S, which instantaneously results in reduction of Mo(VI) to Mo(IV). Re-oxidation of the molybdenum centre occurs by electron transfer to the other redox-active centres of the enzyme, accompanied by de-protonation (facilitated by a conserved glutamate residue, Glu 1261 of the enzyme) of the Mo-SH bond and displacement of bound product by hydroxide from solvent to regenerate the Mo-OH group (Pauff, 2009).

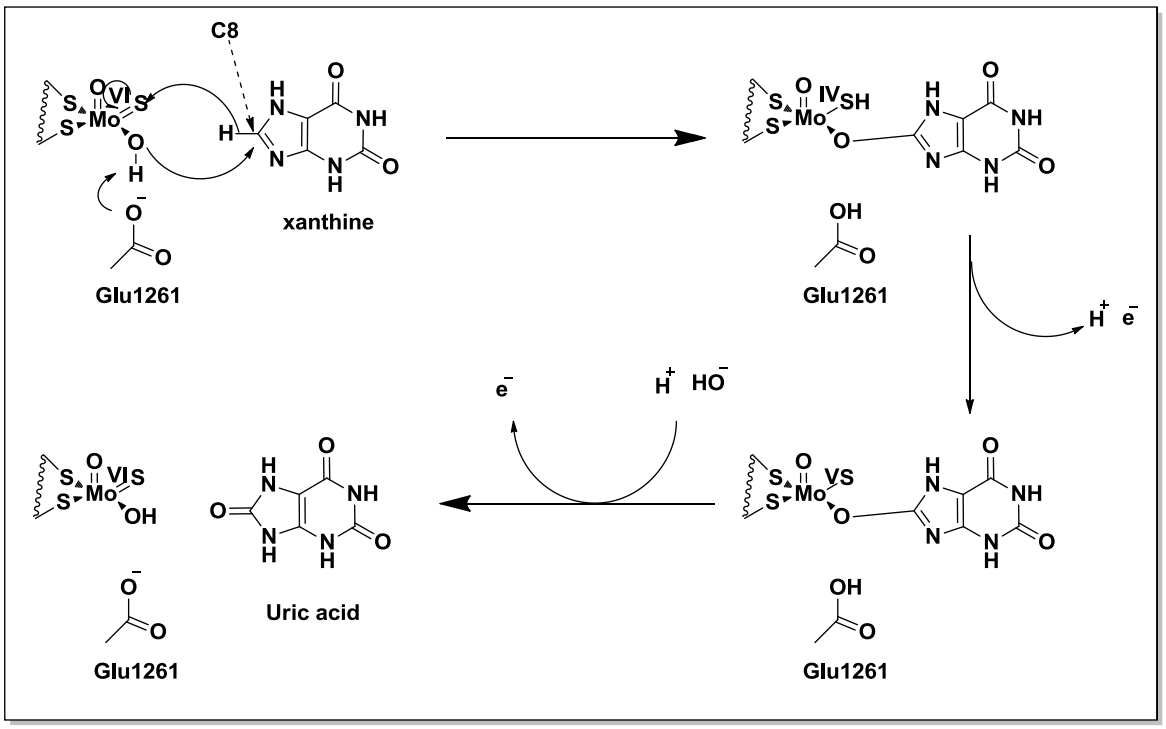

Figure 2.3: The reaction mechanism for xanthine oxidase (Pauff, 2009).

Allopurinol was the first mechanism-based inhibitor (figure 2.4) of the enzyme to be developed, and is still the primary drug for combating hyperuricemia. Allopurinol is hydroxylated by the enzyme to alloxanthine (oxypurinol), which, once formed, coordinates tightly to the reduced form of the molybdenum centre specifically replacing the Mo-OH group of native enzyme (Massey, 1970). Although allopurinol has longstanding use in pharmacotherapy and is efficacious in both lowering urate levels in the body and retarding the metabolism of chemotherapeutic agents such as 6-mercaptopurine, some individuals exhibit hypersensitivity to the drug; in particular, side effects such as vasculitis (especially in those with already

compromised renal function) may occur (Pacher *et al*., 2006). The development of alternative XOR inhibitors thus remains desirable. One such inhibitor developed and approved by FDA which contain non-purine moiety unlike allopurinol is the febuxostat (figure 2.4), (hydroxylated) inhibitor bound to the Mo centre and blocking access to the active site of the enzyme in a manner reminiscent of alloxanthine binding (Okamoto *et al*., 2003). In humans, the enzyme is the target of therapeutic drugs (figure 2.4) against hyperuricemia or gout (Umamaheswari, 2011).

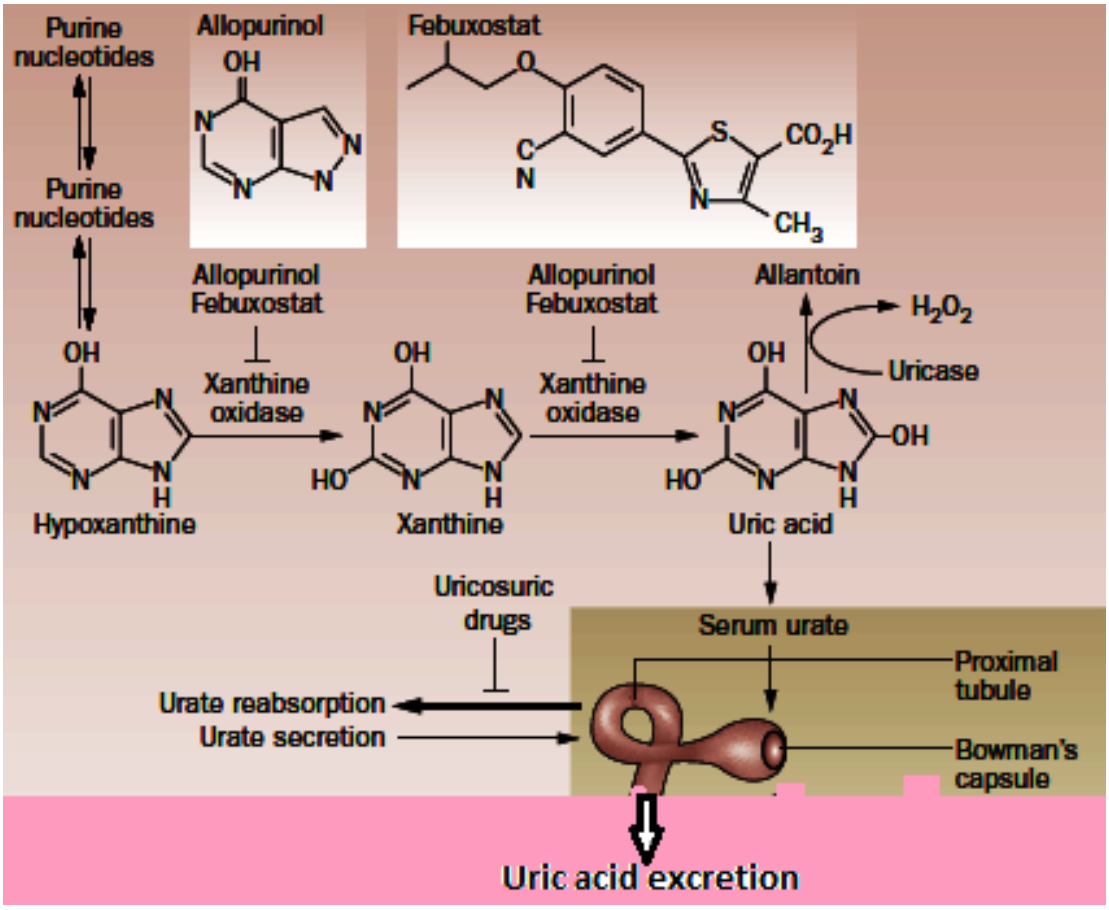

Figure 2.4: Therapeutic sites of actions of hyperuricemia. (Terkeltaub, 2010)

2.2 Therapeutic strategies for hyperuricemia

2.2.1 Anti-inflammatory agents

NSAIDs, steroids, colchicine and IL-1 inhibitors are evidence-based, cost-effective treatments for acute gout (Terkeltaub, 2009) that non-selectively inhibit pathways of the neutrophil-driven inflammation that is characteristic of acute gout. (Cronstein, 2006) NSAIDs are the most commonly used first-line treatment in an acute flare. However, each of these agents is associated with risks of potentially severe adverse effects and drug–drug interactions, particularly in elderly patients and those with

comorbidities such as chronic kidney diseases (CKD) or diabetes mellitus. (Terkeltaub, 2003) Selective inhibition of cyclooxygenase (COX)-2 was found to be fairly effective to NSAID therapy for acute gout, with significantly lesser adverse events. (Terkeltaub, 2010)

2.2.2 Uricosuric therapy

Uricosuric agents were first introduced at the end of the 19th century, they enhance renal clearance of urate (Nuki, 2006). They are used in <15% of gout patients. Uricosurics act primarily by inhibiting proximal renal tubule epithelial cell reabsorption of urate anion by inhibiting ATP binding cassette sub-family G (ABCG), glucose transporter (GLUT) and urate transporter 1 (URAT1) thereby enhancing renal uric acid excretion. They are contraindicated in urate nephropathy or history of acute nephrolithiasis (Richette, 2007). An increased fluid input and output is therefore recommended for all patients. The most available primary uricosuric, probenecid, requires more than once daily dosing and increases the risk of urolithiasis, particularly in acid urine (Rider, 2010). Benzbromarone is metabolized by cytochrome P450 and was withdrawn from widespread use because of serious hepatotoxicity. It has been estimated that the risk of hepatotoxicity is 1 : 17000 taking into account four published cases and 11 cases reported by Sanofi-Synthelabo (Paris, France) (Rider, 2010). All uricosurics also become less effective and ultimately ineffective with progressively lower glomerular filtration rate (Courtney, 2012).

Losartan, an angiotensin II receptor antagonist used for hypertension, and fenofibrate, a fibric acid derivative used in hyperlipidaemia, both have uricosuric actions and saturated uric acid (sUA). The uricosuric action is not a class effect for either drug or neither is licensed in treating gout (Rider, 2010). Losartan inhibits URAT-1, whereas fenofibrate can down-regulate the expression of the inducible COX-2 enzyme, but its exact mechanism is less well understood (Zafar, 2012). This effect of losartan and fenofibrate on sUA is particularly beneficial, given the frequent co-existence of hypertension and hyperlipidaemia with gout. Preferential use of these agents treating comorbidities of gout is recommended (Finney, 2013; Jordan *et al*., 2007). Together, these agents can decrease sUA by 40%; however, fractional UA clearance is increased by 110% and there is a risk of urolithiasis (Stamp, 2013).

2.2.3 Uricolytics

Humans unlike nearly all mammals have mutations in the genes encoding the enzyme uricase. The human uricase gene underwent two separate mutations that independently resulted in truncation of gene transcription. This decreased uricase function, but may have increased antioxidant activity, increased intelligence and improved the ability of humans to retain salt (Finney, 2013). The action of uricase converts urate to allantoin, which is 10 times more soluble and thus more readily excreted (Richette, 2007).

Rasburicase in 1996 was developed by recombinant DNA technique from a genetically modified strain of Saccharomyces cerevisiae. The efficacy of rasburicase in prevention and treatment of tumour lysis syndrome (TLS) has been well demonstrated despite its cost. However, allergenicity and development of antibodies compromise its effectiveness, the risk of which increases with repeated use (Malaguarnera, 2012).

Poly (ethylene) glycol (PEG) (Malik, 2010) – uricase differs from most PEGylated proteins currently in clinical use as it does not closely resemble any human amino acid sequence (Jordan, 2012). PEGylation forms a covalent link between a protein and PEG, and has the advantageous properties of prolonging half-life and decreasing antigenicity (Cammalleri, 2007). The mean termination half-life of PEG–uricase is 2 weeks compared with 19 h for rasburicase. PEG–uricase reduces or eliminates UA excretion, which is an attractive property benefiting patients with UA nephrolithiasis. The most common adverse effect (AE) of PEG–uricase is an acute flare and infusion reactions. Infusion-related events included nausea, vomiting, dizziness, respiratory symptoms, myalgias and rash, but not anaphylaxis. The results of on-going research contract trials (RCTs) are not yet available, but PEG–uricase is another potentially powerful agent for treating refractory gout in those who are unable to tolerate other treatments. PEG–uricase is effective in resolving tophi and could have a role in ‘debulking’ tophi in advanced gout before switching to another agent for maintenance treatment (Yang *et al*., 2012).

2.2.4 Xanthine Oxidase Inhibitors (XOI)

Xanthine oxidase inhibitors (XOI) are much useful, since they possess lesser side effects compared to uricosurics and anti-inflammatory agents (Umamaheswari, 2011). XO inhibitors are broadly classified on the basis of their structural similarities to the natural purines into purine analogues and non-purine analogues.

2.2.4.1 Purine analogues as XO inhibitors

Allopurinol (1,5-dihydro-4*H*-pyrazolo[3,4-*d*]pyrimidin-4-one), a purine analogue, was discovered by Burroughs Wellcome in 1940. Gertrude B. Elion and George H. Hitchings, shared 1988 Nobel Prize in Physiology and Medicine with British scientist James W. Black, for “discoveries of important principles for drug treatment”. Allopurinol was the first XO inhibitor approved by the FDA in 1966 for the treatment of gout and remains a keystone in the therapy of primary and secondary hyperuricemia. Allopurinol acts as a suicide inhibitor of XO and is rapidly oxidized *in-vivo* to its active metabolite oxypurinol which inhibits XO by binding to the molybdenum via covalent linkage (Kumar, 2011). Nagamatsu et al. reported 2-substituted 7*H*-pyrazolo [4,3-*e*]-1,2,4-triazolo-[1,5-*c*]-pyrimidines as more potent XO inhibitors than allopurinol (Ali, 2010; Nagamatsu, 2000). Some of the purine based XO inhibitors are presented in figure 2.5.

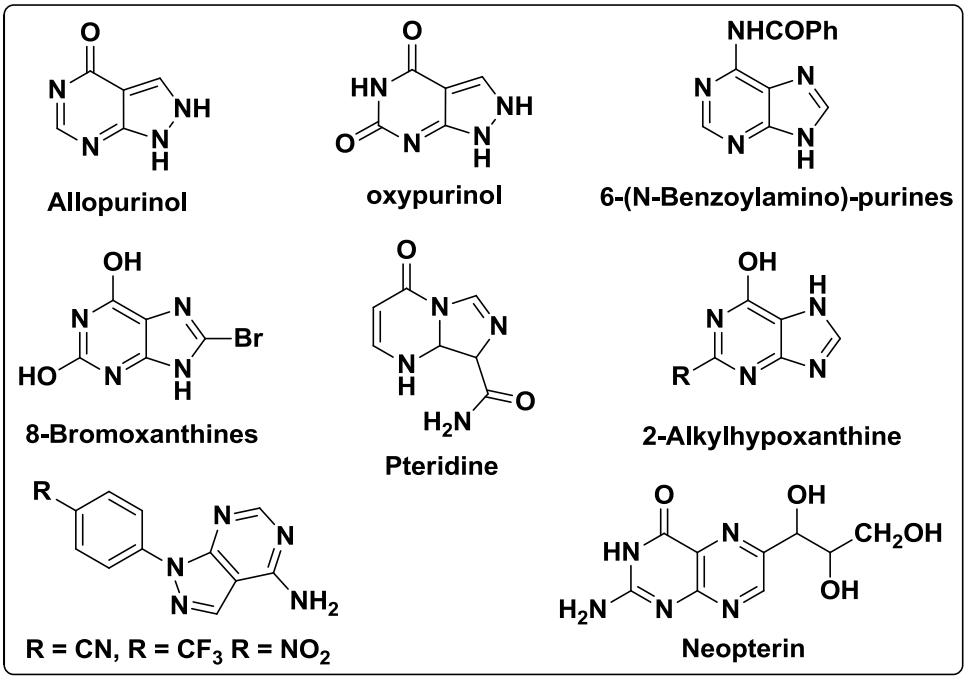

Figure 2.5: Purine analogues of xanthine oxidase inhibitors.

The significant effect of purine-like XO inhibitors on activities of purine and pyrimidine metabolism enzymes such as guanine deaminase, hypoxanthine-guanine phosphoribosyl transferase, purine nucleoside phosphorylase, orotate phosphoribosyl transferase and orotidine-5-monophosphate decarboxylase and the reported hypersensitivity syndrome characterized by fever, skin rash, hepatitis, leukocytosis with eosinophilia and worsening renal function induced in some of the patients by allopurinol use led to the search for XO inhibitors with structurally diverse and novel non-purine isosteres discussed in the next section.

2.2.4.2 Non-purine XO inhibitors

These can be of natural origin and those derived synthetically.

2.2.4.2.1 Natural origin

Shu-Mei Lin et al. isolated 5-hydroxymethylfurfural and 1-methyl-1,2,3,4-tetrahydro-β-carboline-3-carboxylic acid (MTCA) from vinegar possessing potent xo inhibitory activity (Lin, *et al*., 2012). Flavonoids are found to possess very good XO inhibitory activity. Among them apigenin was found to be most active. Quercetin, myricetin and genistein also exhibited good competitive inhibition. Naringenin showed no activity at all which shows that planar structure is necessary for the activity (Lin *et al*., 2002). For a high XO inhibitory activity, a flavonoid compound should possess a small size, high hydrophobic character and a value for torsion angle formed by C3-C2-C1-C2 atoms around 26 - 27 C (Da Silva, 2004). Coumarin derivatives was also reported to have good XO inhibitor activity, especially esculetin and 4-methylesculetin. These have hydroxyl group at -6 and -7 positions (Ferrari, 2007). Phytic acid is a highly phosphorylated molecule abundant in edible legumes, cereals and oil seeds, was reported to have XO inhibitory activity (Muraoka, 2004).

Lithospermic acid (LSA) isolated from roots of Salvia mitiorrhiza, was found to inhibit formation of uric acid and superoxide radicals and exhibited competitive inhibition of XO. LSA have hypouricemic activity on potassium oxonate pre-treated rats *in vivo* and had anti-inflammatory effects in a model of gouty arthritis (Chen *et al*., 2009). Noro *et al*., reported the identification and isolation of a strong *in vitro* uncompetitive XO inhibitor from *Athyrium mesosorum* (Aspidiaceae), which was identified as norathyriol (1,3,6,7-tetrahydroxyxanthone, (Kumar, 2011). Shen and Ji observed by

molecular docking simulations that degradation products of curcumin, vanillin showed good XO inhibitory activity (Kumar, 2011). Tan and co-workers isolated ethanolic extract of Palhinhaea cernua club moss which is in use from several centuries as a traditional Chinese medicine to treat rheumatism. They isolated a new apigenin derivative which showed good XO inhibitory activity (Jiao, 2006). Wang et al. confirmed that essential oil from leaves of Cinnamomum osmophloeum, possess strong XO inhibitory activity, which was attributed to cinnamaldehyde present as the main constituent (Wang *et al*., 2008). Polyhydroxylated and polymethoxylated flavones was reported as XO inhibitory activity. Flavones act as donors in their interaction with the enzyme. Anionic forms having hydroxyl group at C7, C5 and carbonyl at C4 contribute favourable hydrogen bonds and electrostatic interactions between inhibitors and the active site (Costantino, 1996).

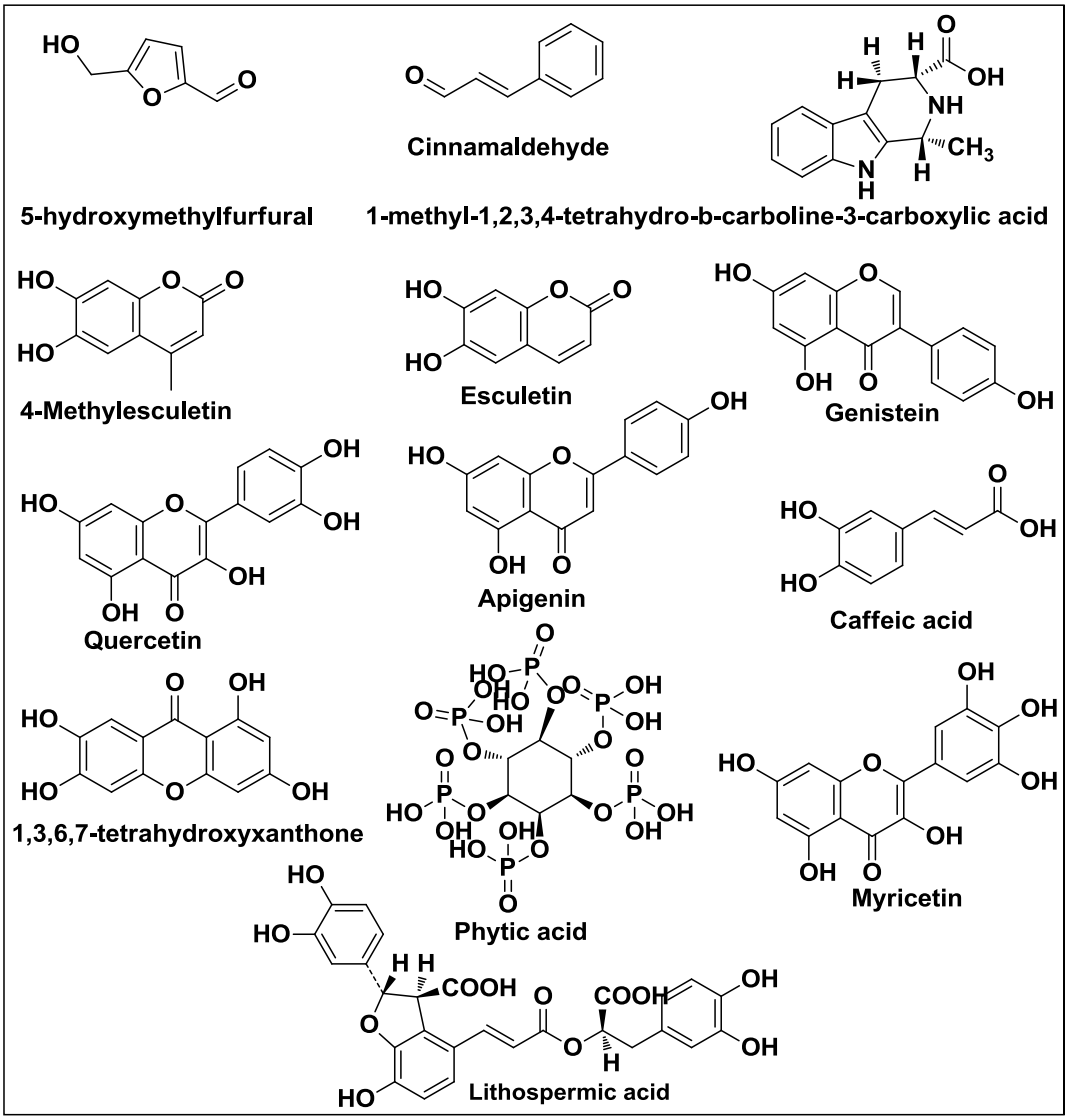

Figure 2.6: Naturally occurring xanthine oxidase inhibitors.

2.2.4.2.2 Synthetic XO inhibitors

Andrija Smelcerovi *et al.* recently synthesized 3-(2-methylpropyl)-6-(propan-2-yl)-4-methyl-morpholine-2,5-dione and 3,6-di(propan-2-yl)-4-methyl-morpholine-2,5-dione a non-purine XOI and evaluated for XO inhibitory activity (Smelcerovic, 2013). Teijin developed Febuxostat (2-[3-cyano- 4-(2-methylpropoxy)-phenyl]-4-methylthiazole-5-carboxylic acid) (TEI-6720; TMX-67). Kumar *et al.*, drug discovery, 1-acetyl-3,5-diaryl-4,5-dihydro(1*H*)pyrazoles was reported as non-purine XO inhibitors and some of them were found to be significantly potent. A structure activity relationship study revealed that nature of two aromatic rings and substituent(s) on these rings greatly affect the XO inhibitory activity. Heteroaryls, in particular such as furan or pyridine, and an *N*-acetyl group was found to be critical for the higher XO inhibitory activity (Nepali, 2011). Ishibuchi et al. synthesized a series of 1-phenylpyrazoles and screened for XO inhibitor activity (Ishibuchi, 2001). Y-700 was found to be most potent. It inhibited XO by obstructing the access of substrate to the active site, a completely different mechanism of inhibition than allopurinol. Similar to febuxostat and Y-700, 5-phenylisoxazole-3-carboxylic acid derivatives was synthesized and screened for XO inhibitory activity by Wang et al. They reported that presence of cyano group at 3-position of the phenyl moiety and isobutoxy group at 4-position plays a significant role in activity and found such compounds to be more potent in the series (Wang *et al*., 2010). Recently, dipyridine triazoles especially FYX-051 are reported to have potent and specific XO inhibitory activity (Okamoto *et al*., 2004).

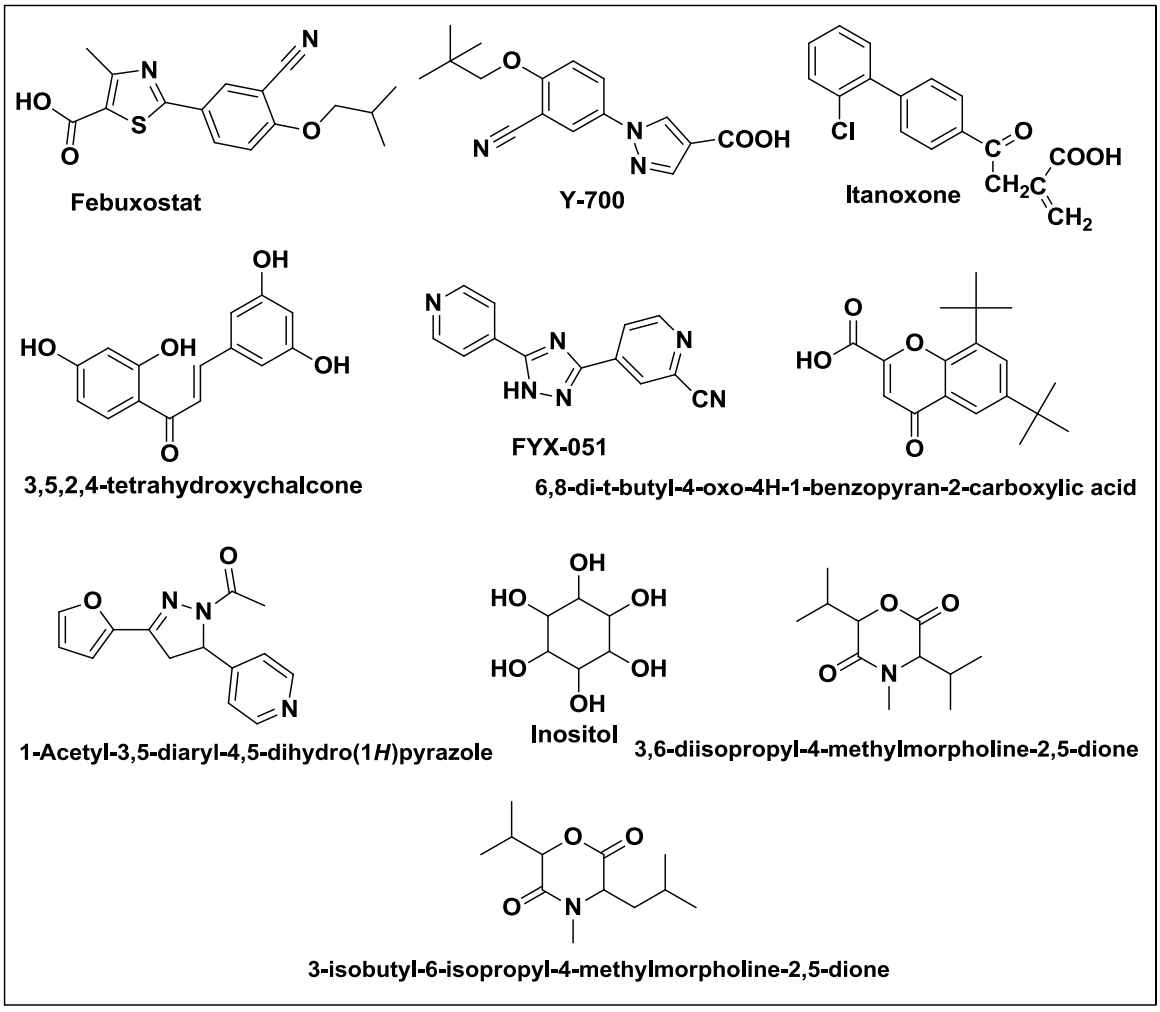

Figure 2.7: Non-purine analogues of xanthine oxidase inhibitors.

2.2.4.3 Non-purine analogues Vs. Purine analogues

Febuxostat binds and inhibits XO independent of the redox state of the enzyme and as such does not induce unwanted ROS formation as in case with allopurinol which gets oxidized to oxypurinol. Oxypurinol requires the Mo-cofactor to be reduced in order for it to bind and inhibit and as such these reducing equivalents must be derived by allopurinol or by substrate. Febuxostat is extensively metabolized by conjugation via uridine diphosphate glucuronosyltransferase and to lesser extent by the cytochrome P450 system. Dose reduction in not required in moderate renal (or hepatic) impairment (Schumacher, 2009). Additionally, it does not interact with warfarin and a safe alternative in patients with allopurinol allergy. Febuxostat is well tolerated, the most common side effects being abnormal liver function tests (LFTs), diarrhoea, joint-related/musculoskeletal/connective tissue symptoms, flushing, dizziness, confusion, myalgia and tachycardia (Schumacher, 2009).

Allopurinol has been the mainstay of chronic treatment and accounts for 90% of uric acid lowering therapy (ULT) (Annemans, 2008; Roddy, 2007). It should be commenced at 100 mg daily and increased by 100 mg every 1 – 2 weeks. (Zhang, 2006). In the UK, however, 97.9 % of patients receive allopurinol doses of 4300 mg/day, which could indicate sub-optimal dosing. One-third on this dose still experiences flares and 23% of those have sUA > 0.36 mmol/l (Annemans, 2008). AEs of allopurinol include life-threatening hypersensitivity reaction, bone-marrow suppression, rash (2%), eosinophilia, hepatitis and decreased renal function (Bruce, 2006). Allopurinol requires reduced dosing in renal impairment, this being its route of excretion. Oxypurinol, the active metabolite of allopurinol, is an alternative in allopurinol allergy, but there is a 40% chance of cross reactivity (Fam, 2005).

A Phase 2 trial demonstrated the efficacy of febuxostat with 56, 76 and 94% of patients achieving sUA < 6 mg/dL within 28 days on 40, 80 and 120 mg, respectively (Schumacher, 2009). A Phase 3 trial compared febuxostat 80 and 120 mg with allopurinol 300 mg for 52 weeks with the same sUA target (Becker *et al*.,2005). The largest reduction in sUA was achieved in those receiving febuxostat 120 mg; however, more patients in this group discontinued treatment. The primary end point was reached in 53% of the patients on 80 mg, 62% on 120 mg of febuxostat and only 21% in those receiving allopurinol. It is difficult to make a direct comparison on the efficacy of febuxostat in comparison with allopurinol due to the doses used. Results from a 5 year febuxostat trial are available, providing longer term safety and efficacy results (Schumacher, 2009). At 5 years, 93% of the patients achieved the target of sUA < 6.0 mg/dL with daily doses between 40 and 120 mg. Twenty-two per cent had palpable tophi and the majority resolved. Efficacy in renal impairment was well-known with no significant relationship between renal function and urate-lowering efficacy found. The most common adverse effect leading to withdrawal from the study was reversible LFT derangement. However, the exclusion criteria of not prescribing in subjects consuming over 14 alcoholic drinks a week must be noted. The most frequently encountered serious AE was atrial fibrillation, but this was not attributed to febuxostat. In December 2008 NICE ruled that febuxostat 80mg could be used in patients intolerant of or with contraindications to allopurinol (http://www.nice.org.uk/ Guidance/TA164).

2.3 Clinical challenges

XO over activity results in deposition of urate crystals which initiates an inflammatory reaction at the joints that includes swelling, redness and pain, the hallmark of inflammation (Rodnan, 1982). As an attempt several purine analogues such as 2-substituted 7*H*-pyrazolo [4,3-*e*]-1,2,4-triazolo-[1,5-*c*]-pyrimidines, 6-(*N*-Benzoylamino)-purines, 2-alkylhypoxanthine, 8-bromoxanthines, neopterine, pteridine was reported as potent XO inhibitors. Purine analogue are useful as drug for inhibiting XO activity. Use of allopurinol however is associated with adverse effects that include allergy, hypersensitivity reactions, gastrointestinal upset, skin rashes and acute interstitial nephritis due to lack of free radical scavenging activity against superoxide anions produced. A large amount of superoxide anion generation by XO has been involved in the pathogenesis of inflammation, mutagenesis, cancer, aging and ischemic reperfusion injury (Halliwell, 1992). Therefore XO inhibitors along with free radical scavengers may prove to be promising agents to treat gout and hyperuricemia conditions and associated side effects. Therefore there is a need for the development of novel compounds with better safety profiles that could be used to relieve associated side effects. Synthetic pyrazolo-pyrimidine derivatives are well known for their pharmacological activities including antitumor, antipyretic, anticancer, antioxidant, anti-inflammatory and XO inhibitory activity (Youssef and Abd-El-Aziz, 2010). Therefore extensive research has been done to report non purine analogues for XO inhibition. Recently one of the non-purine inhibitor, Febuxostat that was approved by the European Medicines Evaluation Agency (EMEA) and Food and Drug Administration (FDA), has attracted worldwide attention (Komoriya, 1993). Our research group has recently reviewed a literature survey on patent analysis on various XOI (Kumar, 2011). Our research group recently also reported synthesis of *N*-(1,3-Diaryl-3-oxopropyl) amides and 1-acetyl-3,5-diaryl-4,5-di-hydrol(1*H*) pyrazoles as a new template for xanthine oxidase inhibition. FYX-051 reported by Takahiro Sato et al. is currently being evaluated in phase-II clinical trial. Y-700 *N*-aryl-5-amino-4-cyanopyrazole, flavonoids, and curcumin also reported to be potent xanthine oxidase inhibitor.

2.4 Clinical significance

Hyperuricemia is a condition of defective purine metabolism characterized by elevated serum uric acid level (7 mg/dL). Normal uric acid levels are 2.4-6.0 mg/dL (female) and 3.4-7.0 mg/dL (male). Hyperuricemia occur either because of decreased renal clearance of uric acid, XO over activity, or a combination of the two mechanisms. Renal impairment accounts for the majority of cases while XO over activity accounts for only a minority of patients presenting with hyperuricemia. Hyperuricemia can be a marker of increased xanthine oxidase (XO) activity, renal dysfunction, or the presence of an inflammatory reaction. However, uric acid per se plays a key role in the development of renal micro vascular disease, inflammation, and activation of RAS and COX-2, which in turn aggravates renal disease and hypertension and induces endothelial dysfunction and cardiovascular disease. Again, these events further increase the uric acid level by increased XO activity decreased renal excretion, or inflammation, making a vicious cycle and complex interrelationship (figure 2.8), which make the initiating event indistinct**.** (Kang, 2005)

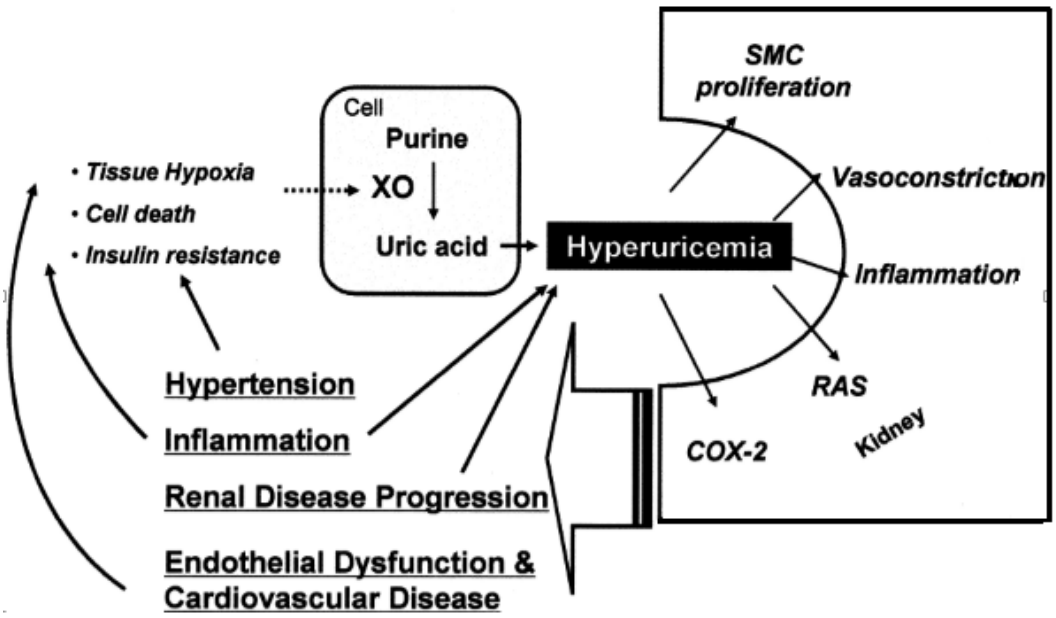

Figure 2.8: Inter-relationship between hyperuricemia and related medical condition (Kang, 2005)

2.4.1 Gout

Gout is one of the most common metabolic disorders with a worldwide distribution and continues to be a major health problem. The first evidence that gout is associated with increased levels of uric acid in the blood was confirmed by Sir Alfred Garrod in the 1800. Excessive serum accumulation of uric acid in the blood leads to gout (Heinig, 2006). The gout is the result of deposition of needle-like crystals of uric acid in joints, capillaries, skin and tissues. Kidney stones also develop through the process of formation and deposition of sodium urate microcrystals (Miner, 2013).

A study found that men who drank two or more sugar-sweetened drinks a day have an 85% higher chance of developing gout than those who drank such beverages infrequently (Malik, 2010). Gout can occur where serum uric acid levels are as low as 6 mg/dL (~357 µmol/L), but an individual can have serum values as high as 9.6 mg/dL (~565 µmol/L) and have no gout (Tausche, 2006). It is characterized by an excessive concentration of uric acid in the blood, causing the accumulation of monosodium urate crystals in the joints and kidneys leading to acute gouty arthritis, tophi of the joints and extremities and uric acid nephrolithiasis. (Harrold, 2009) Approximately two thirds of total body urate is produced endogenously, while the remaining one third is accounted for by dietary purines. Approximately 70% of the urate produced daily is excreted by the kidneys, while the rest is eliminated by the intestines (Punzi, 2013).

2.4.2 Lesch-Nyhan syndrome

Lesch-Nyhan syndrome, an extremely rare inherited disorder, is associated with very high XO activity thus serum uric acid levels. Spasticity, involuntary movement and cognitive retardation as well as manifestations of gout are seen in cases of this syndrome (Nyhan, 2005).

2.4.3 Cardiovascular disease

Although uric acid can act as an antioxidant, excess serum accumulation is often associated with cardiovascular disease. It is not known whether this is causative (e.g., by acting as a prooxidant) or a protective reaction taking advantage of urate's antioxidant properties. The same may account for the putative role of uric acid in the etiology of stroke (Grassi, 2012).

2.4.4 Type 2 diabetes

The association of XO over activity i.e., high serum uric acid with insulin resistance has been known since past, nevertheless, recognition of high serum uric acid as a risk factor for diabetes has been a matter of debate. In fact, hyperuricemia has always been presumed to be a consequence of insulin resistance rather than its precursor. However, a prospective follow-up study showed high serum uric acid is associated with higher risk of type 2 diabetes, independent of obesity, dyslipidaemia, and hypertension (Dehghan, 2008).

2.4.5 Metabolic syndrome

High XO activity is associated with metabolic syndrome. A study has suggested fructose-induced hyperuricemia play a pathogenic role in the metabolic syndrome. This is consistent with the increased consumption in recent decades of fructose-containing beverages (such as fruit juices and soft drinks sweetened with sugar and high-fructose corn syrup) and the epidemic of diabetes and obesity (Malik, 2010).

2.4.6 Uric acid stone formation

Saturated uric acid in blood result in kidney stones when the urate mono crystals crystallizes in the kidney. These uric acid stones are radiolucent and so do not appear on an abdominal plain X-ray, and thus their presence must be diagnosed by ultrasound for this reason. Very large stones may be detected on X-ray by their displacement of the surrounding kidney tissues.

Uric acid stones, which form in the absence of chronic diarrhoea, vigorous exercise, dehydration, and animal protein loading are felt to be secondary to obesity and insulin resistance seen in metabolic syndrome. Increased dietary acid leads to increased endogenous acid production in the liver and muscles, which in turn leads to an increased acid load to the kidneys. This load is handled more poorly because of renal fat infiltration and insulin resistance, which are felt to impair ammonia excretion (a buffer). The urine is therefore quite acidic, and uric acid becomes insoluble, crystallizes and stones form. This explains the high prevalence of uric stones and unusually acidic urine seen in patients with type 2 diabetes. Uric acid crystals is found to be responsible for the formation of calcium oxalate stones acting as "seed crystals" (Pak, 2008).

2.5 Methods for the Evaluation of XOI Activity

Evaluation of XOR activity, usually measures the products of the metabolism of hypoxanthine to xanthine and xanthine to uric acid, as well as the production of superoxide radical, hydrogen peroxide or NADH.

2.5.1 Spectrophotometric measurement of uric acid or NADH production

XO activity can be assayed spectrophotometrically by measuring the production of uric acid, at 290 nm using xanthine or hypoxanthine as the substrate, as air-saturated conditions, at room temperature. XDH activity is measured at the same conditions as XO, but in the presence of NAD+. In this case the formation of NADH can be monitored at 340 nm (Rogers *et al*., 2013).

2.5.2 Ex-vivo measurement of XO and XDH

When the activity of XO and XDH is measured ex-vivo, the samples must be pre-treated in order to avoid the inter-conversion of these two forms and to prevent their inhibition by endogenous compounds. Thus, tissue samples can be treated with phenylmethylsulfonyl fluoride and dithiothreitol, which prevent the conversion of XDH to XO via proteases and sulphahydryl oxidation, respectively. Homogenates and the supernatants are passed through a Sephadex G-25 column to eliminate DTT and endogenous interactions of XO and XDH activity. Enzyme activities are then measured as above mentioned. The quantification of uric acid and its precursors can also be performed by HPLC, a useful methodology when the absolute and/or relative quantities of these compounds need to be measured e.g. in ischemia/reperfusion studies (Villamena, 2013).

2.5.3 Fluorometric measurement of isoxanthopterin production

Activities of XDH and XO can be assayed by fluorimetry, using the oxidation of pterin to isoxanthopterin as a measure of enzyme activity. Excitation is set at 345 nm and emission at 390 nm. The rate of pterin oxidation is measured at the absence and presence of the electron acceptor methylene blue to evaluate the activities of XO and XO plus XDH, respectively (Li, 2013).

2.5.4 Detection of XO induced O_2 - production by the cytochrome c assay

The production of O_2 - can be detected in intact cells using the ferric form of cytochrome C. cells are incubated with Fe^{3+}-cyto c and absorbance is measured at 550nm (Gatto Jr, 2013).

2.5.5 Detection of XO induced H_2O_2 production

During hydroxylation by XO the reduced flavin reacts with dioxygen to form either H_2O_2 or superoxide radical, depending on the overall level of enzyme reduction. Thus XO activity can be measured by the quantification of H_2O_2 formed (Kim, 2013).

2.5.6 Measurement of oxygen consumption

Xanthine/XO reactions have also been studied by continuous time measurements of oxygen consumption using a selective electrode (Rehman, 2013).

CHAPTER 3

RATIONALE OF THE PROJECT

The rationale for the synthesis of non-purine based XO inhibitors includes the following considerations.

1. Purine analogues like allopurinol are associated with very severe and acute side effects like hypersensitivity syndrome, bone marrow depression, aplastic anaemia, Stevens–Johnson syndrome; toxic epidermal necrosis etc. and some of them are even fatal.
2. As many non-purine chemical moieties from natural sources and synthetic literature (Shieh, 2000) are shown to have good xanthine oxidase inhibitory activity which makes it clear that purine nucleus is not an obligatory to find good XO inhibitors.
3. The introduction of some substituted group at N-1 position in pyrazolol [3, 4-d]pyrimidines would exclude the possibility of these compounds being converted, like allopurinol to some other compounds. This was also proved to some extent by high xanthine oxidase inhibitory activity of currently synthesized molecule like Y-700 (1-phenylpyrazole).
4. 5-phenylisoxazole-3-carboxylic acid derivative was reported recently to have potent xanthine oxidase inhibitory activity.
5. Recently reported compound FYX-051 has shown potent and specific activity against XO.

The above points encouraged us to formulate our objectives to synthesize the non-purine based compounds for the inhibitory activity against xanthine oxidase.

CHAPTER 4

OBJECTIVES

With this literature background we set the following objectives:

1) To design and synthesize the compounds pertaining to Formula 1 and Formula 2;

Formula 1

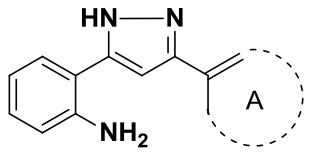

Ring A may be any aryl ring

Formula 2
(R = H or aryl)

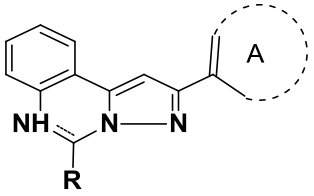

Ring A may be any aryl ring

2) To evaluate the synthesized compounds for their *in vitro* biochemical screening for xanthine oxidase enzyme.

CHAPTER 5

MATERIAL AND METHODS

5.1 Synthesis

5.1.1 General

1. All the reagents were of AR/GR quality and were purchased from Sigma-Aldrich, Loba-Chemie Pt. Ltd., S.D.F.C.L., Sisco Research Laboratory and HiMedia Laboratories Ltd. and were used without further purification.
2. Sartorius analytical balance (BSA224S-CW) was used for the weighing purposes. JSGW heating mantle, Tarson spinot digital, ILMVAC ROdist digital rota vapour, digital hop top and NSW oven/vacuum oven were used during the course of reaction.
3. The progress of the reactions were monitored by TLC, using hexane/ethyl acetate and chloroform/methanol as the mobile phase on pre-coated Merck TLC plates in JSGW UV/fluorescent analysis cabinet and/or iodine chamber.
4. Melting points were recorded on Stuart melting point apparatus (SMP-30) with open glass capillary tubed and was uncorrected.
5. Infrared (IR) spectra of compounds were recorded with KBr on a Bruker FT-IR spectrophotometer.
6. The UV spectra were recorded on a Shimadzu double-beam UV-Visible spectrophotometer in methanol or chloroform.
7. ^{1}H and ^{13}C Nuclear magnetic resonance (NMR) spectra were obtained in $CDCl_3$/d6-DMSO on a Bruker Avance II (400 MHz) NMR spectrometer using TMS ($\delta = 0$) as internal standard.

5.1.2 Synthesis of 3-(2-nitrophenyl)-1-arylprop-2-en-1-one (DK-1)

A mixture of 2-nitrobenzaldehyde (4 g, 26.50 mmol) and aryl ketone (3.18g, 26.50 mmol) in glacial acetic acid (10 mL) (q.s.) was stirred in 100 mL round bottomed flask (RBF). Conc. Sulphuric acid (4-5 drops) was added to the reaction mixture in ice cold condition and further stirred at RT for 24 h. After the completion of the reaction (TLC), the reaction mixture was poured on ice cold water and filtered. The solid was washed with water and dried to afford the crude product. The crude product was recrystallized from methanol to get pure compound.

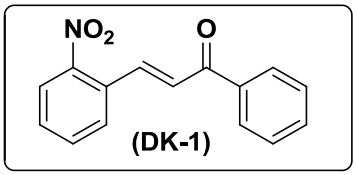

Yield: 85%, 5.69 g, Creamy white solid, MP: 85 - 90 °C

IR (KBr, cm^{-1}): 1666 (C=O), 1610 (C=C), 1510 (N=O), 1342 (N=O)

^{1}H NMR ($CDCl_3$, 300 MHz, δ with TMS = 0): 8.12 (1H, d, *J* = 15.9 Hz), 8.02 (3H, bs), 7.69-7.74 (2H, m), 7.50 - 7.57 (4H, m), 7.34 (1H, d, *J* = 15.9 Hz)

^{13}C NMR ($CDCl_3$, 75 MHz, δ with TMS = 0): 190.22, 148.34, 140.03, 137.20, 133.56, 133.09, 131.08, 130.31, 129.13, 128.62, 126.97, 124.86

5.1.3 Synthesis of 1-(4-chlorophenyl)-3-(2-nitrophenyl)prop-2-en-1-one (DK-1E)

A mixture of 2-nitrobenzaldehyde (2 g, 13.24 mmol) and *p*-chloroacetophenone (2.04 g, 13.24 mmol) in glacial acetic acid (2 mL) (q.s.) was stirred in 50 mL RBF. Conc. Sulphuric acid (4-5 drops) was added to the reaction mixture in ice cold condition and further stirred at RT for 24 h. After the completion of the reaction (TLC), the reaction mixture was poured on ice cold water and filtered. The solid was washed with water and dried to afford the crude product. The crude product was recrystallized from methanol to get pure compound.

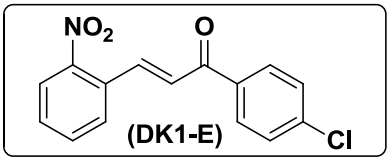

Yield: 78%, 2.97 g, Yellow solid, MP: 90 - 94 °C

IR (KBr, cm^{-1}): 1670 (C=O), 1610 (C=C), 1511 (N=O), 1341 (N=O), 750 (C-Cl)

5.1.4 Synthesis of 5-(2-nitrophenyl)-1-phenyl-4,5-dihydro-1*H*-pyrazole (DK-2)

A mixture of **DK-1** (3.3 g, 13.04 mmol) and hydrazine hydrate (0.63 mL, 13.04 mmol) was refluxed with methanol for 2 h. After completion of the reaction (TLC) pyrazole (**DK-2**) as the pure product was crystallised itself in the reaction mixture which was collected by decanting extra methanol from the reaction mixture and used for next step without further purification.

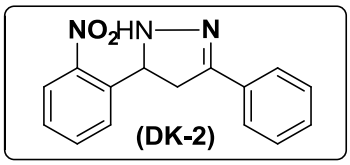

Yield: 97%, 3.2 g, Orange crystalline solid, MP: 140 – 145 °C

IR (KBr, cm^{-1}): 3310 (N-H), 1518 (N=O), 1333 (N=O), 1299 (C=N)

^{1}H NMR ($CDCl_3$, 400 MHz, δ with TMS=0): 7.96 (2H, t, *J* = 8.4 Hz), 7.65 (3H, m), 7.41 (4H, m), 6.05 (D_2O exchangeable NH, 1H, s), 5.42 (1H, t, *J* = 13.2 Hz), 3.80, (1H, q, *J* = 14.2 Hz), 3.01 (1H, q, *J* = 13.2 Hz)

3-(4-chlorophenyl)-5-(2-nitrophenyl)-4,5-dihydro-1*H*-pyrazole (DK-2E)

A mixture of **DK-1E** (1.5 g, 5.23 mmol) and hydrazine hydrate (0.63 mL, 5.23 mmol) was refluxed with methanol for 2 h. After completion of reaction (TLC) pyrazole (**DK-2**) as the pure product was crystallised itself in the reaction mixture which was collected by decanting extra methanol from the reaction mixture and used for next step without further purification.

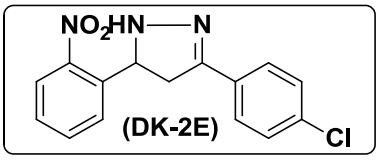

Yield: 97%, 1.46 g, Brownish solid, MP: 134 – 138 °C

IR (KBr, cm^{-1}): 3267 (N-H), 1520 (N=O), 1344 (N=O), 1213 (C-N), 747 (C-Cl)

5.1.5 Synthesis of 5-(2-nitrophenyl)-3-phenyl-1*H*-pyrazole (DK-2A)

DK-2 (3.1 g, 11.70 mmol) was refluxed with catalytic amount of molecular iodine in DMSO at 130 – 140 °C for 2 h. After the completion of reaction (TLC), the reaction mixture was poured in ice cold water; product was extracted using ethyl acetate. Organic layer was washed with brine (10 mL × 3), dried over sodium sulphate and was finally evaporated under reduced pressure using rotary evaporator to obtain the product which was used for next step without further purification.

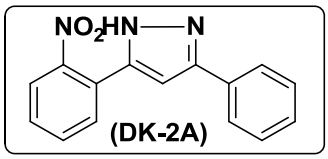

Yield: 92%, 2.85 g, Brownish colour solid, MP: 194 – 198 °C:

IR (KBr, cm^{-1}): 3456 (N-H), 1664 (C=N), 1524 & 1348 (N=O), 1217 (C-N)

^{1}H NMR ($CDCl_3$, 400 MHz, δ with TMS = 0): 7.67-7.76 (3H, m), 7.56-7.63 (3H. m), 7.33-7.51 (5H, m)

^{13}C NMR ($CDCl_3$, 100 MHz, δ with TMS=0): 149.02, 146.37, 146.16, 132.09, 130.97, 129.04, 128.74, 128.04, 126.47, 125.62, 124.56, 123.82, 102.59

5.1.6 Synthesis of 5-(2-nitrophenyl)-3-phenyl-1*H*-pyrazole (DK-2EA)

DK-2E (1.4 g, 4.65 mmol) was refluxed with catalytic amount of molecular iodine in DMSO at 130 – 140 °C for 2 h. After the completion of reaction (TLC), the reaction mixture was poured in ice cold water; product was extracted using ethyl acetate. Organic layer was washed with brine (10 mL × 3), dried over sodium sulphate and was finally evaporated under reduced pressure using rotary evaporator to obtain the product which was used for next step without further purification.

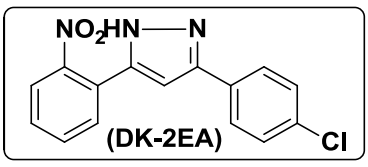

Yield: 92%, 1.28 g, Brownish colour solid, MP: 185 – 188 °C:

5.1.7 Synthesis of 2-(3-phenyl-1*H*-pyrazol-5-yl)aniline (DK-3)

DK-2A (2.75 g, 10.38 mmol) was dissolved in methanol and refluxed with 5-8 equivalent of stannous chloride dihydrate at 70 °C for 2 h. After the completion of the reaction (TLC), the methanol was evaporated under reduced pressure using rotary evaporator followed by neutralization of reaction mixture using 5% NaOH solution. Solid product was than extracted with ethyl acetate. Organic layer was washed with brine (10 mL × 3), dried over sodium sulphate and was finally evaporated under reduced pressure using rotary evaporator to obtain the product which was used for next step without further purification.

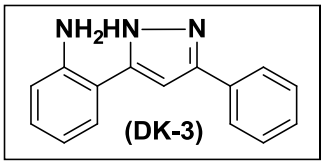

(DK-3)

Yield: 95%, 2.61 g, Yellow solid, MP: 165 – 166 °C.

IR (KBr, cm^{-1}): 3360 (N-H), 3285 (N-H), 1613 (C=N), 1579 (C=C), 1248 (C-N)

^{1}H NMR ($CDCl_3$, 400 MHz, δ with TMS = 0): 13.23 (D_2O exchangeable NH, 1H, bs), 7.81 (1H, s), 7.79 (1H, s), 7.31 - 7.54 (4H, m), 7.00 (2H, s), 6.75 (1H, d, *J* = 7.91 Hz), 6.61 (1H, t, *J* = 7.32 Hz), 6.22 (D_2O exchangeable NH_2, 2H, bs)

MS (ESI): m/z = 236.1 $[M+1]^+$

5.1.8 Synthesis of 2-(3-(4-chlorophenyl)-1*H*-pyrazol-5-yl)aniline (DKE-3)

DK-2EA (1.25 g, 4.17 mmol) was dissolved in methanol and refluxed with 5-8 equivalent of stannous chloride dihydrate at 70 °C for 2 h. After the completion of the reaction (TLC), the methanol was evaporated under reduced pressure using rotary evaporator followed by neutralization of reaction mixture using 5% NaOH solution. Solid product was than extracted with ethyl acetate. Organic layer was washed with brine (10 mL × 3), dried over sodium sulphate and was finally evaporated under reduced pressure using rotary evaporator to obtain the product which was used for next step without further purification.

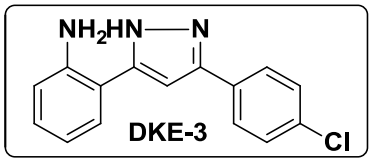

Yield: 95%, 1.21 g, Yellow solid, MP: 184 - 186 °C:

IR (KBr, cm^{-1}): 1614 (C=N), 1490 (C=C), 1215 (C-N), 748 (C-Cl)

^{1}H NMR ($CDCl_3$, 400 MHz, δ with TMS = 0): 13.2 (D_2O exchangeable NH, 1H, bs), 7.82 (2H, d, *J* = 8.3 Hz), 7.46 (2H, d, *J* = 8.3 Hz), 7.04 (2H, m), 6.68 - 6.81 (1H, m), 6.53 - 6.67 (2H, m)

5.1.9 Synthesis of 5-(2,5-dimethoxyphenyl)-2-phenyl-5,6-dihydropyrazolo [1,5-*c*]quinazoline (DK-3A)

A mixture of **DK-3** (100 mg, 0.425 mmol) and 2,5-dimethoxybenzaldehyde (70.64 mg, 0.425 mmol) dissolved in methanol and refluxed for 1h. After the completion of the reaction (TLC), the reaction mixture was left to cool. Precipitated solid was obtained when extra methanol was decanted and was crystallised from methanol.

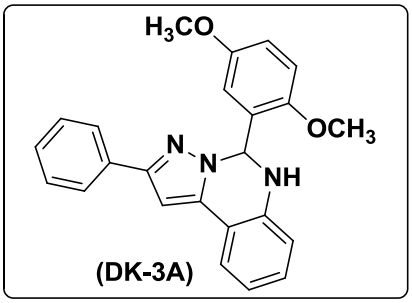

Yield: 80 %, 120 mg, Light yellow solid, MP: 230 – 232 °C

IR (KBr, cm^{-1}): 1644 (C=N), 1587 (C=C), 1220 (C-N), 1123 (C-O)

^{1}H NMR ($CDCl_3$, 400 MHz, δ with TMS = 0): 15.60 (D_2O exchangeable NH, 1H, bs), 8.76 (1H, d, *J* = 8.0 Hz), 8.37 (1H, d, *J* = 8 Hz), 8.04 (2H, m), 7.55 (2H, d, *J* = 8.0 Hz), 7.19 (5H, m), 7.11 (3H, m), 7.27 (1H, d, *J* = 8.27 Hz), 3.70 (3H, s), 3.28 (3H, s)

MS (ESI): m/z = 384 $[M+1]^+$

2-methoxy-4-(2-phenyl-5,6-dihydropyrazolo[1,5-*c*]quinazolin-5-yl)phenol (DK-3B)

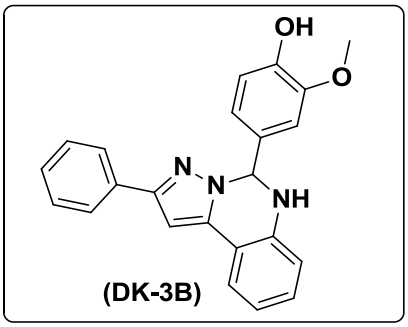

(DK-3B)

Yield: 98%, 143 mg, Light yellow solid, MP: 194 – 198 °C

IR (KBr, cm^{-1}): 3401 (OH), 3015 (C-H), 1673 (C=N), 1590 (C=C), 1216 (C-N)

^{1}H NMR ($CDCl_3$, 400 MHz, δ with TMS = 0): 8.97 (D_2O exchangeable NH, 1H, bs), 7.80 (2H, d, *J* = 1.16 Hz), 7.53 (1H, dd, *J* = 8.68 Hz), 7.37 (2H, m), 7.27 (1H, t, *J*=7.4 Hz), 7.22 (D_2O exchangeable OH, 1H, bs), 7.10 (1H, m), 7.03 (1H, s), 6.95 (1H, t, *J* = 3.32 Hz), 6.87 (1H, d, *J* = 7.97 Hz), 6.77 (1H, m), 6.68 (1H, d, *J* = 8.16 Hz), 6. 57 (2H, t, *J* = 6.24 Hz), 3.70 (3H, s)

^{13}C NMR ($CDCl_3$, 100 MHz, δ with TMS = 0): 150.47, 147.27, 146.73, 140.39, 138.25, 133.18, 131.65, 129.11, 128.37, 127.38, 125.09, 123.55, 118.72, 118.08, 114.92, 114.68, 112.83, 110.49, 96.17, 71.04, 55.44

MS (ESI): m/z = 370 $[M+1]^+$

2-methoxy-5-(2-phenyl-5,6-dihydropyrazolo[1,5-*c*]quinazolin-5-yl)phenol (DK-3C)

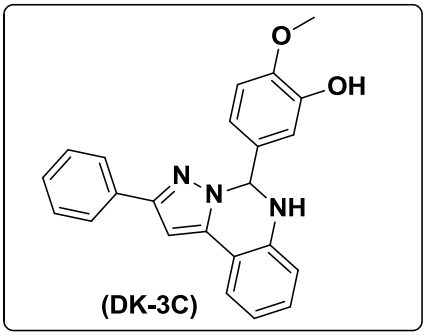

(DK-3C)

Yield: 82%, 119 mg, Yellow solid, MP: 115 – 120 °C

IR (KBr, cm^{-1}): 3384 (OH), 2929 (CH), 2852 (CH), 1617 (C=N), 1439 (C=C), 1130 (C-O), 1217 (C-N)

^{1}H NMR ($CDCl_3$, 400 MHz, δ with TMS = 0): 7.80 – 7.82 (2H, m), 7.52 (1H, d, *J* = 7.52 Hz), 7.35 – 7.39 (2H, m), 7.29 (1H, m), 7.12 – 7.16 (1H, m), 6.84 – 6.91 (3H, m), 6.70 – 6.79 (3H, m), 6.58 (1H, s), 3.82 (3H, s)

4-(2-phenyl-5,6-dihydropyrazolo[1,5-*c*]quinazolin-5-yl)phenol (DK-3E)

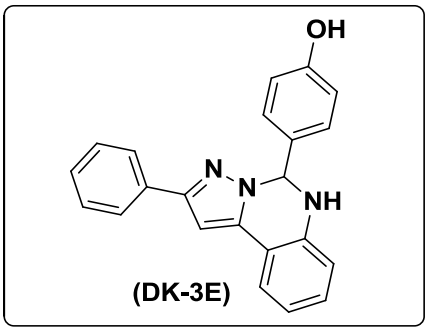

(DK-3E)

Yield: 86%, 124 mg, Brownish solid: MP: 215 – 218 °C

IR (KBr, cm^{-1}): 3387 (OH), 1612 (C=N), 1591 (C=C), 1233 (C-N), 1279 (C-O)

^{1}H NMR ($CDCl_3$, 400 MHz, δ with TMS = 0): 9.34 (D_2O exchangeable NH, 1H, bs), 7.79 (2H, m), 7.51 (1H, dd, *J* = 8.8 Hz), 7.37 (2H, t, *J* = 7.36 Hz), 7.27 (1H, t, *J* = 7.32 Hz), 7.18 (D_2O exchangeable OH,1H, s), 7.10 (3H, q, *J* = 8.6 Hz), 7.01 (1H, s), 6.85 (1H, d, *J* = 7.8 Hz), 6.76 (1H, m), 6.68 (2H, q, *J* = 7.32), 6.57 (1H, s)

5-(3,4-dimethoxyphenyl)-2-phenyl-5,6-dihydropyrazolo[1,5-*c*]quinazoline (DK-3F)

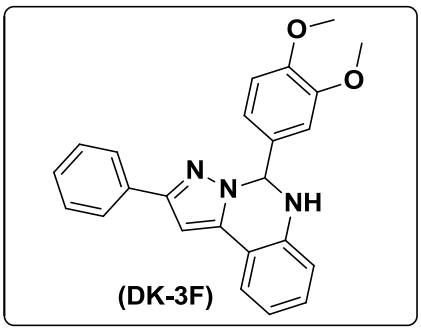

(DK-3F)

Yield: 96%, 145 mg, Yellowish solid, MP: 202 – 203 °C

IR (KBr, cm^{-1}): 3018 (C-H), 1612 (C=N), 1591 (C=C), 1260 (C-O), 1218 (C-N)

^{1}H NMR ($CDCl_3$, 400 MHz, δ with TMS = 0): 7.81 (2H, m), 7.52 (1H, m), 7.38 (2H, m), 7.25 - 7.30 (2H, m), 7.10 (1H, m), 7.00 (2H, m), 6.87 (1H, d, *J* = 7.6 Hz), 6.77 (2H, m), 6.67 (1H, m), 6.63 (1H, s), 3.73 (3H, s), 3.71 (3H, s)

5-(2-nitrophenyl)-2-phenyl-5,6-dihydropyrazolo[1,5-*c*]quinazoline (DK-3G)

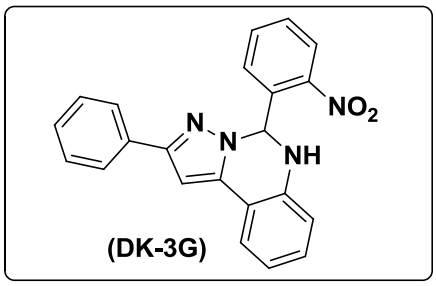

Yield: 98%, 153 mg, Orange solid, MP: 201 – 204 °C

IR (KBr, cm^{-1}): 3020 (CH), 1589 (C=N), 1531 (NO_2), 1346 (NO_2), 1215 (C-N)

^1H NMR ($CDCl_3$, 400 MHz, δ with TMS = 0): 8.13 (1H, m), 7.83 (1H, m), 7.59 (1H, m), 7.36 - 7.44 (6H, m), 7.31 - 7.35 (1H, m), 7.12 (1H, m), 6.97 (1H, s), 6.89 (1H, m), 6.67 (1H, m), 6.39 (1H, m)

5-(3-nitrophenyl)-2-phenyl-5,6-dihydropyrazolo[1,5-*c*]quinazoline (DK-3H)

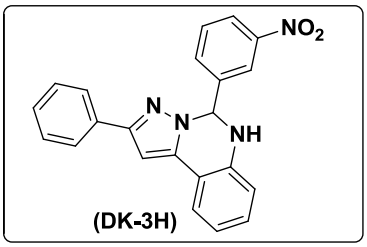

Yield: 97%, 151 mg, Orange solid, MP: 130 – 135 °C

IR (KBr, cm^{-1}): 3020 (CH), 1617 (C=N), 1534 (NO_2), 1351 (NO_2), 1214 (C-N)

^1H NMR ($CDCl_3$, 400 MHz, δ with TMS = 0): 8.27 (1H, t, *J* = 1.92 Hz), 8.15 - 8.17 (1H, m), 7.81 (2H, m), 7.61 (1H, d, *J* = 7.8 Hz), 7.56 (1H, m), 7.47 (1H, t, *J* = 7.96 Hz), 7.37 - 7.41 (2H, m), 7.29 - 7.33 (1H, m), 7.18 - 7.23 (1H, m), 6.96 (1H,s), 6.95 - 6.99 (1H, m), 6.90 (1H, s), 6.84 (1H, m), 6.79 (1H, s)

^{13}C NMR ($CDCl_3$, 100 MHz, δ with TMS = 0): 152.53, 148.43, 141.78, 138.60, 138.22, 132.94, 132.83, 129.88, 129.83, 128.68, 128.16, 125.82, 124.32, 123.98, 121.91, 120.94, 116.04, 114.60, 97.31, 71.04

MS (ESI): m/z = 369 $[M+1]^+$

2,4-dichloro-6-(2-phenyl-5,6-dihydropyrazolo[1,5-*c*]quinazolin-5-yl)phenol (DK-3I)

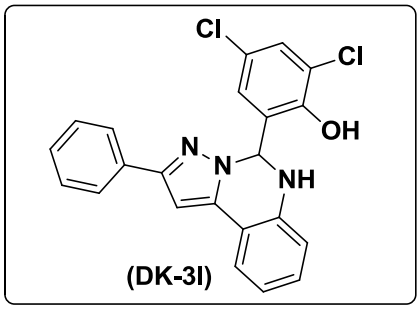

(DK-3I)

Yield: 86%, 149 mg, Creamy solid, MP: 208 – 210 °C

IR (KBr, cm^{-1}): 3300 (O-H), 1614 (C=N), 1584 (C=C), 1220 (C-N), 776 (C-Cl)

^{1}H NMR ($CDCl_3$, 400 MHz, δ with TMS = 0): 10.30 (D_2O exchangeable NH, 1H, bs), 7.81 (2H, d, *J* = 7.2 Hz), 7.59 (1H, m), 7.40 (2H, t, *J*=7.36 Hz), 7.29 - 7.35 (2H, m), 7.12 (3H, m), 7.03 (1H, s), 6.92 (1H, d, *J* = 7.96 Hz), 6.82 (1H, t, *J* = 7.24 Hz), 6.50 (1H, d, *J* = 2.53 Hz)

5-(3a,7a-dihydro-1*H*-indol-3-yl)-2-phenyl-5,6-dihydropyrazolo[1,5-*c*]quinazoline (DK-3J)

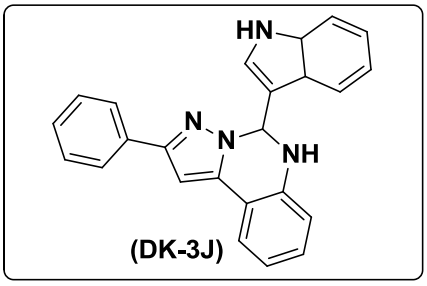

(DK-3J)

Yield: 90%, 139, mg, Creamy solid: MP: 204 – 206 °C

IR (KBr): 3394 (N-H), 1617 (C=N), 1558 (C=C), 1251 (C-N)

^{1}H NMR ($CDCl_3$, 400 MHz, δ with TMS = 0): 10.97 (D_2O exchangeable NH, 1H, bs), 7.76 (2H, d, *J* = 7.36 Hz), 7.62 (1H, d, *J* = 7.97 Hz), 7.55 (1H, d, *J* = 7.48 Hz), 7.35 (3H, t, *J* = 7.36 Hz), 7.25 (1H, t, *J* = 7.28 Hz), 7.00 - 7.16 (5H, m), 6.92 (3H, m), 6.78 (1H, t, *J* = 7.44 Hz)

^{13}C NMR ($CDCl_3$, 100 MHz, δ with TMS = 0): 150.03, 141.07, 138.08, 136.44, 133.30, 129.02, 128.30, 127.22, 125.00, 123.89, 123.51, 121.22, 119.53, 118.82, 117.87, 114.69, 114.59, 112.89, 111.42, 95.93, 66.39

MS (ESI): m/z = 363 $[M+1]^+$

4-(2-phenyl-5,6-dihydropyrazolo[1,5-*c*]quinazolin-5-yl)benzonitrile (DK-3P)

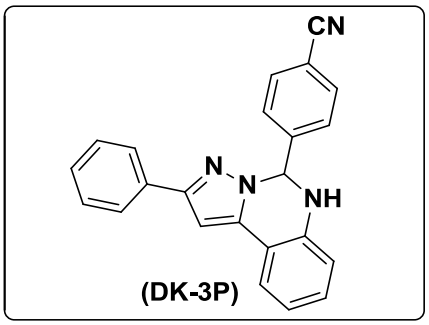

(DK-3P)

Yield: 65%, 96 mg, Off white solid: MP: 178 – 180 °C

IR (KBr, cm^{-1}): 3059 (C-H), 2229 (CN), 1613 (C=N), 1591 (C=C), 1219 (C-N)

^1H NMR ($CDCl_3$, 400 MHz, δ with TMS = 0): 9.34 (D_2O exchangeable NH, 1H, bs), 7.79 (2H, t), 7.51 (1H, q), 7.37 (2H, t), 7.27 (1H, t), 7.18 (1H, s), 7.10 (3H, q), 7.01 (1H, s), 6.85 (1H, d), 6.76 (1H, m), 6.68 (2H, q), 6.57 (1H, s)

5.1.10 Synthesis of 2-phenylpyrazolo[1,5-*c*]quinazoline (DK-3D)

A mixture of **DK3** (100 mg, 0.425 mmol) and triethyl orthoformate (63 mg, 0.425 mmol) was dissolved in acetonitrile and refluxed for 1 h. After the completion of the reaction (TLC), the reaction mixture was left to cool. Precipitated solid was obtained when extra acetonitrile was decanted and was crystallised from methanol.

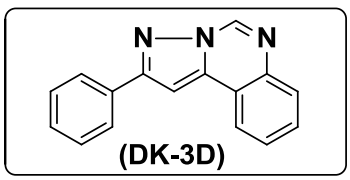

(DK-3D)

Yield: 95%, 99 mg, Creamy solid: MP: 145 – 150 °C:

IR (KBr, cm^{-1}): 3019 (CH), 1620 (C=N), 1539 (C=C), 1215 (C-N)

^{1}H NMR ($CDCl_3$, 400 MHz, δ with TMS = 0): 9.11 (1H, s), 8.00 - 8.06 (3H, m), 7.95 (1H, m), 7.58 - 7.68 (2H, m), 7.47 - 7.51 (2H, m), 7.41-7.45 (1H, m), 7.24 (1H, s)

^{13}C NMR ($CDCl_3$, 100 MHz, δ with TMS = 0): 155.95, 140.09, 139.72, 139.31, 132.15, 129.85, 129.32, 128.84, 128.75, 128.18, 126.73, 123.32, 119.99, 95.42

MS (ESI): m/z = 246 $[M+1]^+$

5.1.11 Synthesis of 2-(2-chlorophenyl)pyrazolo[1,5-*c*]quinazoline (DKE-3D)

A mixture of **DKE-3** (100 mg, 0.370 mmol) and triethyl orthoformate (54.81 mg, 0.370 mmol) was dissolved in acetonitrile and refluxed for 1h. After the completion of the reaction (TLC), the reaction mixture was left to cool. Precipitated solid was obtained when extra acetonitrile was decanted and was crystallised from methanol.

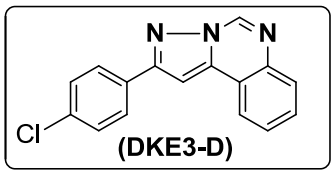

(DKE3-D)

Yield: 86%, 89 mg, Off white solid: MP: 200 – 205 °C

IR (KBr, cm^{-1}): 3019 (C-H), 1619 (C=N), 1477 (C=C), 1215 (C-N), 773 (C-Cl)

^{1}H NMR ($CDCl_3$, 400 MHz, δ with TMS = 0): 9.33 (1H, s), 8.23 – 8.26 (1H, m), 8.05 – 8.09 (2H, m), 7.90 – 7.93 (1H, m), 7.76 (1H, d, *J* = 0.6 Hz), 7.67 – 7.74 (2H, m), 7.53 – 7.57 (2H, m)

^{13}C NMR ($CDCl_3$, 100 MHz, δ with TMS = 0): 153.57, 139.50, 139.40, 139.13, 133.89, 130.66, 129.77, 128.82, 128.13, 128.09, 127.83, 123.49, 119.39, 95.95

5.1.12 Synthesis of 4-(2-(2-chlorophenyl)-5,6-dihydropyrazolo[1,5-*c*]quinazolin-5-yl)-2-methoxyphenol (DKE-3B)

A mixture of **DKE-3** (100 mg, 0.370 mmol) and 4-hydroxy-3-methoxybenzaldehyde (56.30 mg, 0.370 mmol) dissolved in methanol and refluxed for 1h. After completion of the reaction (TLC), the reaction mixture was left to cool. Precipitated solid was obtained when extra methanol was decanted and was crystallised from methanol.

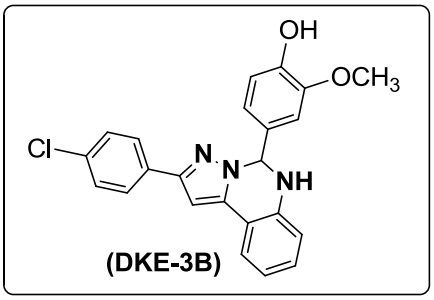

(DKE-3B)

Yield: 86%, 128 mg, Off white solid: MP: 195-198°C

IR (KBr, cm^{-1}): 3010 (C-H), 1616 (C=N), 1515 (C=C), 1218 (C-N), 744 (C-Cl)

4-(2-(2-chlorophenyl)-5,6-dihydropyrazolo[1,5-*c*]quinazolin-5-yl)phenol (DKE-3E)

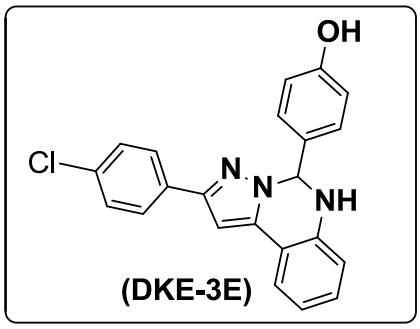

(DKE-3E)

Yield: 76%, 105 mg, Off white solid: MP: 230 – 235 °C

IR (KBr, cm^{-1}): 3302 (OH), 1615 (C=N), 1590 (C=C), 1247 (C-N), 748 (C-Cl)

^{1}H NMR ($CDCl_3$, 400 MHz, δ with TMS = 0): 9.38 (D_2O exchangeable NH, 1H, bs), 7.78 (2H, t, *J* = 6.8 Hz), 7.51 (1H, dd, *J* = 0.84 Hz), 7.41 (2H, m), 7.22 (D_2O exchangeable OH, 1H, bs), 7.08 (4H, m), 6.86 (1H, d, *J* =7.92 Hz) , 6.77 (1H, t, *J* = 7.53 Hz), 6.68 (2H, t, *J* = 6.4 Hz), 6.57 (1H, s)

^{13}C NMR ($CDCl_3$, 100 MHz, δ with TMS = 0): 157.60, 149.31, 140.43, 138.35, 132.13, 131.98, 129.21, 128.40, 127.51, 126.63, 123.58, 118.00, 114.91, 114.63, 96.31, 71.00

MS (ESI): m/z = 373 $[M+1]^+$

2-(2-chlorophenyl)-5-(3,4-dimethoxyphenyl)-5,6-dihydropyrazolo[1,5-*c*] quinazoline (DKE-3F)

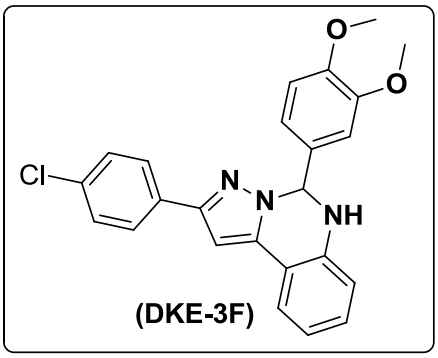

(DKE-3F)

Yield: 74%, 114.5 mg, Off white solid, MP: 140 – 145 °C

IR (KBr, cm^{-1}): 2925 (CH), 1598 (C=N), 1514 (C=C), 1215 (C-N)

^1H NMR ($CDCl_3$, 400 MHz, δ with TMS = 0): 9.86 (D_2O exchangeable NH, 1H, bs), 7.73 (1H, d, *J* = 8.56 Hz), 7.53 (1H, d, *J* = 8.64 Hz), 7.47 (1H, dd, *J* = 1.84 Hz), 7.42 (1H, d, *J* = 1.8 Hz), 7.29 - 7.34 (2H, m), 7.16 (1H, d, *J* = 6.6 Hz), 6.98 (1H, d, *J* = 8.16 Hz), 6.93 (1H, t, *J* = 1.52 Hz), 6.75 - 6.83 (5H, m), 6.56 (1H, s), 3.97 (3H, s), 3.95 (3H, s)

5.2 Biology

5.2.1 Chemicals

1. Xanthine oxidase enzyme as lyophilised powder was purchased from SRL Pt. Ltd. and stored at temperature below 4°C.
2. Allopurinol was purchased from SRL Pt. Ltd.
3. Potassium phosphate monobasic (KH_2PO_4) and dibasic (K_2HPO_4), DMSO of AR grade was purchased from Loba Chemie Pt. Ltd.
4. DMSO, extra pure AR was purchased from SRL.
5. Methanol was purchased from SDFCL.
6. H_2DCFDA (from Molecular Probes).

5.2.2 Instruments

1. Analytical balance (JB1603-c/FACT) and pH meter (Mettler Toledo) for the purpose of weighing and measuring the pH.
2. REMI laboratory refrigerator and ice flaking machine (MSW-136) by Macro scientific works was used for storing solutions.
3. Double-beam UV-Visible spectrophotometer (Shimadzu) for measuring absorbance.
4. TARSONS micropipette (0.5 µL -1000 µL) was used with different micro tip.

5.2.3 Evaluation of XO inhibitory activity

5.2.3.1 Principle of the XO Assay

Xanthine oxidase assay is an enzymatic reaction in which xanthine oxidase produces uric acid during oxidation of xanthine as depicted in figure 5.2.1. Uric acid can be easily analysed with an absorption wavelength of 290 nm quantifying xanthine oxidase activity (Hille *et al.*, 1998).

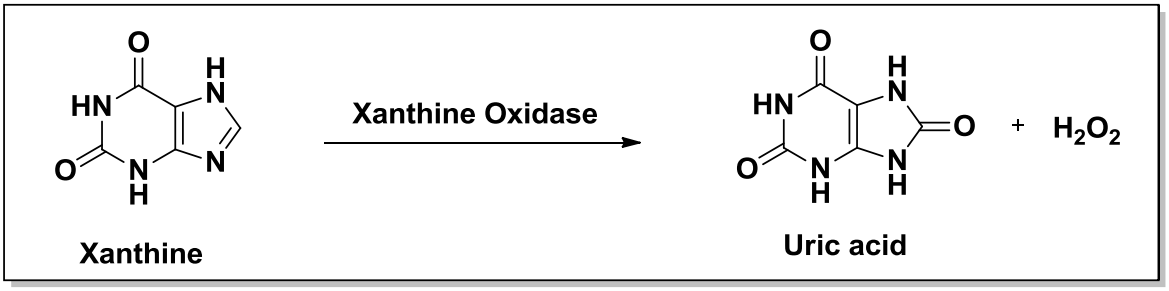

Figure 5.2.1: Principle of the XO assay

5.2.3.2 Preparation of reagents

Phosphate buffer (50 mM)

For the preparation of 50 mM phosphate buffer at pH 7.5, 9.4 mL (1M) KH_2PO_4 (Potassium phosphate monobasic) and 40.6 mL (1M) K_2HPO_4 (Potassium phosphate dibasic) was diluted up to 1000 mL with deionised water.

Xanthine solution (0.10 mM)

Stock solution of 0.1 (M) xanthine was prepared by dissolving 15.2 mg of xanthine in 1 mL of (1M) NaOH solution. Working solution was made in accordance with 1µL/mL in deionised water and pH was maintained with 1 (N) HCl.

XO enzyme solutions (0.1 - 0.2 unit/mL)

Stock solution of 16U/mL was prepared by dissolving 1mg of lyophilised powder of xanthine oxidase enzyme in 1 mL of cold phosphate buffer reagent. For working solution stock solution was diluted up to required volume.

5.2.3.3 Procedure

The inhibitory effect on XO was measured spectrophotometrically at 290 nm under aerobic condition. Allopurinol was used as a positive control for the inhibition test. The reaction mixture consisted of 1.5 mL of 50 mM potassium phosphate buffer (pH 7.5), 1 mL test sample solution (5, 10, 25, 50 & 100 µM) was dissolved in dimethylsulphoxide (DMSO), 0.5 mL of freshly prepared XO enzyme solution (0.2 units/mL of xanthine oxidase in phosphate buffer). The assay mixture was pre-incubated at RT for 15 minutes. Then, 1 mL of substrate solution (0.10 mM of xanthine) was added into the mixture. The mixture was incubated at RT for 30 minutes. Next, the reaction was stopped with the addition of 1 mL of 1 M hydrochloric acid. The absorbance was measured using UV-VIS spectrophotometer against a blank prepared in the same way but the xanthine was replaced with the phosphate buffer. Readings were taken in triplicate.

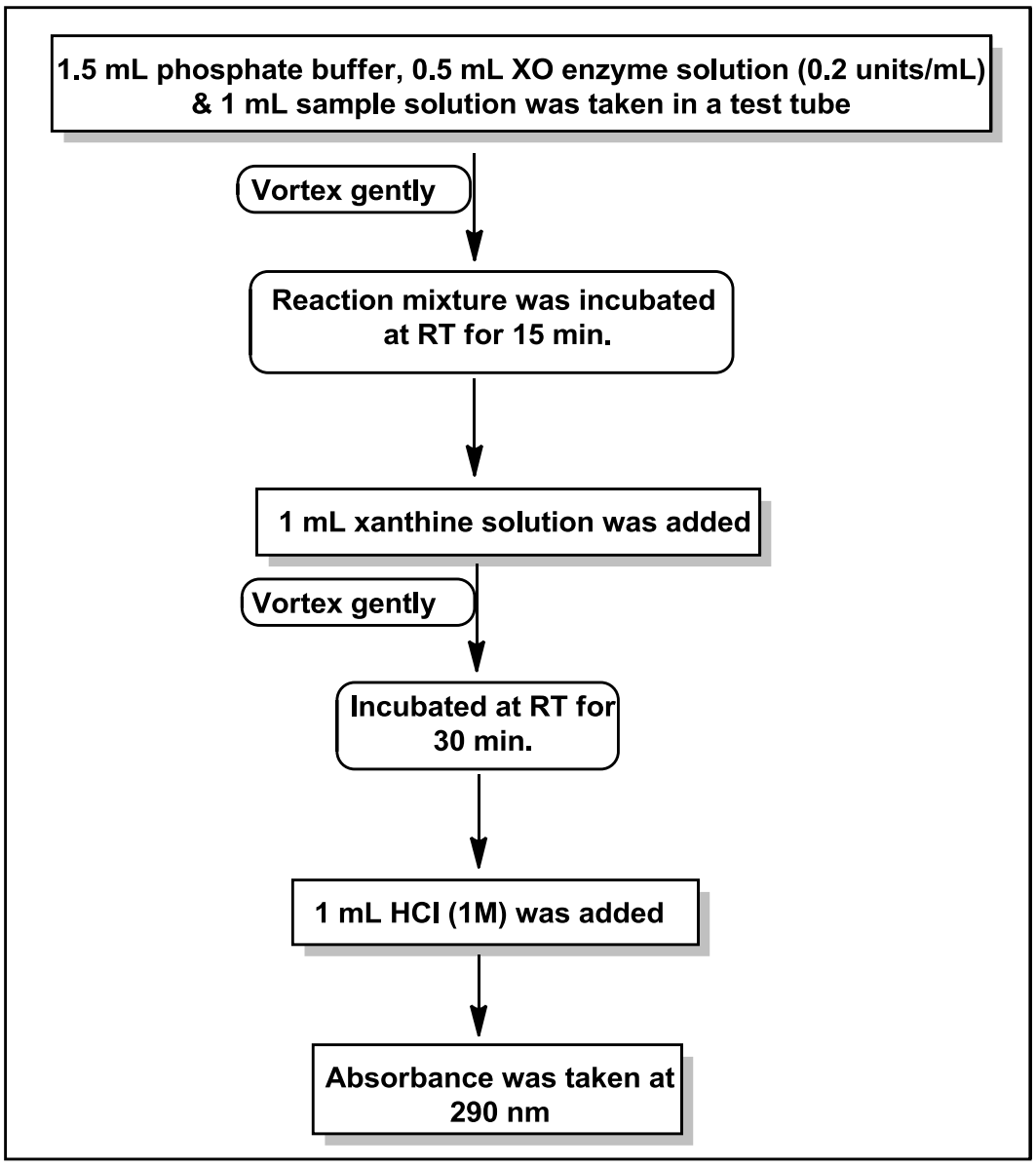

Figure 5.2.2: Protocol used for XO assay.

5.2.3.4 Calculation of Inhibition

The degree of XO inhibitory activity was calculated by following formula

$$\% \text{ Inhibition} = [(A_c - A_s)/A_c] \times 100$$

Where A_c = Absorbance of control (Sample in absence of XO inhibitors)

A_s = Absorbance of sample (Sample with potential XO inhibitors)

5.2.4 Evaluation of Antioxidant activity

Reactive oxygen species can harm various biomolecules including DNA and consequences are oxidative stress in the biological systems. Antioxidants are known to act via reducing the oxidative stress by scavenging of the free radicals and therefore, prevent many diseases including cancer. Hence, we performed DPPH assay to study the antioxidant activity of our compounds *in vitro*. DPPH assay was used to determine the total antioxidant activity by scavenging of the stable DPPH free radical. Antioxidant activity was observed to escalate in the concentration dependent manner (Musa *et al.*, 2013; Szabo *et al.*, 2007).

5.2.4.1 Principle of DPPH Assay

The principle of the assay is the use of the stable free radical for estimating antioxidant activity diphenylpicrylhydrazyl (DPPH) which gets reduced and thus stabilized in presence of a hydrogen donating substance as depicted in figure 5.2.3 (Szabo *et al.*, 2007).

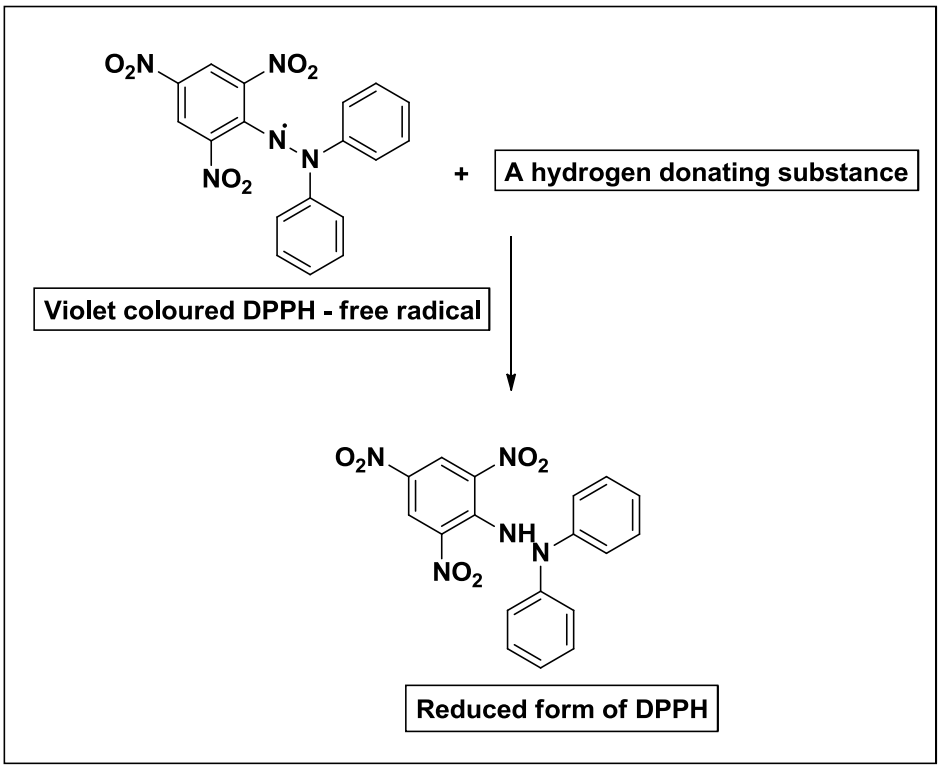

Figure 5.2.3: Principle of DPPH assay.

5.2.4.2 Procedure

2 mL of the different concentrations of compounds in methanol were added to 2 mL of 0.135 mM methanolic solution of DPPH. The mixture was shaken vigorously and was left to stand for 30 minutes in the dark. Absorbance was recorded at 517 nm against the blank. Blank was prepared without the addition of DPPH. BHT was used as standard.

5.2.4.3 Calculation of Inhibition

The ability to scavenge DPPH radical was calculated by the following equation:

$$\text{DPPH radical scavenging activity (\%)} = [(A_c - A_s)/A_c] \times 100$$

Where A_c = Control (Absorbance of DPPH radical + methanol)

A_s = Sample (Absorbance of DPPH radical + compound)

5.3 Molecular Docking

The coordinates of bovine milk XO complexed with hypoxanthine were obtained from protein data bank (PDB entry: 3NRZ) (Cao *et al*., 2010). The *R* and *S* isomers of **DK-3I** were drawn in MOE builder tool and subjected to the addition of partial charges and energy minimization *via* MMFF94x force field. The ligands were docked in to the active site of XO using the MOE (Chemical Computing Group, CCG), MOE performs drug design through molecular simulation, protein structure analysis, data processing of small molecules, docking study of proteins and small molecules, and so on under the unified operations. It utilizes GBVI/WSA dG (Generalized-Born Volume Integral/Weighted Surface area) scoring function (Corbeil, 2012) to evaluate the various conformations of ligand at the binding site and comprises of four components: protein–ligand hydrogen bond energy, protein–ligand van der Waals (vdw) energy, ligand internal vdw energy, and ligand torsional strain energy. Each isomer was docked 10,000 times and each pose was ranked according to its MOE GBVI/WSA dG Score. The conformations with highest score were selected for discussion (Vilar, 2008).

CHAPTER 6

RESULTS AND DISCUSSION

6.1 Chemistry

The pharmacophore pertaining to formula II, 2-phenyl-5,6-dihydropyrazolo[1,5-*c*]quinazolines (**1**, figure 6.1.1) have already been identified as privileged pharmacophore as Gly/NMDA receptor and excitatory amino acid antagonists (Varano, 2002), potent phosphodiesterase 10A and Eg5 ATPase inhibitors and potential vaccinia virus inhibitors (Guo, 2013), adenosine receptor antagonists, AMPA and kainate receptor antagonist (Catarzi, 2012; Varano, 2008).

There are some synthetic strategies reported for the synthesis of **1** which are outlined in the figure 6.1.1. Xiaobo *et al.* developed one pot two step synthesis of **1** by treating **2** with hydrazine hydrochloride in presence of Cs_2CO_3 as the base and DMSO as the solvent in first step followed by addition of acetamidine hydrochloride under nitrogen atmosphere in second step as shown in route A (Yang *et al*., 2012). Shenghai *et al*. synthesized **1** by treating **3** with different aldehydes in presence ammonia hydrate, copper iodide and DMF at 100 °C for 24 h as depicted in route B (Guo, 2013). Colotta *et al.* synthesized **1** by refluxing **3** with paraformaldehyde in benzene for 4 - 5 h through route C (Colotta, 1996). Catarzi *et al*. synthesized **1** by treating 4 with NH_2CN for amine derivative of pyrazolo[1,5-c]quinazoline through route D (Catarzi, 2012).

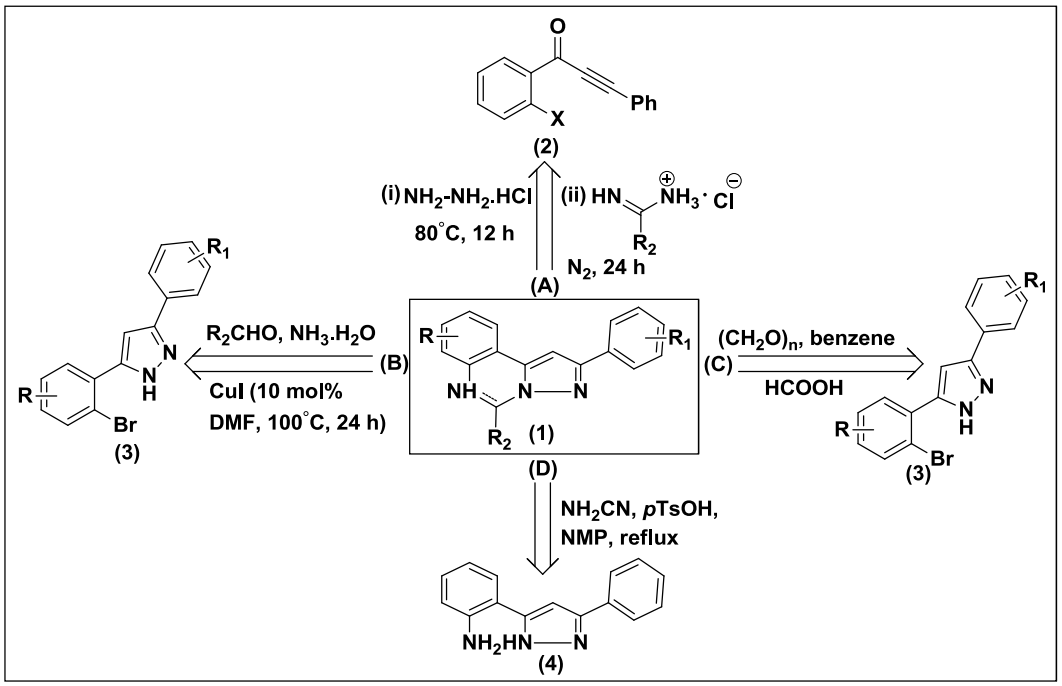

Figure 6.1.1: Retrosynthetic approaches for 2-phenyl-5,6-dihydropyrazolo[1,5-*c*]quinazoline.

While these synthetic methods are generally efficient however, they usually suffer from one or another disadvantages like difficult to obtain starting materials, harsh reaction conditions, use of high boiling solvents and expensive catalysts. Therefore, a more practical and general pathway towards pyrazolo[1,5-*c*]quinazoline skeleton starting from simple and easy to obtain starting materials is desirable.

For the synthesis of target compounds (formula I & II) we have followed the route as depicted in scheme 6.1.1. Briefly, the 2-nitrobenzaldehyde was condensed with aryl ketones to afford nitro substituted 1,3-diaryl propenones under acid catalysed conditions. Introduction of pyrazoline ring system was made feasible by refluxing diaryl propenones with hydrazine hydrate in methanol (Lévai, 2005). Dehydrogenation of pyrazolines was carried out by refluxing them with iodine and DMSO (Lokhande, 2005). Subsequently, reduction of aromatised pyrazole derivative was carried out using stannous chloride and methanol (Bellamy, 1984). The reduced product was eventually cyclized either using different aldehydes by refluxing in methanol or using triethyl orthoformate.

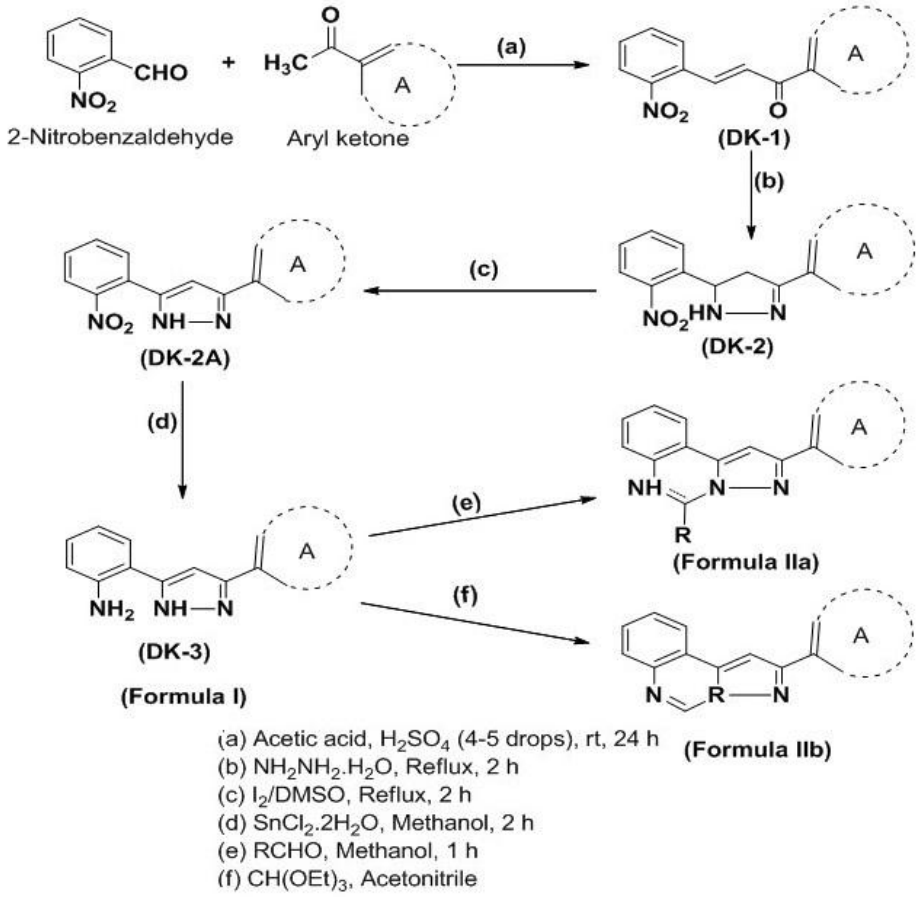

Scheme 6.1.1: Synthetic scheme for the formation of target compound.

6.1.1 Synthesis of nitro substituted 1,3-diarylpropenones

The synthesis of nitro substituted 1, 3-diaryl propenones was carried out through Claisen – Schmidt condensation of 2-nitrobenzaldehyde with aryl ketones in presence of glacial acetic acid and few drops of conc. H_2SO_4 (scheme 6.1.2).

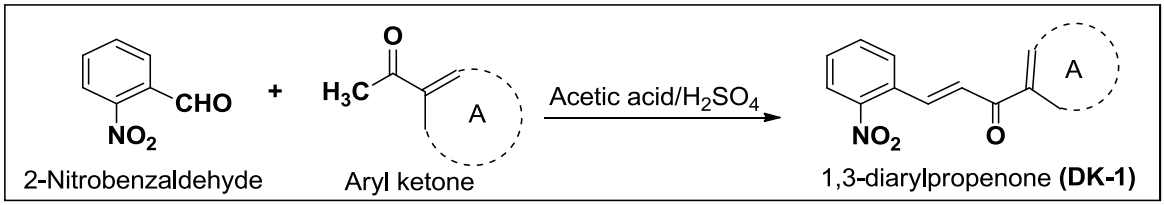

Scheme 6.1.2: Synthesis of 1, 3-diaryl propenones

Mechanistically, acid catalysed Claisen-Schmidt condensation involves the nucleophile attack of carbanion on the electrophilic carbon of the aldehyde in the process rendering the oxygen electron rich which takes up the proton from reaction solution (scheme 6.1.3). The final step of the reaction is dehydration which affords the nitro substituted 1, 3-diaryl propenones (figure 6.1.2).

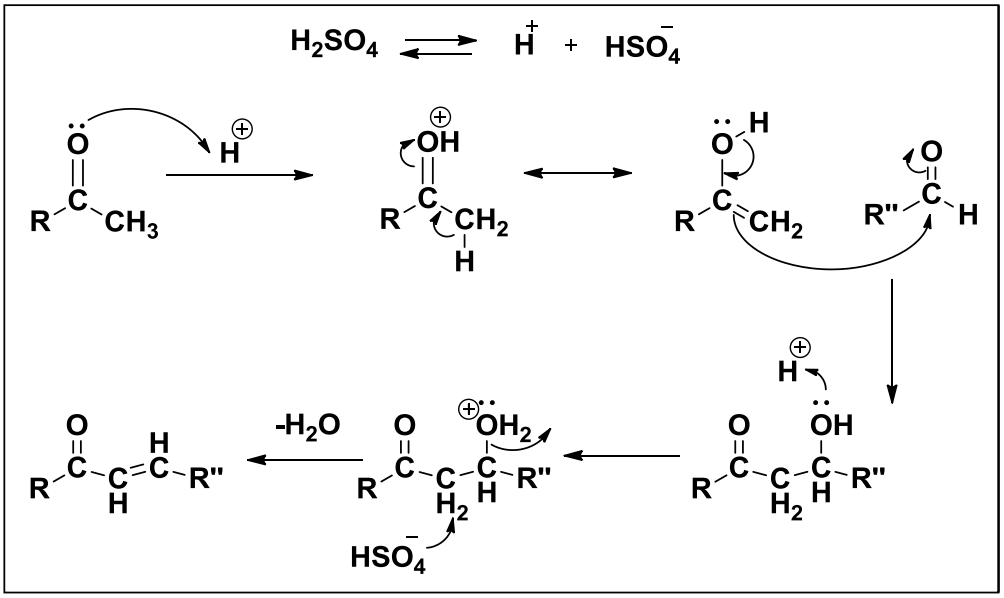

Scheme 6.1.3: Mechanism for formation of 1, 3-diaryl propenones

The compounds was characterized by melting point (MP), Infrared spectroscopy (IR) and Nuclear Magnetic Resonance (NMR) spectroscopy. For all the synthesized compounds, characteristic IR absorptions peaks were observed at 1660 - 1670 cm^{-1} for carbonyl group which was much lower than the normal value of 1710 cm^{-1}. The reason for this decrease is the conjugation of α, β double bond with the carbonyl compound. Conjugation is known to increase the single bond character of the C=O

and C=C bonds in the resonance hybrid, lowering their force constants and as a result lowering the frequencies. Other peaks obtained were at 1610 cm^{-1} (C=C stretch), 1510 and 1342 cm^{-1} (N=O stretch) 1284 - 1281 cm^{-1} (C-O stretch), 1653 - 1585 cm^{-1} (C=C aromatic). Melting point for these compounds was seen to be in the range of 85 – 95 ˚C which are uncorrected.

In ^{1}H NMR spectra we always detected the following typical peaks of 8.12 ppm for CH close to nitro group and 7.34 ppm for CH away from nitro group. For all the compound the aromatic protons appeared as multiplet at above 7.00 ppm. The ^{13}C NMR indicated the characteristic peak at 190.22 ppm for carbonyl carbon (C=O) and 148.34 ppm for C=N carbon.

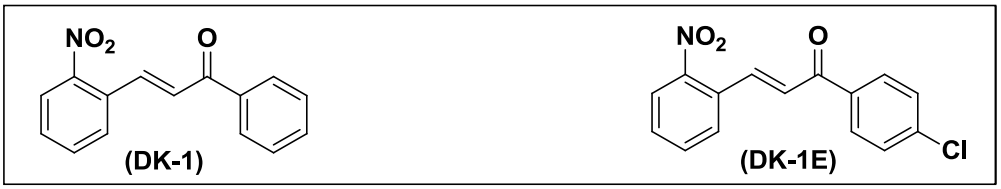

Figure 6.1.2: Chemical structures of nitro substituted 1,3-diaryl propenones

6.1.2 Synthesis of 3-(2-nitrophenyl)-1-aryl-4,5-dihydro-1*H*-pyrazolines

Synthesis of 3-(2-nitrophenyl)-1-phenyl-4,5-dihydro-1*H*-pyrazoline (scheme 6.1.4) mainly follows the mechanism for Michael Addition which takes place between the hydrazine hydrate and enone moiety of the 1, 3- diaryl propenones. This reaction was carried out in the presence of methanol.

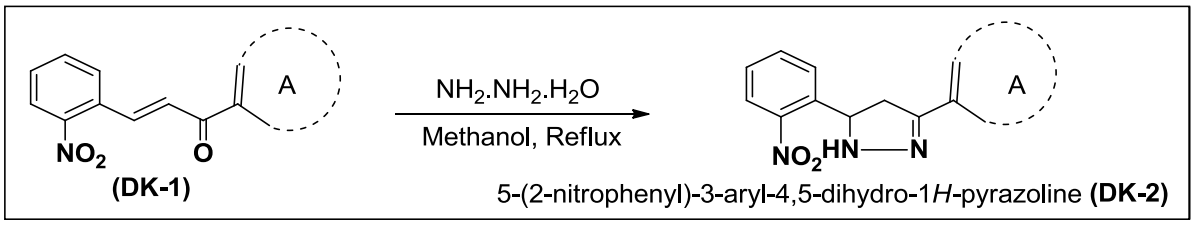

Scheme 6.1.4: Synthesis of 2*H*-pyrazolines

All the pyrazolines obtained were pure and were characterized by MP, IR and NMR.

IR spectrum showed absorptions which fell in between 3250 - 3350 cm^{-1} (NH), 1632 - 1590 cm^{-1} (C=N stretch), 1223 - 1176 cm^{-1} (C-N stretch).

The ^{1}H NMR spectra of the pyrazoline derivatives showed the ABX system with three double doublets out of which one double doublet was de-shielded and

appeared more downfield than the other two. The three double doublets represent the three protons of the pyrazoline nucleus; confirming its formation. The chemical shift for these protons appeared in the range of 5.55 - 5.91 ppm with the *J* values falling in the range of 3.76 – 12 Hz, 3.15 - 1.47 Hz with the *J* values falling in the range of 3.90 and 18 Hz, 3.56 - 3.86 ppm and their *J* values falling in the range of 11.36 Hz and 18.56 Hz. The protons of the benzene ring appeared in the range of 7.24 - 7.78 ppm, varying according to the substitution on the ring.

The ^{13}C NMR spectra obtained for one of the pyrazoline compound showed the peak for carbon adjacent to the electronegative atom in the range of 115 – 125 ˚C.

Figure 6.1.3: Chemical structures of 2*H*-pyrazolines synthesized

6.1.3 Synthesis of 5-(2-nitrophenyl)-3-aryl-1*H*-pyrazole

Dehydrogenation of 4,5-dihydropyrazoline using I_2/DMSO resulted in the aromatization of pyrazoline ring (scheme 6.1.5).

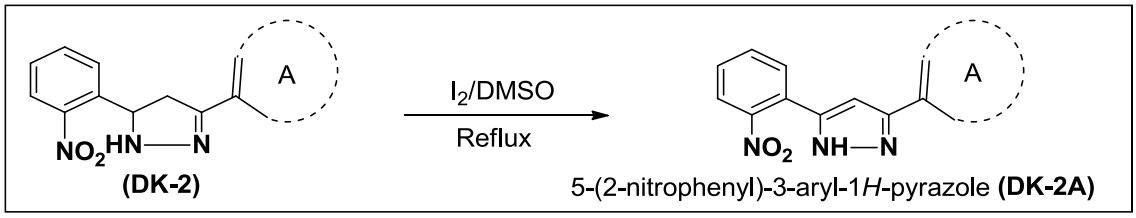

Scheme 6.1.5: Synthesis of 1*H*-pyrazoles

All the pyrazoles (figure 6.1.4) so obtained were characterized by MP, IR and NMR.

IR spectra showed absorptions which fell in range of 1605 – 1615 cm^{-1} (C=C) owing to aromatization in addition to other IR peaks.

^1H NMR showed the disappearance of ABX pattern due to aromatisation. Appearance of peak at 6.69 ppm further confirmed the formation of Pyrazole.

^{13}C NMR showed three most characteristic peaks at 149.02, 146.37 and 146.16 ppm for de-shielded carbon attached to NO_2, NH and N respectively. Peak corresponding to 102.59 ppm appeared due to pyrazole carbon.

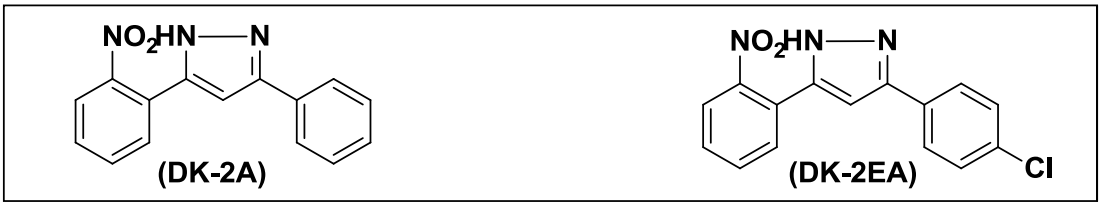

Figure 6.1.4: Chemical structures of 1*H*-pyrazoles synthesized

6.1.4 Synthesis of 2-(3-aryl-1*H*-pyrazol-5-yl)aniline

Next we planned to reduce the nitro of **DK-2A** and various attempts were made (figure 6.1.5). Unfortunately we were unsuccessful to obtain the desired reduced products. Fortunately the reduction were successful when carried out with $SnCl_2.2H_2O$ in methanol under reflux (scheme 6.1.6).

The ease of reduction of the aromatic nitro group depends on the nature of the other substituents on the ring and on the reducing potential of the environment.

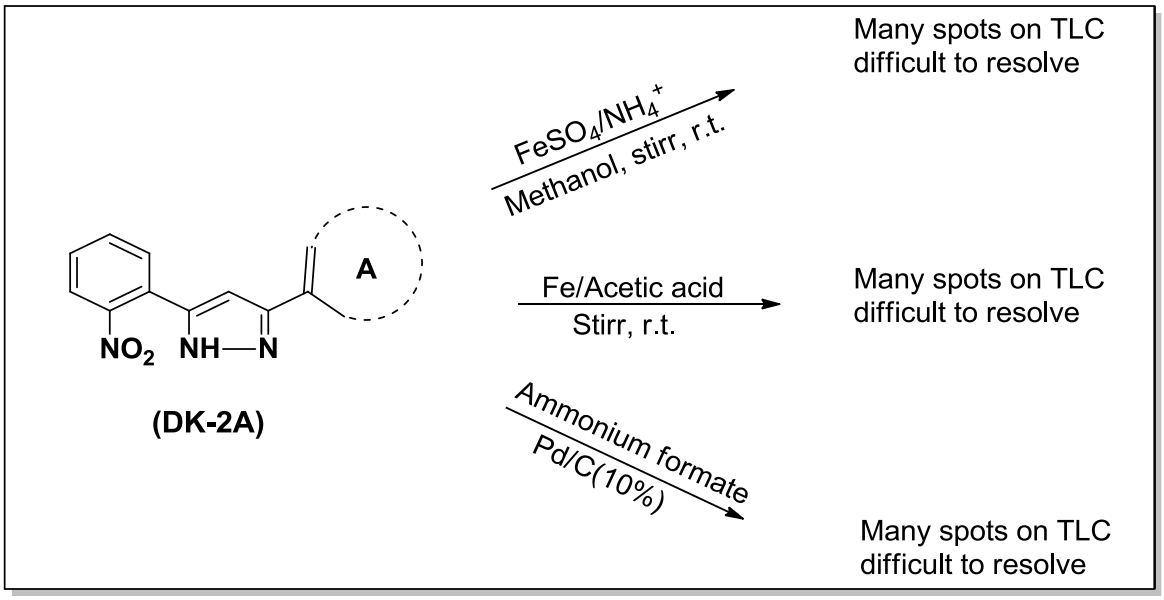

Figure 6.1.5: Reduction of nitro group under various conditions.

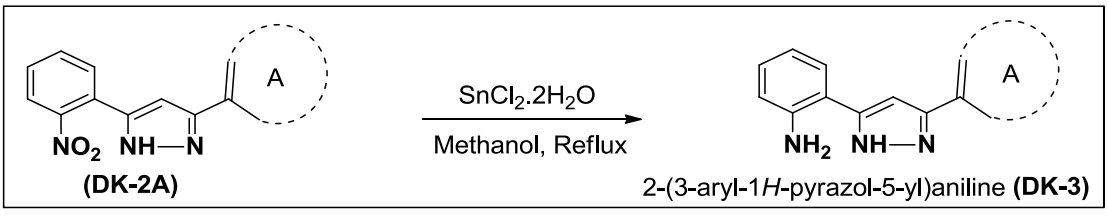

Scheme 6.1.6: Synthesis of anilines

Mechanistically the nitro reduction could follow the steps as shown in scheme 6.1.7.

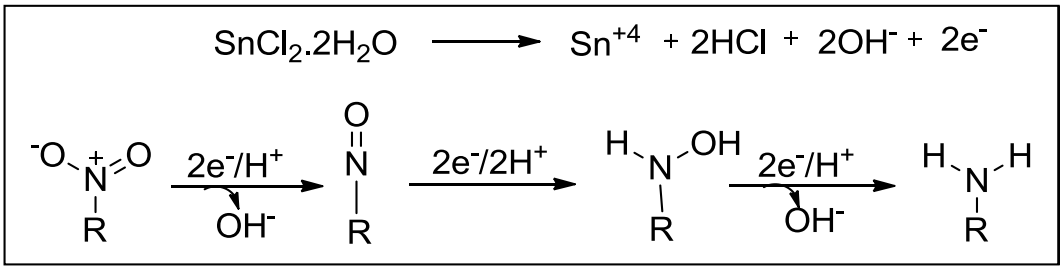

Scheme 6.1.7: Mechanism of synthesis of anilines

The MP of all the compounds were found to be in range of 166 - 186°C.

IR spectra confirmed the product formation due to appearance of a sharp characteristic peak of primary amine (NH_2) at 3350 - 3380 cm^{-1} and secondary amine (NH) at 3250 - 3270 cm^{-1} and 1613 cm^{-1} for C=C.

The ^{1}H NMR spectra showed a characteristic singlet peak at 13.23 ppm for proton of NH this was due to the fact that nitrogen causes downfield shifting because of de-shielding of protons, 7.00 ppm for proton of NH_2 aromatic proton occupied peak between 7.00 - 8.00 ppm. ^{13}C NMR showed three most characteristic peaks at 152.59, 145.55 and 142.24 ppm for de-shielded carbon attached to NH_2, NH and N respectively. Peak corresponding to 99.5 ppm was due to pyrazole carbon. 115.59 & 115.18 ppm value represents aromatic carbon attached next to the carbon of NH_2 on either side. 129.23, 128.67, 127.81, 127.66 and 125.16 ppm are the normal aromatic carbon peak.

Mass spectra showed the molecular ion peaks at $[M+1]^+$ that is 236.1 in case of **DK-3** compounds and 270.1 for **DKE-3** compounds (figure 6.1.6).

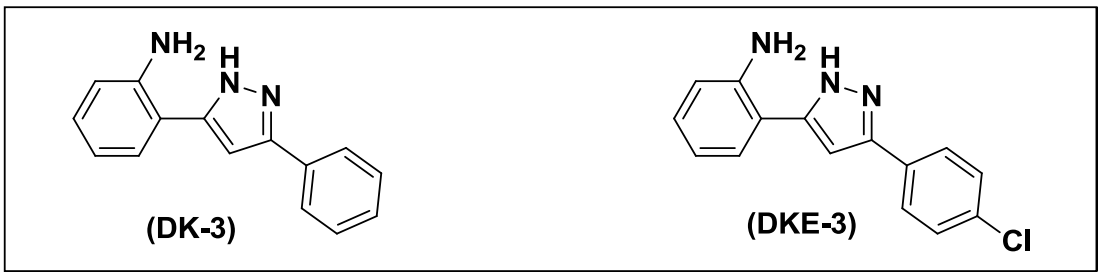

Figure 6.1.6: Chemical structures of anilines synthesized.

6.1.5 Synthesis of 2-aryl-5,6-dihydropyrazolo[1,5-*c*]quinazoline

2-(3-aryl-1*H*-pyrazol-5-yl)anilines were allowed to react either with a variety of aldehydes or triethyl orthoformate to afford quinazolines (figure 6.1.7 and 6.1.8). The reaction was carried out in methanol under reflux. Crude precipitate so obtained were purified through crystallization from methanol to afford the pure products.

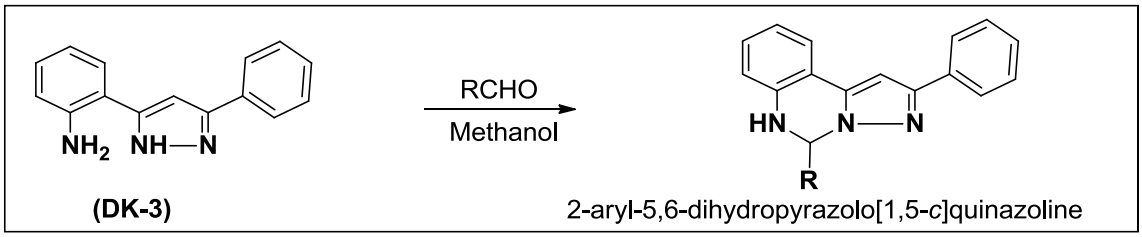

Scheme 6.1.8: Synthesis of 2-aryl-5,6-dihydropyrazolo[1,5-*c*]quinazolines

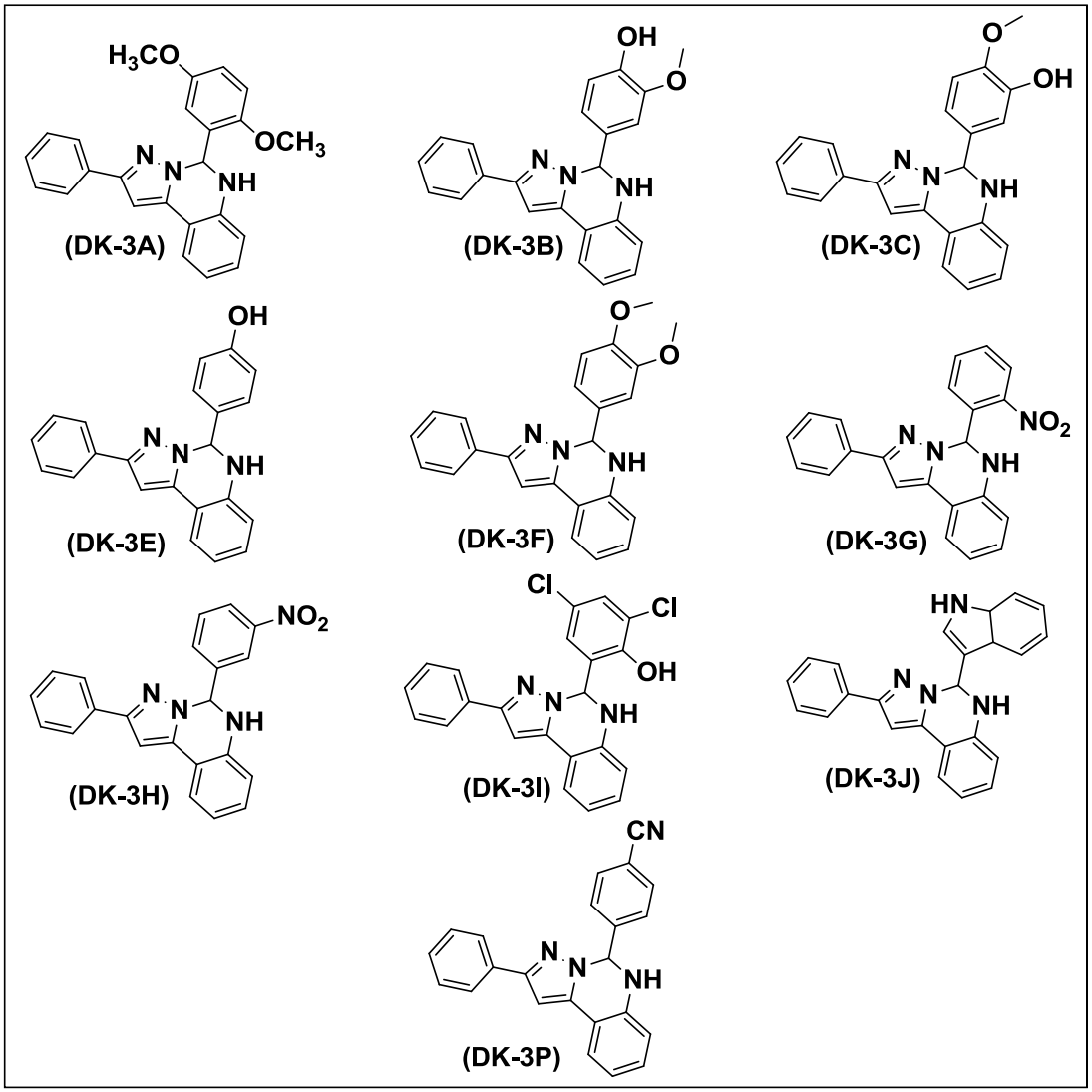

Figure 6.1.7: Chemical structures of 2-aryl-5,6-dihydro pyrazolo[1,5-*c*]quinazolines synthesized.

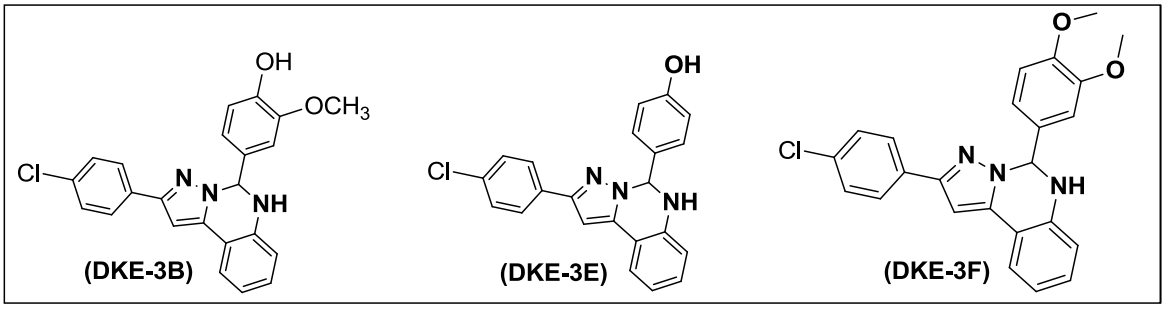

Figure 6.1.8: Chemical structures of 2-aryl-5,6-dihydropyrazolo[1,5-c]quinazolines synthesized.

All the products were characterized by MP, IR, NMR and MS.

The MP of all the compounds were found to be in the range of 115 – 235 °C.

The IR spectroscopy showed the most characteristic peak in the range from 2900 - 3100 cm^{-1} for amine of quinazoline, other characteristic peaks was obtained at 2229 cm^{-1} (CN), 1600 - 1700 cm^{-1} (C=N), 1210 - 1220 cm^{-1} (C-N), 770 - 780 cm^{-1} (C-Cl).

The ^{1}H NMR spectra highlighted the characteristic sharp singlet peak of NH in the range of 8 - 14 ppm this was due to the downfield shifting of proton by nitrogen. Peaks for aromatic protons was found in the region above 7 – 8 ppm. ^{13}C NMR confirmed the pyrazole carbon in the range between 95 - 100 ppm, quinazoline carbon attached with phenyl showed peak in between 70 - 75 ppm, carbon attached with oxygen at 145 - 150 ppm the reason being oxygen is more electronegative causes de-shielding.

Mass spectra showed the molecular ion peak at $[M+1]^{+}$ and most common fragment peak at 236.1 in case of **DK-3** compounds and 270.1 for **DKE-3** compound.

6.1.6 Synthesis of 2-arylpyrazolo[1,5-*c*]quinazolines

2-(3-aryl-1*H*-pyrazol-5-yl)anilines were condensed with triethyl orthoformate in acetonitrile (scheme 6.1.9) under reflux to afford the products (figure 6.1.9).

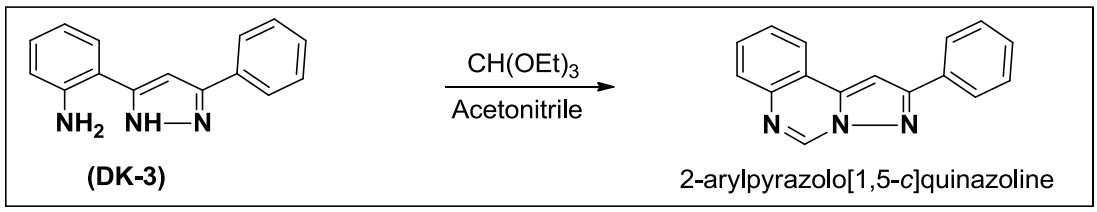

Scheme 6.1.9: Synthesis of 2-arylpyrazolo[1,5-*c*]quinazolines.

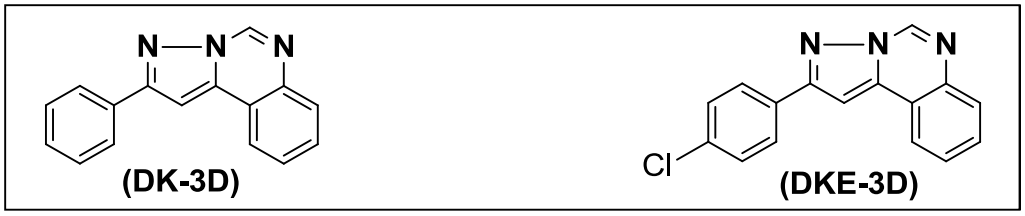

Figure 6.1.9: Chemical structures of 2-arylpyrazolo[1,5-*c*]quinazolines synthesized

All the products were characterized by MP, IR, NMR and MS.

The MP of all the compounds were found to be in the range of 145 – 205 °C.

The IR spectroscopy showed the characteristic peaks in the range of 2900 - 3100 cm^{-1} for NH of quinazoline, other characteristic peaks were obtained at 2229 cm^{-1} (CN), 1600 - 1700 cm^{-1} (C=N), 1210 - 1220 cm^{-1} (C-N), 770 - 780 cm^{-1} (C-Cl).

The ^{1}H NMR spectra highlighted characteristic sharp singlet peak of NH in the range of 8 -14 ppm this was due to the downfield shifting of proton by nitrogen. Peaks for aromatic protons was found in the region above 6.2 – 6.8 ppm. ^{13}C NMR confirmed the pyrazole carbon in the range between 95 - 100 ppm, quinazoline carbon attached with phenyl showed peak in between 70 - 75 ppm.

Mass spectra showed the molecular ion peaks at $[M+1]^{+}$ that is 236.1 in for **DK-3D.**

6.2 Biological Evaluation

6.2.1 XO Inhibitory Activity

In humans, Xanthine oxidase (XO), is the terminal enzyme of purine catabolism, catalysing the hydroxylation of purines to uric acid. When acting as an NADH oxidase, XO is a generator of superoxide, a powerful ROS. XO has also been noted to produce hydrogen peroxide (H_2O_2) and superoxide during ischemia-reperfusion injury (Brown, 1988). These ROS affect various molecular components of the cell, with excess amounts leading to cell degeneration and death. XO is present in nearly all species. In mammalian tissues, XO is found predominantly in the liver and intestine. Human XO activity is almost exclusively limited to these tissues, with only trace levels found elsewhere in the body. However, in several disease states, levels of circulating XO have been seen to increase dramatically. This is especially true of liver disease, during which circulating levels of XO may be 1,000 fold greater. This dramatic increase in XO activity results hyperuricemia.

In order to evaluate the biological activities of synthesized compounds, *in-vitro* biochemical screening was carried out using xanthine oxidase enzyme with UV-Visible spectrophotometer at 290 nm. Four different concentrations of compounds were used for inhibiting the xanthine oxidase enzyme i.e., uric acid formation as described in experimental section. XO activity i.e. uric acid formation was started by addition of xanthine substrate in different concentration of compounds (5, 10, 25 and 50 µM). The uric acid absorbance was measured spectrophotometrically at 290 nm after an incubation of 30 minutes. The more potent compounds tend to bind more strongly with XO and reduces the uric acid formation.

Out of 17 compounds synthesized only 15 compounds were screened (2 were not soluble under given conditions). As evident from table 6.2.1 and figure 6.2.2, it was observed that some of the compounds **DK-3, DK-3B, DK-3F, DK-3G, DK-3H** and **DK-3I** showed significant xanthine oxidase inhibition and significant reduction in uric acid formation. The compounds exhibited the good inhibitory potential mainly at concentrations of 25 µM and 50 µM except **DK-3H** which was observed to exhibit the XO inhibitory activity at 5 µM concentrations. Percentage inhibition of XO exhibited by **DK-3H** and **DK-3I** at 25 µM concentrations was found to be comparable to allopurinol (used as positive control)

Table 6.2.1: Percent inhibition of XO with synthesized compounds at concentrations of 5 µM, 10 µM, 25 µM and 50 µM.

Compounds	% Inhibition [a]				IC $_{50}$ (Fig. 6.2.1)
	5 µM	10 µM	25 µM	50 µM	
DK-3	9.84	9.63	25.08	60.74	43 µM
DK-3B	8.06	13.96	19.86	45.53	>50 µM
DK-3F	4.07	7.39	11.46	62.59	44 µM
DK-3G	6.2	10.59	25.84	41.6	>50 µM
DK-3H	35.99	47.96	69.38	73.76	14 µM
DK-3I	17.95	23.98	57.32	87.78	24 µM
Allopurinol	38.96	42.03	46.53	59.23	32 µM

[a] values are means of three readings

The compounds **DK-3** and **DK-3B** were found to have very good xanthine oxidase inhibitory activity in the concentration range of 25 µM to 50 µM. But, at lower concentrations range i.e. 5 µM and 10 µM **DK-3B** was found to be more active than **DK-3**. **DK-3F** exhibited the best inhibitory activity at 50 µM but at lower concentrations, it was not much active. Among **DK-3G, DK-3H** and **DK-3I** at 50 µM concentration **DK-3I** was found to be more active followed by **DK-3H** and **DK-3G.** But at 25 µM the **DK-3H** was found to more active followed by **DK-3I** and **DK-3G**. At lower concentrations range i.e. 5 µM and 10 µM **DK-3H** was found to be more active followed by **DK-3I** and **DK-3G. DK-3I** and **DK-3H** showed even comparable activity than standard allopurinol. The IC $_{50}$ values of some of the significantly active compounds are shown in figure 6.2.1.

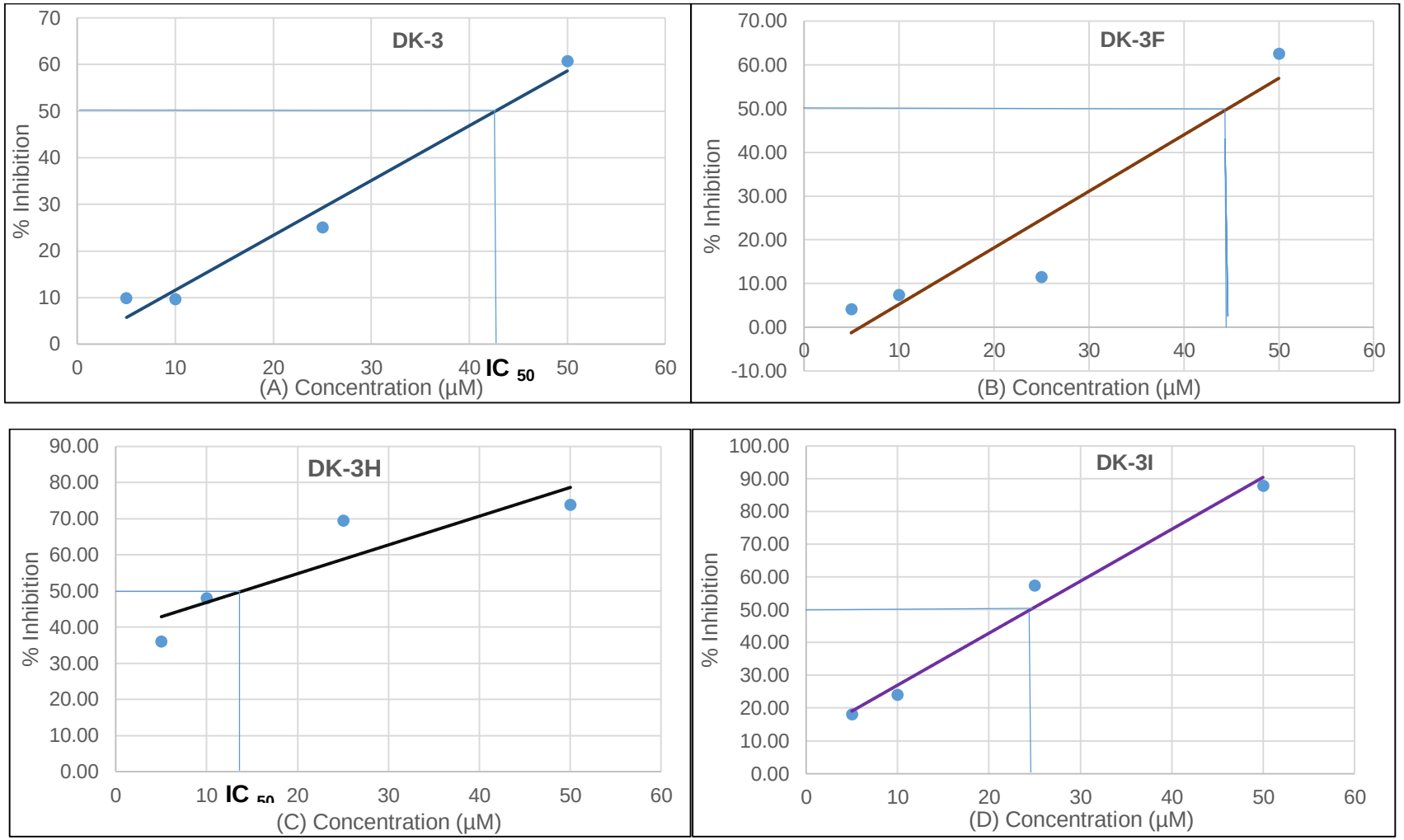

Figure 6.2.1:: Plot of Concentration Vs. % Inhibition showing IC 50 values of significantly active compounds **DK-3** (A), **DK-3F** (B), **DK-3H** (C) and **DK-3I** (D).

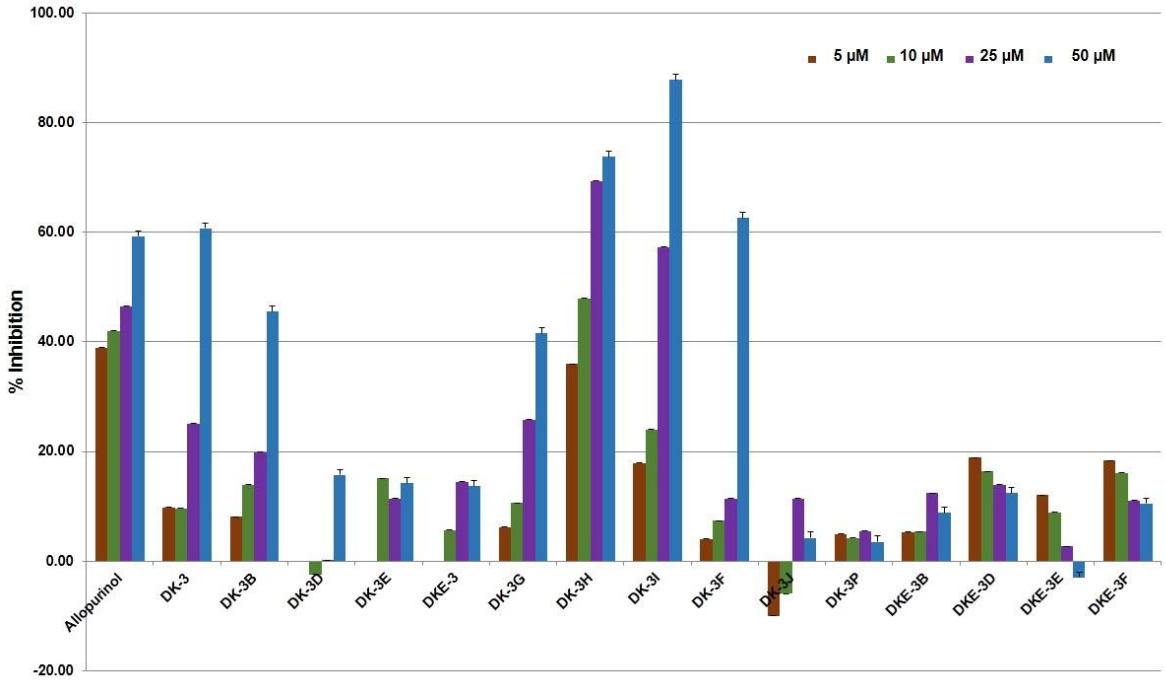

Figure 6.2.2: Percent inhibition of XO with synthesized compounds at concentrations of 5 µM, 10 µM, 25 µM and 50 µM. Data is expressed as mean values ± S.D. of three independent experiment.

6.2.2 Structure Activity Relationship (SAR) of compounds for XO Activity

The compounds without any substitution at ring A (**DK-3**), was found to be more active in comparison to ring A substituted compounds (**DKE-3)**.

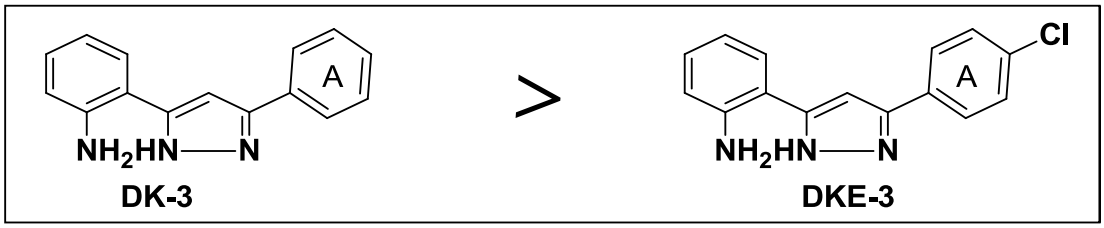

Figure 6.2.3: Comparison of XO inhibitory activity of 1*H*-pyrazol-5-yl)anilines

But, when **DK-3** is cyclised with triethyl orthoformate there were no any significant change in activity observed. Simple cyclisation process i.e. R = H (**DK-3D** and **DKE-3D**) did not affected any significant change in activity thus we replaced R with substituted aryl group by cyclising **DK-3** with different types of aryl aldehydes and we found significant change in activity (figure 6.2.4).

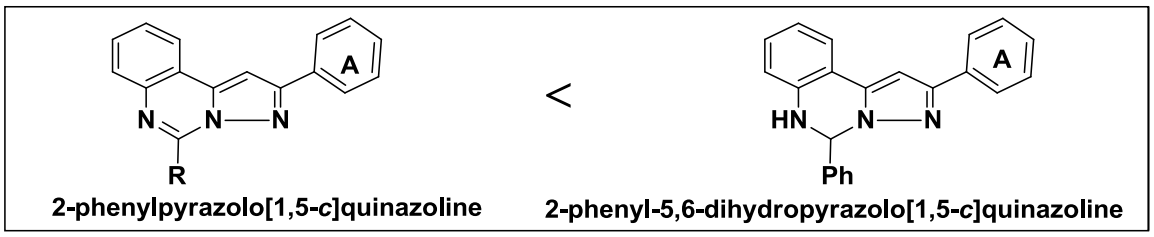

Figure 6.2.4: Comparison of XO inhibitory activity of 2-phenylpyrazolo[1,5-*c*]quinazoline and 2-aryl-5,6-dihydropyrazolo[1,5-*c*]quinazoline.

In general, the compounds bearing electron withdrawing groups at ring B were observed to increase the XO inhibitory activity.

The compounds having meta nitro on ring B (**DK-3H**) found to be more active than the one having nitro at ortho (**DK-3G**). The compounds having para hydroxy on ring B (**DK-3E**) showed lesser XO inhibitory activity than the one having chloro on meta position on both side in addition to para hydroxy ring B (**DK-3I**) figure 6.2.5 .

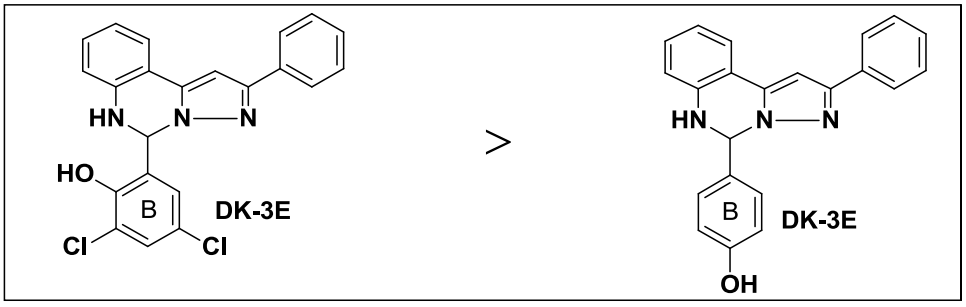

Figure 6.2.5: Comparison of XO inhibitory activity of compounds having electron withdrawing groups.

The compounds bearing methoxy at meta and para positions (**DK-3F)** were observed as more active XO inhibitor than the one having only one methoxy at meta and hydroxy at para on ring B (**DK-3B**). The compounds containing more number of methoxy group were found to be more active as XO inhibitory activity of **DK-3F** (2 methoxy group) was found to be maximum followed by **DK-3B** (1 methoxy group) and **DK-3E** (no methoxy group) as shown in figure 6.2.6.

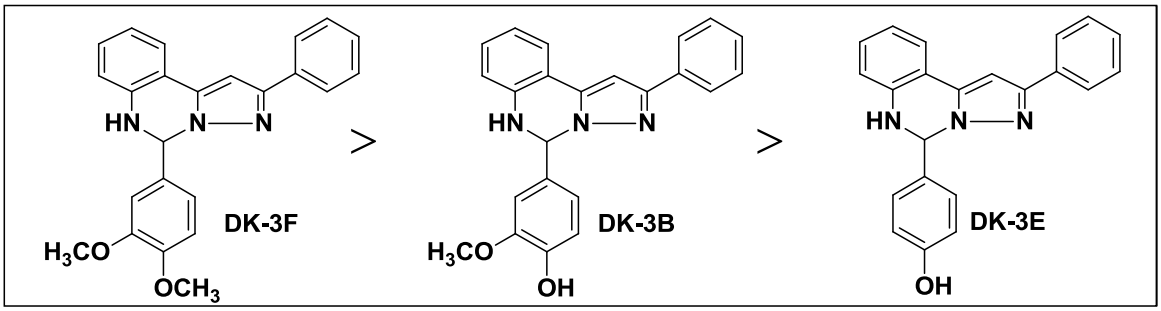

Figure 6.2.6**:** Comparison of XO inhibitory activity of compounds containing methoxy group.

6.2.3 Antioxidant Activity

In order to confirm the antioxidant potential of best XO inhibitory compounds, **DK-3H** and **DK-3I** were tested of which both of them were observed to possess very good antioxidant activity (**DK-3H,** 99 % and **DK-3I,** 96 %) as they showed significant decrease in the level of DPPH free radical (table 6.2.2 and figure 6.2.7).

Table 6.2.2: Percentage inhibition of various compounds against DPPH.

S.No	Compound	% Inhibition
1	**DK-3H (4 mM)**	99 **%**
2	**DK-3I (4 mM)**	96 **%**
3	**BHT (5 mM)**	95 %

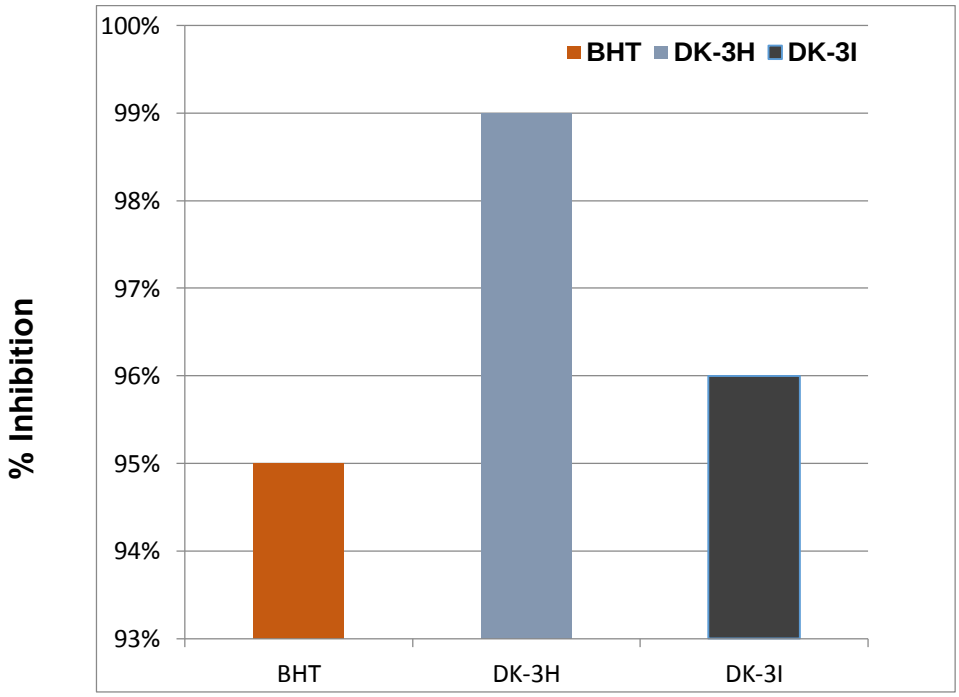

Figure 6.2.7**:** Percentage inhibition of various compounds against DPPH

So it may be considered that the synthesized compounds showed XO inhibitory activity as well as very good antioxidant activity.

6.2.4 Molecular docking

In order to theoretically investigate the recognition process of *R*- and *S*- enantiomers of the most potent identified XO inhibitor **DK-3I** flexible docking experiments using MOE software (Evaluation License) (Shadnia, 2009) were performed assuming that it gets accommodated into the hypoxanthine XO active site. The docking study showed that *S*-enantiomer of **DK-3I** fits well in the XO binding cavity. The binding site residues and overall binding mode have been found to be similar to those observed with hypoxanthine. The planar ring A of the inhibitor aligned parallel to the Phe914 ring (Figure 6.2.8). This arrangement of energetically favourable arene/arene interactions has also been seen in the co-crystal structure of XO with salicylate and fabuxostat. This conservation argues for an important role in stabilizing the binding positions of aromatic substrates and might well represent one of the key features of the substrate recognition. The *O*H group of the inhibitor gets positioned near the hydrogen atom of free hydroxyl group of Ser876. The docked conformation of *R*- enantiomer was differing from the *S*- enantiomer. The favourable binding conformation and higher interaction energy of *S*- enantiomer suggests its prevailing role in XO inhibitory activity.

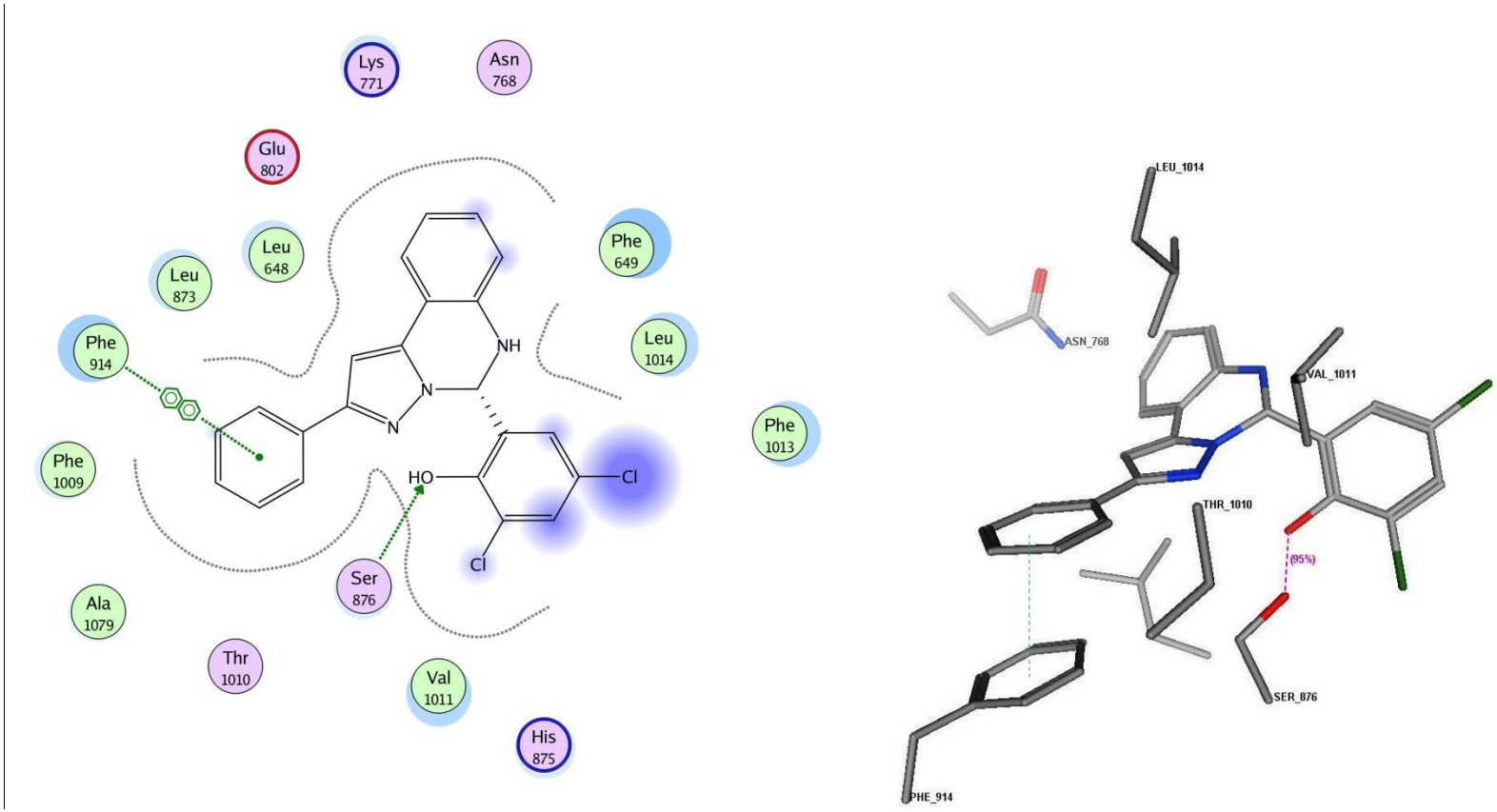

A **B**

Figure 6.2.8. (**A**). 2D-Docking conformation of *S* isomers of **DK-3l** at hypoxanthine binding site of XO and, (B) 3D-Docking conformation of *S* isomers of **DK-3l** at hypoxanthine binding site of XO.

CHAPTER 7

CONCLUSION

Hyperuricemia and gout remain the main indications for the development of novel XO inhibitors. Novel XO inhibitors must preferably be more potent, more effective, and possess better pharmacodynamic profile than allopurinol/oxypurinol as such purine analogues offer some serious life threatening problems like hypersensitivity reaction (Stevens rationally designed, synthesized and evaluated *in- vitro* XO inhibitory activity of Johnson syndrome, tissue epidermal necrolysis, bone marrow depression etc.). These are resulted from the metabolic conversion of the drugs to corresponding nucleotides through the action of phosphoribosyl transferase. This has prompted the researcher to develop new XO inhibitors that are structurally distinct from purines. We have 1*H*-pyrazol-5-yl)anilines and their cyclized products 2-arylpyrazolo[1,5-*c*]quinazolines and 2-aryl-5,6-dihydropyrazolo[1,5-c]quinazolines respectively. The purity of all the compounds were ascertained by melting point, UV, IR, NMR and Mass spectrometry.

XO inhibitory activity was evaluated spectrophotometrically at 290 nm by measuring absorbance of uric acid at concentrations of 5, 10, 25 and 50 µM. Some of the compounds showed very good XO inhibitory activity at lower concentrations. The information about XO inhibitory potential of the compounds acquired from the XO assay results helped us to explore the structural relationship studies and highlighted the modifications which led to increase in the activity.

Two best active derivatives were further evaluated for their potential to exhibit antioxidant activity especially against free radical scavenging activity. Both the compounds showed significant antioxidant property.

Molecular docking of the selected compound **DK-3l** (particularly *S* enantiomer) revealed the compound occupy the same active site where the substrate goes and also have all the important interactions with amino acid residues of the active site conserved.

In future, the lead compounds so obtained may be further optimized for the design of more potent XO inhibitors which may be evaluated *in-vivo* for antigout and antihyperuricemic activity in order to exhibit their potential at preclinical level.

REFERENCES

Ali, H. I., Fujita, T., Akaho, E. and Nagamatsu, T. (2010). A comparative study of AutoDock and PMF scoring performances, and SAR of 2-substituted pyrazolotriazolopyrimidines and 4-substituted pyrazolopyrimidines as potent xanthine oxidase inhibitors. *Journal of Computer-Aided Molecular Design* ***24***(1), 57-75.

Annemans, L., Spaepen, E., Gaskin, M., Bonnemaire, M., Malier, V., Gilbert, T. and Nuki, G. (2008). Gout in the UK and Germany: prevalence, comorbidities and management in general practice 2000–2005. *Annals of the Rheumatic Diseases* ***67***(7), 960-966.

Barrett, D. and Davidson, N. A. (1975). Xanthine dehydrogenase accumulation in developing Drosophila eyes. *Journal of insect physiology* ***21***(8), 1447-1452.

Becker, M. A., MacDonald, P. A., Hunt, B. J. and Jackson, R. L. (2013). Diabetes and gout: efficacy and safety of febuxostat and allopurinol. *Diabetes, Obesity and Metabolism* ***64***(2), 256-261.

Becker, M. A., Schumacher Jr, H. R. Wortmann, R. L., MacDonald, P. A., Eustace, D., and Palo, W. A., Streit, J. and Joseph-Ridge, N. (2005). Febuxostat compared with allopurinol in patients with hyperuricemia and gout. *New England Journal of Medicine* ***353***(23), 2450-2461.

Becker, S. L. (1983). Will milk make them grow. *Parascandola, J. Whorton, JC eds. Chemistry and Modern Society* **1983**: 61-83.

Beedkar, S. D., Khobragade, C. N., Chobe, S. S., Dawane, B. S. and Yemul, O. S. (2012). Novel thiazolo-pyrazolyl derivatives as xanthine oxidase inhibitors and free radical scavengers. *International Journal of Biological Macromolecules* ***50***(4), 947-956.

Bellamy, F. D. and Ou, K. (1984). Selective reduction of aromatic nitro compounds with stannous chloride in non acidic and non aqueous medium. *Tetrahedron Letters* ***25***(8), 839-842.

Brown, J. M., Terada, L. S., Grosso, M. A., Whitmann, G. J., Velasco, S. E., Patt, A. Harken, A. H. and Repine, J. E. (1988). Xanthine oxidase produces hydrogen peroxide which contributes to reperfusion injury of ischemic, isolated, perfused rat hearts. *Journal of Clinical Investigation* ***81***(4), 1297.

Bruce, S. P. (2006). Febuxostat: a selective xanthine oxidase inhibitor for the treatment of hyperuricemia and gout. *The Annals of Pharmacotherapy* ***40***(12), 2187-2194.

Cammalleri, L. and Malaguarnera, M. (2007). Rasburicase represents a new tool for hyperuricemia in tumor lysis syndrome and in gout. *International Journal of Medical Sciences* ***4***(2), 83.

Cao, H., Pauff, J.M., and Hille, R. (2010). Substrate orientation and catalytic specificity in the action of xanthine oxidase: the sequential hydroxylation of hypoxanthine to uric acid. *The Journal of Biological Chemistry* ***285***(36), 28044-53.

Catarzi, D., Colotta, V.,Varano, F., Poli, D., Squarcialupi, L., Filacchioni, G., Varani, K., Vincenzi, F., Borea, P., Andrea, B. and Diego D. (2012). Pyrazolo [1, 5-c] quinazoline derivatives and their simplified analogues as adenosine receptor antagonists. Synthesis, structure-affinity relationships and molecular modeling studies. *Bioorganic and Medicinal Chemistry* ***21***(1), 283-294.

Chen, J., Rogers, S. C., and Kavdia, M. (2013). Analysis of Kinetics of Dihydroethidium Fluorescence with Superoxide Using Xanthine Oxidase and Hypoxanthine Assay. *Annals of Biomedical Engineering* ***41***(2), 327-337.

Chen, L., Wang, W., and Wang, Y. (2009). Inhibitory effects of lithospermic acid on proliferation and migration of rat vascular smooth muscle cells. *Acta Pharmacologica Sinica* ***30***(9), 1245-1252.

Colotta, V., Catarzi, D., Varano, F., Filacchioni, G., Cecchi, L., Galli, A. and Costagli, C. (1996). Synthesis and binding activity of some pyrazolo [1, 5-c] quinazolines as tools to verify an optional binding site of a benzodiazepine receptor ligand. *Journal of Medicinal Chemistry* ***39***(15), 2915-2921.

Corbeil, C. R., Williams, C. I. and Labute, P. (2012). Variability in docking success rates due to dataset preparation. *Journal of Computer-Aided Molecular Design* ***26***(6), 775-786.

Costantino, L., Rastelli, G. and Albasini, A. (1996). A rational approach to the design of flavones as xanthine oxidase inhibitors. *European Journal of Medicinal Chemistry* ***31***(9), 693-699.

Courtney, P. and Doherty, M. (2012). Management of gout in the patient with renal disease *Rheumatology and the Kidney* (2 ed., pp. 415): Oxford University Press, Oxford.

Cronstein, B. N. and Terkeltaub, R. (2006). The inflammatory process of gout and its treatment. *Arthritis Research and Therapy* ***8***(1), S3.

Da Silva, S. L., Da Silva, A., Honório, K. M., Marangoni, S., Toyama, M. H. and Da Silva, A. B. F. (2004). The influence of electronic, steric and hydrophobic properties of flavonoid compounds in the inhibition of the xanthine oxidase. *Journal of Molecular Structure: Theochem* ***684***(1), 1-7.

Dehghan, A., van Hoek, M., Sijbrands, E. J., Hofman, A. and Witteman, J. C. (2008). High serum uric acid as a novel risk factor for type 2 diabetes. *Diabetes Care* ***31***(2), 361-362.

Della Corte, E. and Stirpe, F. (1972). The regulation of rat liver xanthine oxidase. Involvement of thiol groups in the conversion of the enzyme activity from dehydrogenase (type D) into oxidase (type O) and purification of the enzyme. *Biochemical Journal* ***126***(3), 739.

Dixon, M. (1926). Studies on xanthine oxidase: the specificity of the system. *Biochemical Journal* ***20***(4), 703.

Fam, A. G. (2005). Gout: excess calories, purines, and alcohol intake and beyond. Response to a urate-lowering diet. *Journal of Rheumatology* ***32***(5), 773-777.

Ferrari, A. M., Sgobba, M., Gamberini, Maria C., and Rastelli, G. (2007). Relationship between quantum-chemical descriptors of proton dissociation and experimental acidity constants of various hydroxylated coumarins. Identification of the biologically active species for xanthine oxidase inhibition. *European Journal of Medicinal Chemistry* ***42***(7), 1028-1031.

Finney, D. (2013). Managing gout: not a trivial matter. *Practice Nursing* ***24***(4), 179.

Gatto Jr, G. J., Ao, Z., Kearse, M. G., Zhou, M., Morales, C. R., Daniels, E., Bradley, B. T., Goserud, M. T., Goodman, K. B. and Douglas, S. A. (2013). NADPH oxidase-dependent and-independent mechanisms of reported inhibitors of reactive oxygen generation. *Journal of Enzyme Inhibition and Medicinal Chemistry* ***28***(1), 95-104.

Grassi, D., Ferri, L., Desideri, G., Di Giosia, P., Cheli, P., Del Pinto, R., Properzi, G. and Ferri, C. (2012). Chronic Hyperuricemia, Uric Acid Deposit and Cardiovascular Risk. *Current Pharmaceutical Design* ***19***(13), 2432-2438.

Guo, S., Wang, J., Fan, X., Zhang, X. and Guo, D. (2013). Synthesis of Pyrazolo [1, 5-c] quinazoline Derivatives through Copper-Catalyzed Tandem Reaction of 5-(2-Bromoaryl)-1 H-pyrazoles with Carbonyl Compounds and Aqueous Ammonia. *The Journal of Organic Chemistry* ***78***(7), 3262-3270.

Halliwell, B. (1992). JMC Gutteridge and CE Cross. *Journal of Laboratory and Clinical Medicine* ***119***(6), 598-620.

Harrold, L. R., Andrade, S. E., Briesacher, B. A., Raebel, M. A., Fouayzi, H., Yood, R. A. and Ockene, I. S. (2009). Adherence with urate-lowering therapies for the treatment of gout. *Arthritis Research & Therapy* ***11***(2), R46.

Hediger, M. A., Johnson, R. J., Miyazaki, H. and Endou, H. (2005). Molecular physiology of urate transport. *Physiology* ***20***(2), 125-133.

Heinig, M. and Johnson, R. J. (2006). Role of uric acid in hypertension, renal disease, and metabolic syndrome. *Cleveland Clinic Journal of Medicine* ***73***(12), 1059-1064.

Hille, R., Rétey, J., Bartlewski-Hof, U., Reichenbecher, W. and Schink, B. (1998). Mechanistic aspects of molybdenum-containing enzymes. *FEMS Microbiology Reviews* ***22***(5), 489-501.

Ishibuchi, S., Morimoto, H., Oe, T., Ikebe, T., Inoue, H., Fukunari, A., Kamezawa, M., Yamada, I. and Naka, Y. (2001). Synthesis and structure activity relationships of 1-phenylpyrazoles as xanthine oxidase inhibitors. *Bioorganic and Medicinal Chemistry Letters* ***11***(7), 879-882.

Jiao, R. H., Ge, H. M., Shi, D. H. and Tan, R. X. (2006). An Apigenin-Derived Xanthine Oxidase Inhibitor from Palhinhaea c ernua. *Journal of Natural Products* ***69***(7), 1089-1091.

Jordan, K. M. (2012). Up-to-date management of gout. *Current Opinion in Rheumatology* ***24***(2), 145-151.

Jordan, K. M., Cameron, J. S., Snaith, M., Zhang, W., Doherty, M., Seckl, J., Hingorani, A., Jaques, R. and Nuki, G. (2007). British Society for Rheumatology and British Health Professionals in Rheumatology guideline for the management of gout. *Rheumatology* ***46***(8), 1372-1374.

Kang, D. H. and Nakaqawa, T. (2005). Uric acid and chronic renal disease: Possible implication of hyperuricemia on progression of renal disease. *Seminars in Nephrology* ***25***(1), 43-49.

Kim, B. S., Serebreni, L., Hamdan, O., Wang, L., Parniani, A., Sussan, T., Scott Stephens, R., Boyer, L., Damarla, M. and Hassoun, P. M. (2013). Xanthine oxidoreductase is a critical mediator of cigarette smoke-induced endothelial cell DNA damage and apoptosis. *Free Radical Biology and Medicine* **60**: 1-354.

Komoriya, K., Osada, Y., Hasegawa, M., Horiuchi, H., Kondo, S., Couch, R. C. and Griffin, T. B. (1993). Hypouricemic effect of allopurinol and the novel xanthine oxidase inhibitor TEI-6720 in chimpanzees. *European Journal of Pharmacology* ***250***(3), 455-460.

Kumar, R., Sharma, S. and Singh, R. (2011). Xanthine oxidase inhibitors: a patent survey. *Expert Opinion on Therapeutic Patents* ***21***(7), 1071-1108.

Lévai, A. (2005). Synthesis of chlorinated 3, 5-diaryl-2-pyrazolines by the reaction of chlorochalcones with hydrazines. *Arkivoc* **9**: 344-352.

Li, Z., Guan, R. and Liu, H. (2013). A Sensitive Reversed-Phase High-Performance Liquid Chromatography Method for the Quantitative Determination of Milk Xanthine Oxidase Activity. *Open Journal of Medicinal Chemistry* ***3***(2), 26-30.

Lin, C. M., Chen, C. S., Chen, C. T., Liang, Y. C. and Lin, J K. (2002). Molecular modeling of flavonoids that inhibits xanthine oxidase. *Biochemical and Biophysical Research Communications* ***294***(1), 167-172.

Lin, S. M., Wu, J. Y., Su, C., Ferng, S., Lo, C. Y. and Chiou, R. Y. Y. (2012). Identification and Mode of Action of 5-Hydroxymethyl-2-furfural (5-HMF) and 1-Methyl-1, 2, 3, 4-tetrahydro-β-carboline-3-carboxylic Acid (MTCA) as Potent Xanthine Oxidase Inhibitors in Vinegars. *Journal of Agricultural and Food Chemistry* ***60***(39), 9856-9862.

Lokhande, P. D., Waghamare, B. Y. and Sakate, S. S. (2005). Regioselective one-pot synthesis of 3, 5-diaryl-pyrazoles. *Indian Journal of Chemistry Section B* ***44***(11), 2338.

Malaguarnera, G., Giordano, M. and Malaguarnera, M. (2012). Rasburicase for the treatment of tumor lysis in hematological malignancies. *Expert Review of Hematology* ***5***(1), 27-38.

Malik, V. S., Popkin, B. M., Bray, G. A., Despres, J. P., Willett, W. C. and Hu, F. B. (2010). Sugar-sweetened beverages and risk of metabolic syndrome and type 2 diabetes: a meta-analysis. *Diabetes Care* ***33***(11), 2477-2483.

Massey, V., Komai, H., Palmer, G. and Elion, G. B. (1970). On the mechanism of inactivation of xanthine oxidase by allopurinol and other pyrazolo [3, 4-d] pyrimidines. *Journal of Biological Chemistry* ***245***(11), 2837-2844.

Menon, A. and Nair, C. K. N. (2013). Ayurvedic formulations ameliorate cisplatin-induced nephrotoxicity: Preclinical studies on Brahma Rasayana and Chyavanaprash. *Journal of Cancer Research and Therapeutics* ***9***(2), 230.

Miner, J., Girardet, J. l. and Quart, B. D. (2013). Treatment of Gout: US Patent 20,130,059,868.

Muraoka, S. and Miura, T. (2004). Inhibition of xanthine oxidase by phytic acid and its antioxidative action. *Life Sciences* ***74***(13), 1691-1700.

Musa, K. H., Abdullah, A., Kuswandi, B. and Amrun Hidayat, M. (2013). A novel high throughput method based on the DPPH dry reagent array for determination of antioxidant activity. *Food Chemistry* ***141***(4), 4102–4106

Nagamatsu, T., Fujita, T. and Endo, K. (2000). Novel xanthine oxidase inhibitor studies. Part 3.1 Convenient and general syntheses of 3-substituted 7*H*-pyrazolo [4, 3-*e*]-1, 2, 4-triazolo [4, 3-*c*] pyrimidin-5 (6*H*)-ones as a new class of potential xanthine oxidase inhibitors. *Journal of the Chemical Society, Perkin Transactions* ***1*** (1), 33-42.

Neogi, T., George, J., Rekhraj, S., Struthers, A. D., Choi, H. and Terkeltaub, R. A. (2012). Are either or both hyperuricemia and xanthine oxidase directly toxic to the vasculature? A critical appraisal. *Arthritis and Rheumatism* ***64***(2), 327-338.

Nepali, K., Singh, G., Turan, A., Agarwal, A., Sapra, S., Kumar, R., Banerjee, U. C., Verma, P. K., Satti, N. K. and Gupta, M. K. (2011). A rational approach for the design and synthesis of 1-acetyl-3, 5-diaryl-4, 5-dihydro (1*H*) pyrazoles as a new class of potential non-purine xanthine oxidase inhibitors. *Bioorganic and Medicinal Chemistry* ***19***(6), 1950-1958.

Nishino, T., Okamoto, K., Eger, B. T., Pai, E. F. and Nishino, T. (2008). Mammalian xanthine oxidoreductase–mechanism of transition from xanthine dehydrogenase to xanthine oxidase. *FEBS Journal* ***275***(13), 3278-3289.

Nuki, G. and Simon, P. A. (2006). A concise history of gout and hyperuricemia and their treatment. *Arthritis Research and Therapy* ***8***(1), S1.

Nyhan, W. L. (2005). Lesch-Nyhan Disease. *Journal of the History of the Neurosciences* ***14***(1), 1-10.

Okamoto, K., Eger, B. T., Nishino, T., Kondo, S., Pai, E. F. and Nishino, T. (2003). An extremely potent inhibitor of xanthine oxidoreductase. Crystal structure of the enzyme-inhibitor complex and mechanism of inhibition. *The Journal of Biological Chemistry* ***278***(3), 1848-1855.

Okamoto, K., Matsumoto, K., Hille, R., Eger, B. T., Pai, E. F. and Nishino, T. (2004). The crystal structure of xanthine oxidoreductase during catalysis:

implications for reaction mechanism and enzyme inhibition. *Proceedings of the National Academy of Sciences of the United States of America* ***101***(21), 7931-7936.

Pacher, P., Nivorozhkin, A. and Szabó, C. (2006). Therapeutic effects of xanthine oxidase inhibitors: renaissance half a century after the discovery of allopurinol. *Pharmacological reviews* ***58***(1), 87-114.

Pak, C. Y. (2008). Medical stone management: 35 years of advances. *The Journal of Urology* ***180***(3), 813-819.

Pauff, J. M. and Hille, R. (2009). Inhibition studies of bovine xanthine oxidase by luteolin, silibinin, quercetin, and curcumin. *Journal of Natural Products* ***72***(4), 725-731.

Punzi, L. and So, A. (2013). Serum uric acid and gout: from the past to molecular biology. *Current Medical Research and Opinion* ***29***(S3), 3-8.

Rajagopalan, K. and Handler, P. (1967). Purification and properties of chicken liver xanthine dehydrogenase. *Journal of Biological Chemistry* ***242***(18), 4097-4107.

Rehman, A. U., Cser, K., Sass, L. and Vass, I. (2013). Characterization of singlet oxygen production and its involvement in photodamage of Photosystem II in the cyanobacterium Synechocystis PCC 6803 by histidine-mediated chemical trapping. *Biochimica et Biophysica Acta (BBA)-Bioenergetics* ***1827***(6), 689-698.

Richette, P., Brière, C., Hoenen-Clavert, V., Loeuille, D. and Bardin, T. (2007). Rasburicase for tophaceous gout not treatable with allopurinol: an exploratory study. *The Journal of Rheumatology* ***34***(10), 2093-2098.

Rider, T. G. and Jordan, K. M. (2010). The modern management of gout. *Rheumatology* ***49***(1), 5-14.

Roddy, E., Zhang, W. and Doherty, M. (2007). Concordance of the management of chronic gout in a UK primary-care population with the EULAR gout recommendations. *Annals of the Rheumatic Diseases* ***66***(10), 1311-1315.

Rodnan, G. P. (1982). Treatment of the gout and other forms of crystal-induced arthritis. *Bulletin on the Rheumatic Diseases* ***32***(5), 43.

Saka, B., Barro-Traoré, F., Atadokpédé, F. A., Kobangue, L., and Niamba, P. A., Adégbidi, H., Yedomon, H. G., Traoré, A. and Pitché, V. P. (2013). Stevens–Johnson syndrome and toxic epidermal necrolysis in sub-Saharan Africa: a

multicentric study in four countries. *International Journal of Dermatology* ***52***(5), 575-579.

Schumacher, H. R., Becker, M. A., Lloyd, E., MacDonald, P. A. and Lademacher, C. (2009). Febuxostat in the treatment of gout: 5-yr findings of the FOCUS efficacy and safety study. *Rheumatology* ***48***(2), 188-194.

Shadnia, H. (2009) uDock 2.5 flexible docking program for MOE/smp clusters User Manual

Shieh, D., Liu, L. T. and Lin, C. C. (2000). Antioxidant and free radical scavenging effects of baicalein, baicalin and wogonin. *Anticancer Research* ***20***(5A), 2861.

Smelcerovic, A., Rangelov, M., Veljkovic, A.,Cherneva, E., Yancheva, D., Nikolic, G. M., Petronijevic, Z. and Kocic, G. (2013). Two 6-(propan-2-yl)-4-methyl-morpholine-2, 5-diones as new non-purine xanthine oxidase inhibitors and anti-inflammatory agents. *Food and Chemical Toxicology* **55**: 493-497.

Stamp, L. K. and Chapman, P. T. (2013). Gout and its comorbidities: implications for therapy. *Rheumatology* ***52***(1), 34-44.

Stirpe, F. and Della Corte, E. (1969). The regulation of rat liver xanthine oxidase conversion in vitro of the enzyme activity from dehydrogenase (type D) to oxidase (type O). *Journal of Biological Chemistry* ***244***(14), 3855-3863.

Szabo, M., Idiţoiu, C., Chambre, D. and Lupea, A. (2007). Improved DPPH determination for antioxidant activity spectrophotometric assay. *Chemical Papers* ***61***(3), 214-216.

Tausche, A. K., Unger, S., Richter, K., Wunderlich, C., Grassler, J., Roch, B. and Schroder, H. E. (2006). Hyperuricemia and gout: diagnosis and therapy. *Internist (Berl)* ***47***(5), 509-520; quiz 521.

Terkeltaub, R. (2010). Update on gout: new therapeutic strategies and options. *Nature Reviews Rheumatology* ***6***(1), 30-38.

Terkeltaub, R. A. (2003). Gout. *New England Journal of Medicine* ***349***(17), 1647-1655.

Terkeltaub, R. A. (2009). *Colchicine update: 2008.* Paper presented at the Seminars in arthritis and rheumatism ***38***(6)*,* 411-419

Ultra, C. (2001). 6.0 and Chem3D Ultra. *Cambridge Soft Corporation, Cambridge, USA*.

Umamaheswari, M., Madeswaran, A., Asok kumar, K., Sivashanmugam, T., Subhadradevi, V. and Jagannath, P. (2011). Study of potential xanthine oxidase inhibitors: In silico and in vitro biological activity. *Bangladesh Journal of Pharmacology* ***6***(2), 117-123.

Varano, F., Catarzi, D., Colotta, V., Filacchioni, G., Galli, A., Costagli, C. and Carlà, V. (2002). Synthesis and biological evaluation of a new set of pyrazolo [1, 5-c] quinazoline-2-carboxylates as novel excitatory amino acid antagonists. *Journal of Medicinal Chemistry* ***45***(5), 1035-1044.

Varano, F., Catarzi, D., Colotta, V., Filacchioni, G., Galli, A., Costagli, C. and Carlà, V. (2008). Novel AMPA and kainate receptor antagonists containing the pyrazolo [1, 5-*c*] quinazoline ring system: Synthesis and structure–activity relationships. *Bioorganic and Medicinal Chemistry* ***16***(5), 2617-2626.

Vilar, S., Cozza, G. and Moro, S. (2008). Medicinal chemistry and the molecular operating environment (MOE): application of QSAR and molecular docking to drug discovery. *Current Topics in Medicinal Chemistry* ***8***(18), 1555-1572.

Villamena, F. A. (2013). *Molecular Basis of Oxidative Stress: Chemistry, Mechanisms, and Disease Pathogenesis* (1 ed.): John Wiley and Sons, Incorporated.

Wang, S., Yan, J., Wang, J., Chen, J., Zhang, T., Zhao, Y. and Xue, M. (2010). Synthesis of some 5-phenylisoxazole-3-carboxylic acid derivatives as potent xanthine oxidase inhibitors. *European Journal of Medicinal Chemistry* ***45***(6), 2663-2670.

Wang, S. Y., Yang, C. W., Liao, J. W., Zhen, W. W., Chu, F. H. and Chang, S. T. (2008). Essential oil from leaves of Cinnamomum osmophloeum acts as a xanthine oxidase inhibitor and reduces the serum uric acid levels in oxonate-induced mice. *Phytomedicine* ***15***(11), 940-945.

Waud, W. R., Brady, F. O., Wiley, R. D. and Rajagopalan, K. (1975). A new purification procedure for bovine milk xanthine oxidase: effect of proeolysis on the subunit structure. *Archives of biochemistry and biophysics* ***169***(2), 695-701.

Yang, X., Jin, Y., Liu, H., Jiang, Y. and Fu, H. (2012). Easy and efficient one-pot synthesis of pyrazolo [1, 5-c] quinazolines under mild copper-catalyzed conditions. *RSC Advances* ***2***(29), 11061-11066.

Yang, X., Yuan, Y., Zhan, C. G. and Liao, F. (2012). Uricases as therapeutic agents to treat refractory gout: current states and future directions. *Drug Development Research* ***73***(2), 66-72.

Youssef, A. M., Neeland, E. G., Villanueva, E. B., White, M., El-Ashmawy, I. M., Patrick, B., Klegeris, A. and and Abd-El-Aziz, A. S. (2010). Synthesis and biological evaluation of novel pyrazole compounds. *Bioorganic and Medicinal Chemistry* ***18***(15), 5685-5696.

Zafar, I., Khan, M., Turab, S. M. and Khan, R. A. (2012). Efficacy and Safety of Fenofibrate in Patients with Hyperuricemia. *Journal of the Dow University of Health Sciences* ***6***(1), 3-6.

Zhang, W., Doherty, M., Bardin, T., Pascual, E., Barskova, V., Conaghan, P., Gerster, J., Jacobs, J., Leeb, B. and Liote, F. (2006). EULAR evidence based recommendations for gout. Part II: Management. Report of a task force of the EULAR Standing Committee for International Clinical Studies Including Therapeutics (ESCISIT). *Annals of the Rheumatic Diseases* ***65***(10), 1312-1324.

APPENDIX

Manuscript

Kumar, D. and Kumar R. (2013). Synthesis and Biological Evaluation of 2-aryl-5,6-dihydropyrazolo[1,5-*c*]quinazolines as Xanthine Oxidase Inhibitors. *Manuscript under preparation*.

SPECTRAL DATA

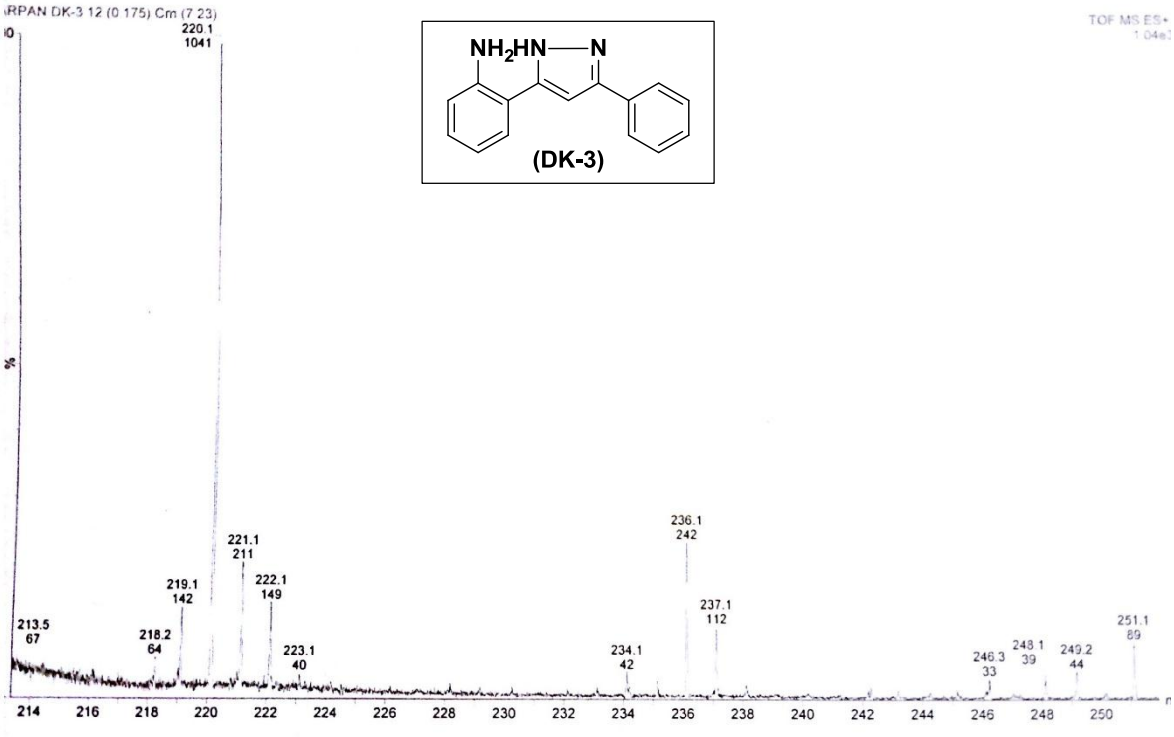

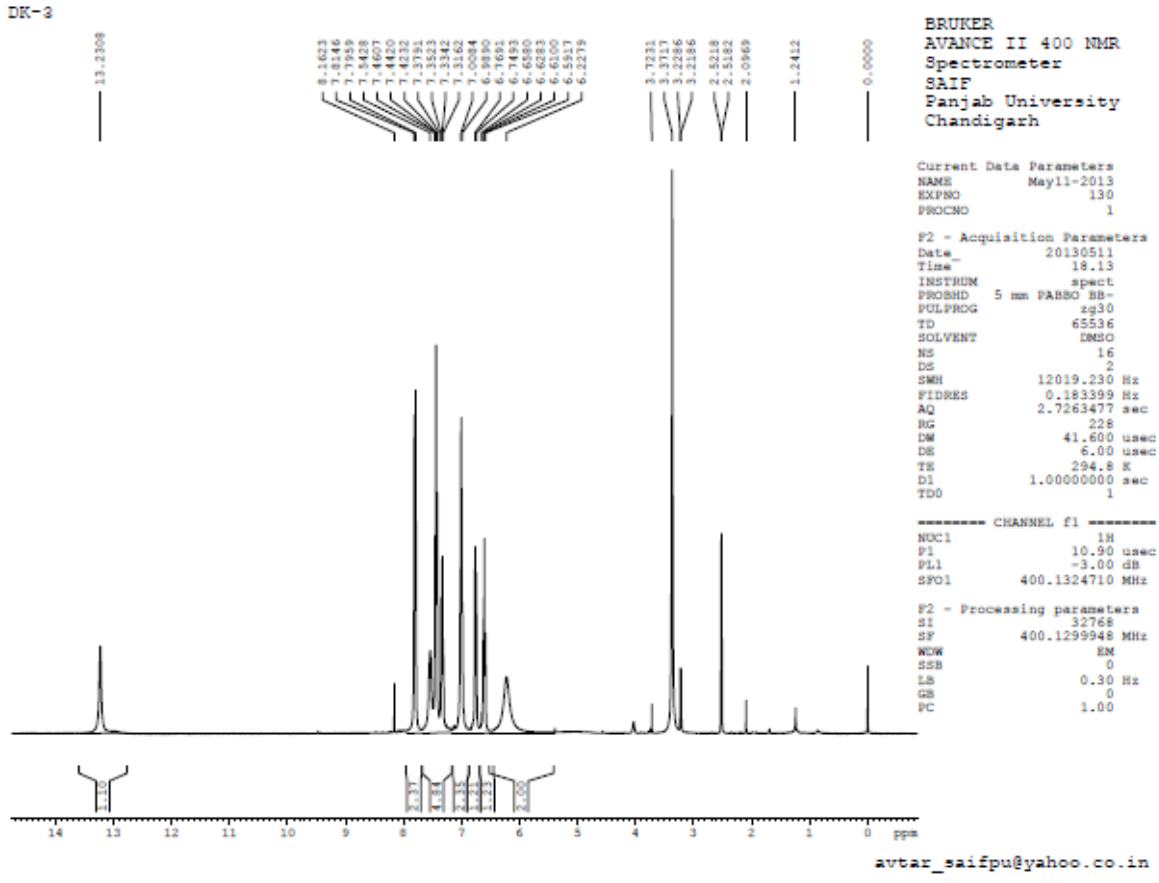

avtar_saifpu@yahoo.co.in

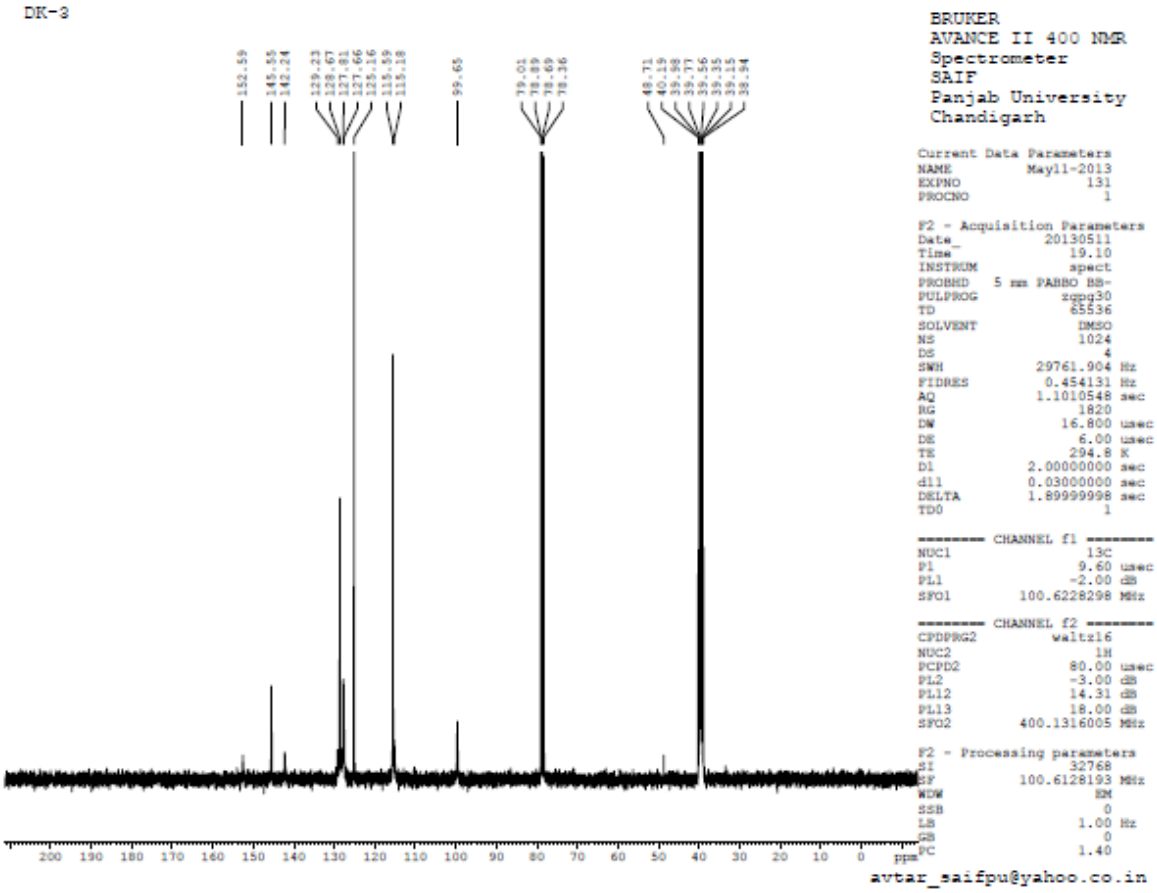
DK-3
152.59
145.55
142.24
129.23
128.67
127.81
127.66
125.16
115.59
115.18
99.65
79.01
78.89
78.69
78.36
48.71
40.19
39.98
39.77
39.56
39.35
39.15
38.94
BRUKER
AVANCE II 400 NMR
Spectrometer
SAIF
Panjab University
Chandigarh
Current Data Parameters
NAME May11-2013
EXPNO 131
PROCNO 1
F2 - Acquisition Parameters
Date_ 20130511
Time 19.10
INSTRUM spect
PROBHD 5 mm PABBO BB-
PULPROG zgpg30
TD 65536
SOLVENT DMSO
NS 1024
DS 4
SWH 29761.904 Hz
FIDRES 0.454131 Hz
AQ 1.1010548 sec
RG 1820
DW 16.800 usec
DE 6.00 usec
TE 294.8 K
D1 2.00000000 sec
d11 0.03000000 sec
DELTA 1.89999998 sec
TD0 1
======== CHANNEL f1 ========
NUC1 13C
P1 9.60 usec
PL1 -2.00 dB
SFO1 100.6228298 MHz
======== CHANNEL f2 ========
CPDPRG2 waltz16
NUC2 1H
PCPD2 80.00 usec
PL2 -3.00 dB
PL12 14.31 dB
PL13 18.00 dB
SFO2 400.1316005 MHz
F2 - Processing parameters
SI 32768
SF 100.6128193 MHz
WDW EM
SSB 0
LB 1.00 Hz
GB 0
PC 1.40
200 190 180 170 160 150 140 130 120 110 100 90 80 70 60 50 40 30 20 10 0 ppm
avtar_saifpu@yahoo.co.in

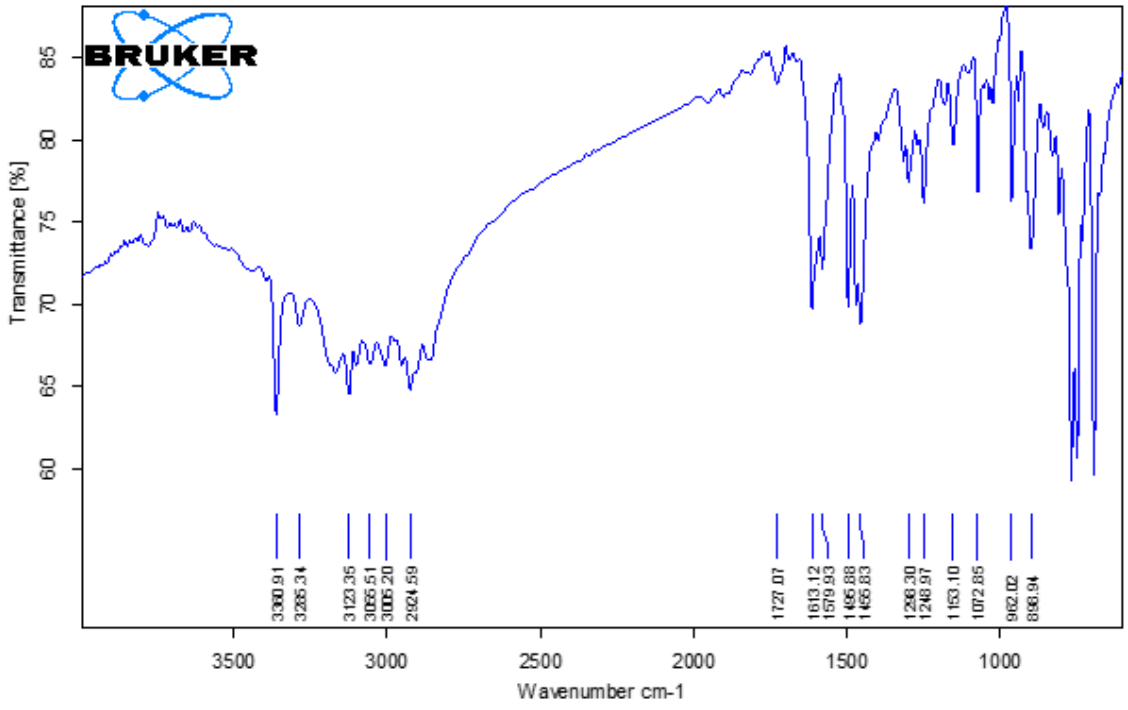
BRUKER
Transmittance [%]
85
80
75
70
65
60
3360.91
3285.34
3123.35
3066.51
3005.20
2924.59
1727.07
1613.12
1579.93
1496.88
1455.83
1298.30
1248.97
1153.10
1072.85
962.02
898.94
3500
3000
2500
2000
1500
1000
Wavenumber cm-1

WATERS, Q-TOF MICROMASS (LC-MS)
DEEPENDRA DK-3H 19 (0.213) Cm (7:28)

SAIF/CIL,PANJAB UNIVERSITY,CHANDIGARH
TOF MS ES+
3.63e3

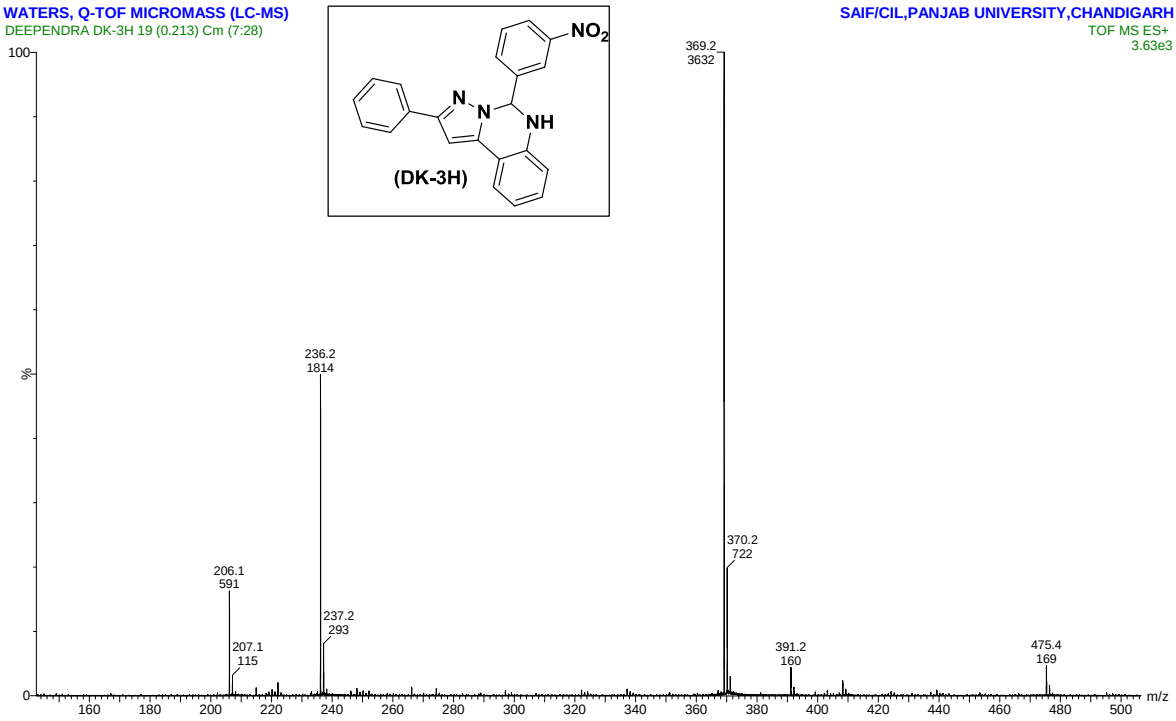

DK-3H

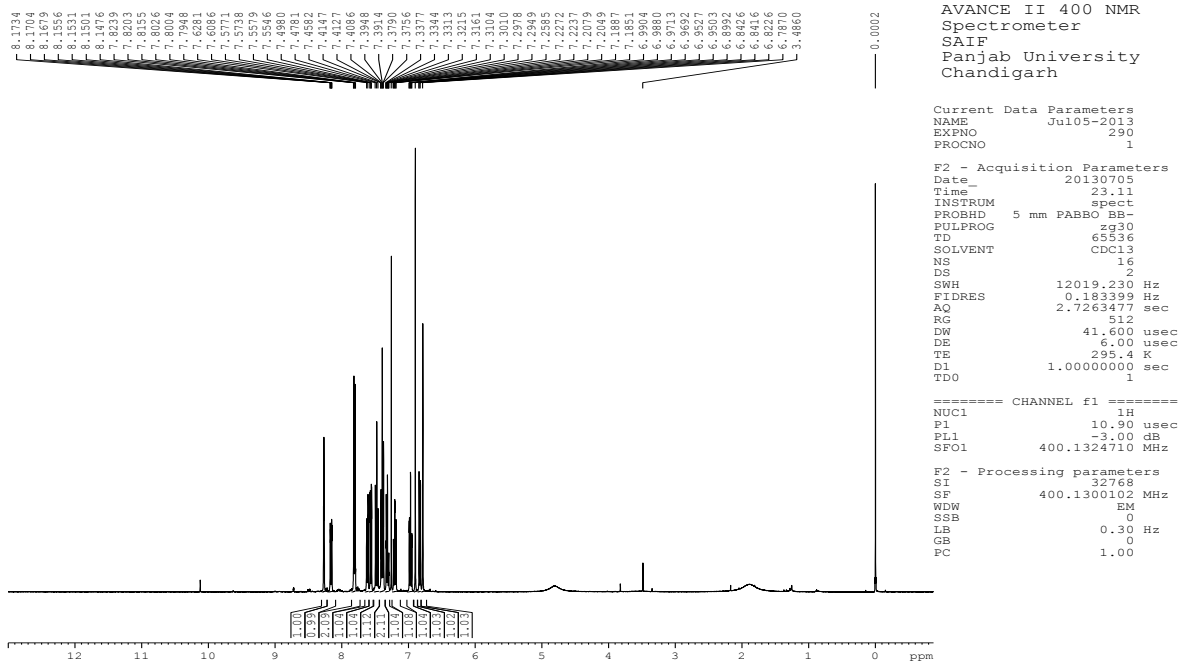

BRUKER
AVANCE II 400 NMR
Spectrometer
SAIF
Panjab University
Chandigarh

```
Current Data Parameters
NAME                  Jul05-2013
EXPNO                        290
PROCNO                         1

F2 - Acquisition Parameters
Date_                   20130705
Time                       23.11
INSTRUM                    spect
PROBHD    5 mm PABBO BB-
PULPROG                    zg30
TD                        65536
SOLVENT                   CDCl3
NS                           16
DS                            2
SWH                  12019.230 Hz
FIDRES                0.183399 Hz
AQ                   2.7263477 sec
RG                          512
DW                       41.600 usec
DE                        6.00 usec
TE                       295.4 K
D1                  1.00000000 sec
TD0                            1

======== CHANNEL f1 ========
NUC1                         1H
P1                       10.90 usec
PL1                      -3.00 dB
SFO1                400.1324710 MHz

F2 - Processing parameters
SI                         32768
SF                  400.1300102 MHz
WDW                           EM
SSB                            0
LB                        0.30 Hz
GB                             0
PC                          1.00
```

avtar_saifpu@yahoo.co.in

DK-3H

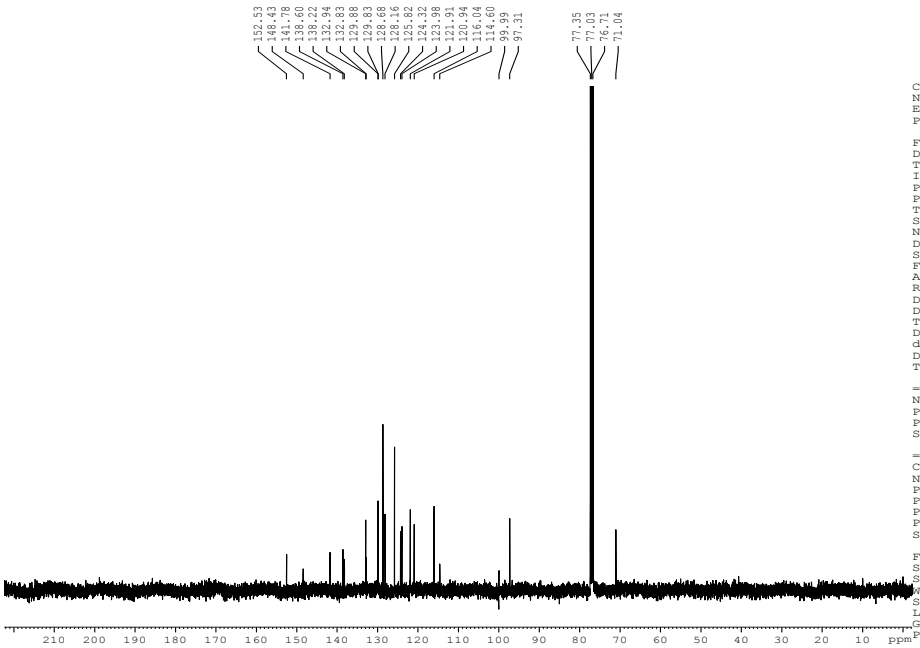

BRUKER
AVANCE II 400 NMR
Spectrometer
SAIF
Panjab University
Chandigarh

```
Current Data Parameters
NAME                  Jul05-2013
EXPNO                        291
PROCNO                         1

F2 - Acquisition Parameters
Date_                   20130705
Time                       23.41
INSTRUM                    spect
PROBHD     5 mm PABBO BB-
PULPROG                 zgpg30
TD                       65536
SOLVENT                  CDCl3
NS                         512
DS                           4
SWH                  29761.904 Hz
FIDRES                0.454131 Hz
AQ                   1.1010548 sec
RG                          36
DW                      16.800 usec
DE                       6.00 usec
TE                       295.7 K
D1                  2.00000000 sec
d11                 0.03000000 sec
DELTA               1.89999998 sec
TD0                            1

======== CHANNEL f1 ========
NUC1                        13C
P1                         9.60 usec
PL1                       -2.00 dB
SFO1               100.6228298 MHz

======== CHANNEL f2 ========
CPDPRG2                 waltz16
NUC2                        1H
PCPD2                     80.00 usec
PL2                       -3.00 dB
PL12                      14.31 dB
PL13                      18.00 dB
SFO2               400.1316005 MHz

F2 - Processing parameters
SI                          32768
SF                 100.6127690 MHz
WDW                            EM
SSB                             0
LB                           1.00 Hz
GB                              0
PC                           1.40
```

avtar_saifpu@yahoo.co.in

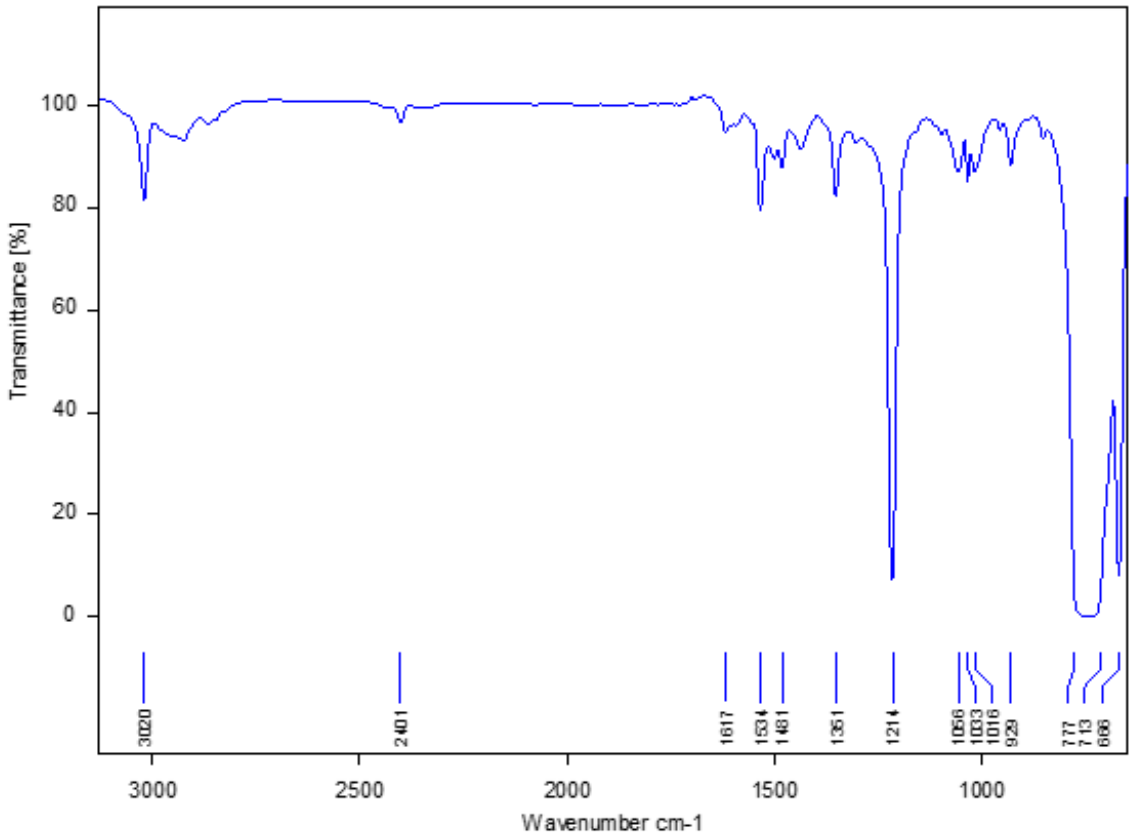

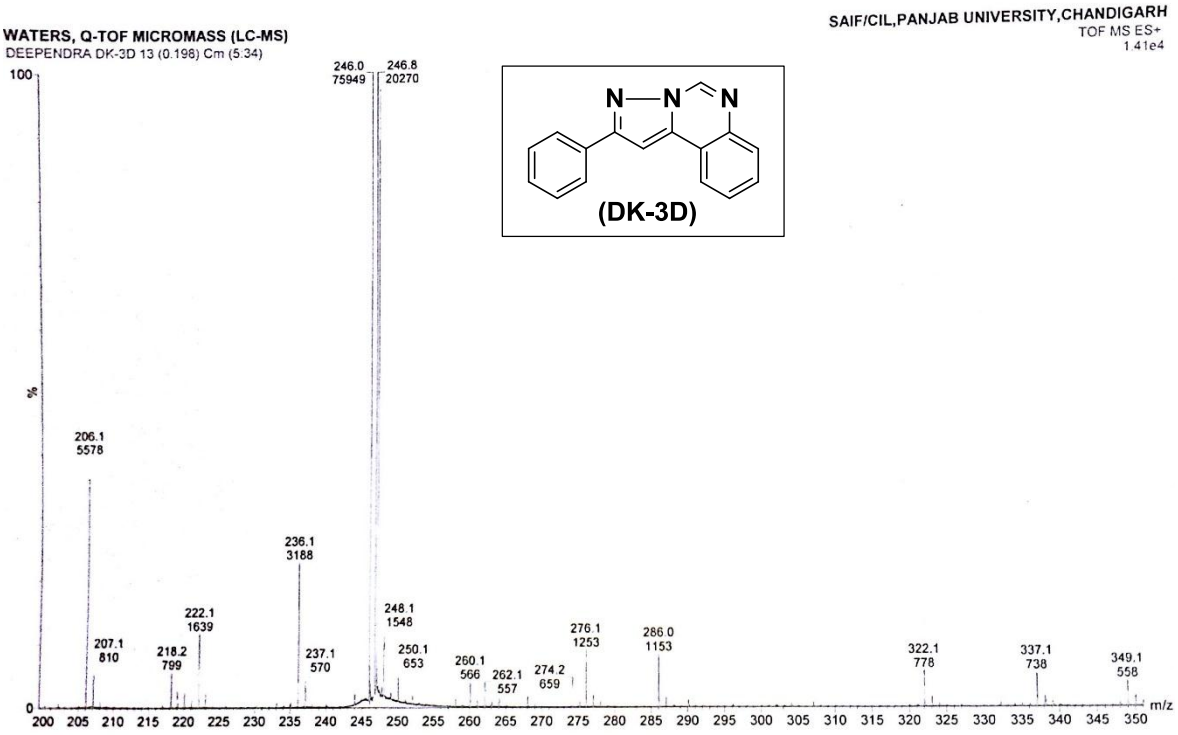

DK-3D

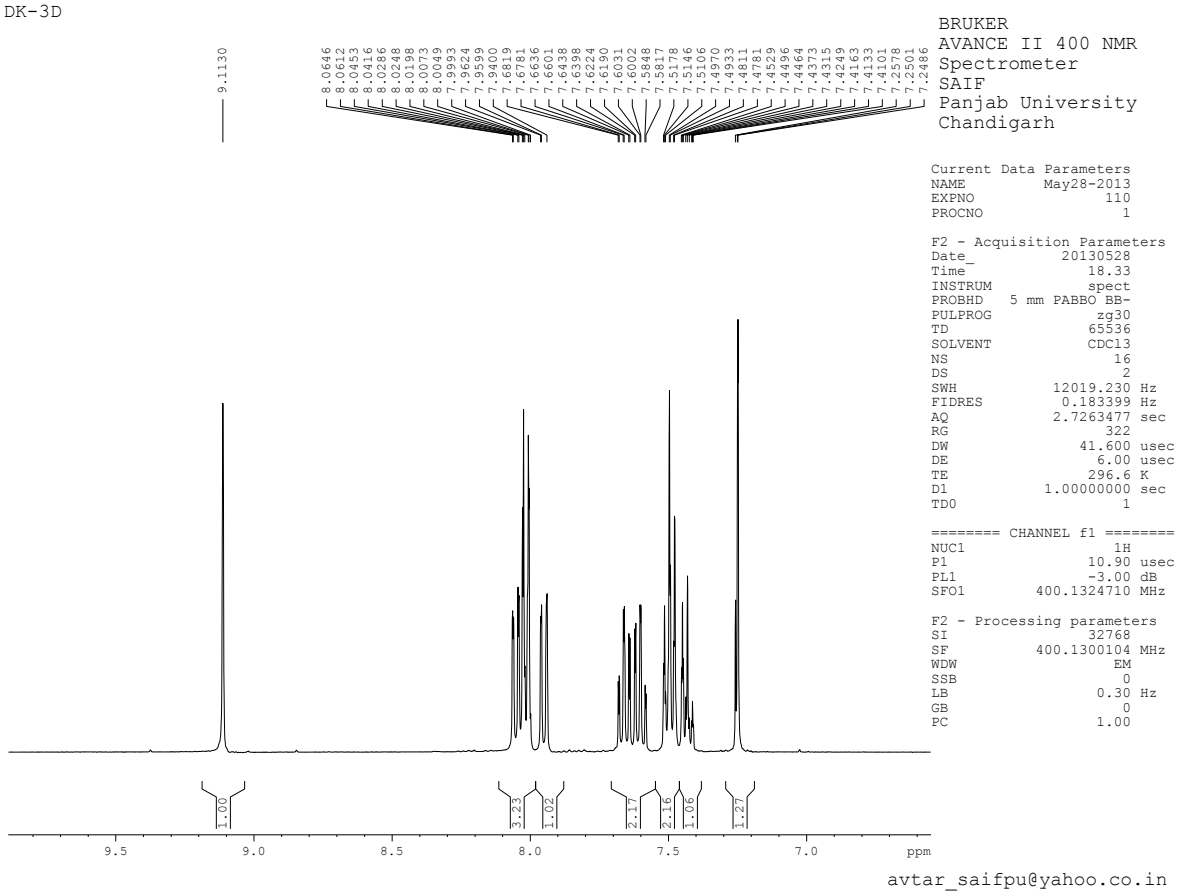

BRUKER
AVANCE II 400 NMR
Spectrometer
SAIF
Panjab University
Chandigarh

```
Current Data Parameters
NAME          May28-2013
EXPNO                110
PROCNO                 1

F2 - Acquisition Parameters
Date_           20130528
Time               18.33
INSTRUM            spect
PROBHD   5 mm PABBO BB-
PULPROG             zg30
TD                 65536
SOLVENT            CDCl3
NS                    16
DS                     2
SWH            12019.230 Hz
FIDRES          0.183399 Hz
AQ             2.7263477 sec
RG                   322
DW                41.600 usec
DE                 6.00 usec
TE                296.6 K
D1           1.00000000 sec
TD0                    1

======== CHANNEL f1 ========
NUC1                  1H
P1                10.90 usec
PL1               -3.00 dB
SFO1         400.1324710 MHz

F2 - Processing parameters
SI                 32768
SF           400.1300104 MHz
WDW                   EM
SSB                    0
LB                  0.30 Hz
GB                     0
PC                  1.00
```

avtar_saifpu@yahoo.co.in

DK-3D

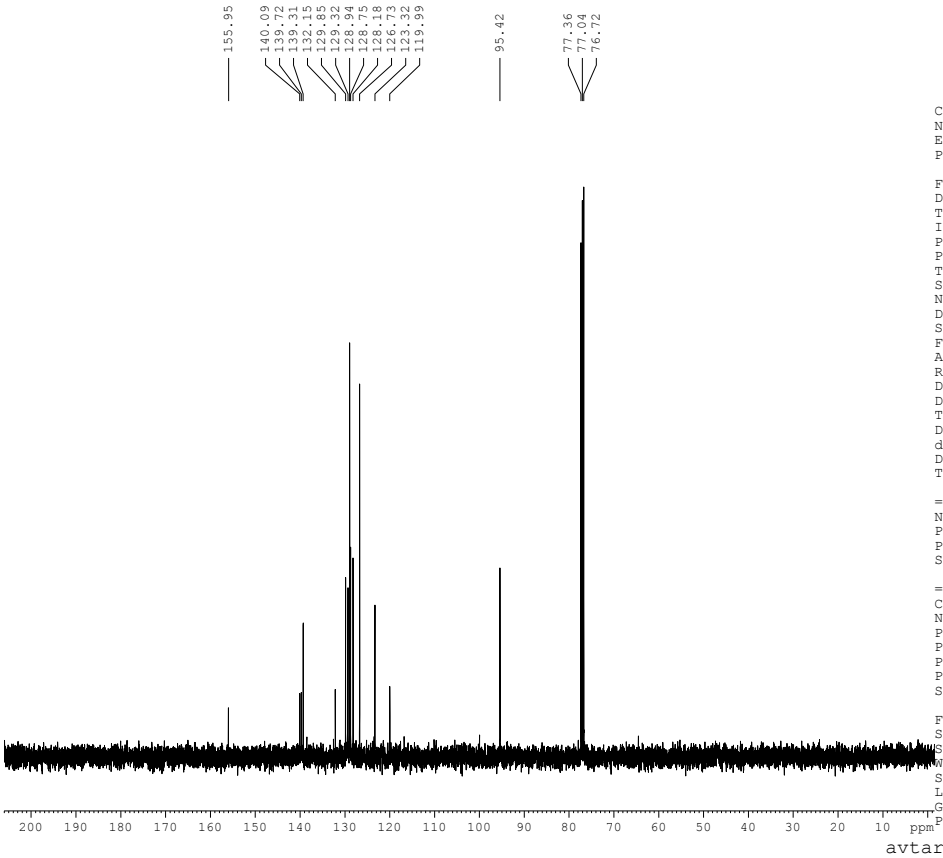

BRUKER
AVANCE II 400 NMR
Spectrometer
SAIF
Panjab University
Chandigarh

```
Current Data Parameters
NAME          May28-2013
EXPNO                111
PROCNO                 1

F2 - Acquisition Parameters
Date_           20130528
Time               18.41
INSTRUM            spect
PROBHD   5 mm PABBO BB-
PULPROG          zgpg30
TD                65536
SOLVENT           CDCl3
NS                 1024
DS                    4
SWH           29761.904 Hz
FIDRES        0.454131 Hz
AQ            1.1010548 sec
RG                   36
DW               16.800 usec
DE                6.00 usec
TE                297.2 K
D1           2.00000000 sec
d11          0.03000000 sec
DELTA        1.89999998 sec
TD0                   1

======== CHANNEL f1 ========
NUC1                 13C
P1                 9.60 usec
PL1               -2.00 dB
SFO1        100.6228298 MHz

======== CHANNEL f2 ========
CPDPRG2          waltz16
NUC2                 1H
PCPD2             80.00 usec
PL2               -3.00 dB
PL12              14.31 dB
PL13              18.00 dB
SFO2        400.1316005 MHz

F2 - Processing parameters
SI                32768
SF          100.6127690 MHz
WDW                  EM
SSB                   0
LB                 1.00 Hz
GB                    0
PC                 1.40
```

avtar_saifpu@yahoo.co.in